Escola de Camins
Escola Tècnica Superior d'Enginyeria de Camins, Canals i Ports
UPC BARCELONATECH

TREBALL FINAL DE GRAU

Pseudo-static approach to the structural vulnerability of an off-shore windmill

Treball realitzat per:
Robert Ortells Sesé

Dirigit per:
Juan José Egozcue Rubí
Maribel Ortego Martínez

Grau en:
Enginyeria Civil

Barcelona, 17 de juny de 2014

Departament de Matemàtica Aplicada III

Abstract

PSEUDO-STATIC APPROACH TO THE STRUCTURAL VULNERABILITY OF AN OFF-SHORE WINDMILL

Author: Robert Ortells Sesé
Advisors: Juan José Egozcue Rubí, Maribel Ortego Martínez

key words: vulnerability, risk, off-shore, windmill, multiple linear regression, sample importance re-sampling, Monte Carlo simulation, compositional data.

The present project is aimed to study the structural vulnerability of an off-shore windmill of the Danish Northern Sea. The main objective has been to model the potential risk an off-shore windmill is under as a function of the external actions that it comes across: wind speed, swell sea conditions and degree of structural fatigue. To evaluate the potential damage on the windmill, three states have been defined: service state, blade damage and tower destruction. Studying the *vulnerability* has meant finding a model which can provide the conditional probabilities to be in these three states as long as the external actions are known.

In order to address the problem, a multiple linear regression model has been proposed. However, the construction of such model demands *experimental data*, which we have obtained through a Monte Carlo simulation. Therefore, the following steps have been carried out. First, we have modelled the physical behaviour of the windmill, by keeping in mind that for a wind speed under 25 m/s it operates normally whereas above that level the system is inactive. Secondly, we have carried out a Monte Carlo simulation to take into consideration all the random parameters of the model. This simulation has been aimed to provide us data about *what the probabilities to be in the three states are for certain fixed external actions*. Finally, once the probabilities for different sets of external actions have been obtained, we have proposed a multiple regression model to fit this simulated data in order to be able to evaluate these probabilities for whatsoever external actions.

With reference to the regression, however, we have to point out that since probabilities are values bounded between zero and one, they do not belong to the real scale, so they cannot be fitted directly through a conventional multiple regression approach. In other words, given that the values we are trying to predict with our regression model are not in the real scale, they *need to be treated appropriately to take its nature into consideration.* Therefore, the compositional data analysis has been considered.

With reference to the results, the linear regression model which predicts the probabilities to be in the three states as a function of the external actions has been proved to be meaningful and admissibly accurate, according to the simplicity of the model we have proposed. Moreover, regarding the potential usefulness of the results, we should understand such project as a supporting tool to the decision making process of the design of an off-shore windmill plant.

Abstract

ANÁLISIS PSEUDO-ESTÁTICO DE LA VULNERABILIDAD ESTRUCTURAL DE UN MOLINO OFF-SHORE

Autor: Robert Ortells Sesé
Tutores: Juan José Egozcue Rubí, Maribel Ortego Martínez

palabras clave: vulnerabilidad, riesgo, off-shore, molino, regresión lineal múltiple, muestreo de importancia, simulación de Monte Carlo, datos composicionales.

El presente proyecto trata de estudiar la vulnerabilidad estructural de un molino de viento off-shore situado en el Mar del Norte de Dinamarca. El objetivo principal ha sido modelizar el riesgo potencial del molino en función de las condiciones de contorno con las que se encuentra: velocidad del viento, situación del mar de fondo y grado de fatiga estructural. Para evaluar el daño potencial sobre la estructura se han definido tres estados posibles: servicio, ruptura de palas y destrucción completa de la torre. El proceso de *estudiar la vulnerabilidad* ha consistido en construir un modelo capaz de predecir cuál es la probabilidad de que el molino se halle en estos tres estados en función de cuáles son las acciones externas con las que se encuentra.

Para afrontar el problema, se ha planteado una regresión lineal múltiple. Sin embargo, dicha regresión precisa de unos *datos experimentales* que ajustar, datos que hemos obtenido mediante un proceso de simulación de Monte Carlo. Por lo tanto, se han llevado a cabo los siguientes pasos. En primer lugar, se ha propuesto un modelo de comportamiento para el molino, teniendo en cuenta que el molino está activo bajo condiciones de velocidad de viento inferiores a 25 m/s, y que está inactivo por motivos de seguridad una vez se supera dicho umbral. En segundo lugar, se ha planteado una simulación de Monte Carlo para obtener las probabilidades de estar en los tres estados para valores concretos de las acciones externas, teniendo en consideración que varios de los parámetros del modelo son variables aleatorias. Finalmente, a partir de los datos obtenidos en la simulación se ha definido una regresión lineal múltiple, mediante la cual se ha intentado ajustar los valores de las probabilidades para poder hacer una estimación del riesgo estructural bajo condiciones externas arbitrarias.

En referencia a la regresión, sin embargo, debemos mencionar que dado que las probabilidades son valores acotados entre 0 y 1, no pertenecen a la recta real, de forma que no admiten un ajuste mediante un proceso de regresión convencional. En otras palabras, como las variables que estamos intentando predecir mediante la regresión no son variables cuyo dominio sea la recta real, precisamos de *un tratamiento apropiado que tenga en cuenta su naturaleza.* Por consiguiente, se ha procedido a utilizar el tratamiento composicional.

En cuanto a los resultados, el modelo de regresión lineal múltiple que predice las probabilidades de estar en los tres estados que hemos definido como función de las acciones externas ha resultado tener sentido y proporcionar unos resultados admisiblemente buenos teniendo en cuenta la simplicidad del modelo que hemos considerado. En relación a la utilidad de un proyecto de estas características, debemos entender el presente estudio como una herramienta adicional para la toma de decisiones en el contexto de la fase de diseño de molinos de viento off-shore.

Abstract

ANÀLISI PSEUDO-ESTÀTICA DE LA VULNERABILITAT ESTRUCTURAL D'UN MOLÍ OFF-SHORE

Autor: Robert Ortells Sesé
Tutors: Juan José Egozcue Rubí, Maribel Ortego Martínez

paraules clau: vulnerabilitat, risc, off-shore, molí, regressió lineal múltiple, mostreig d'importància, simulació de Monte Carlo, dades composicionals.

El present projecte tracta d'estudiar la vulnerabilitat estructural d'un molí de vent off-shore situat al Mar del Nord de Dinamarca. L'objectiu principal ha estat modelitzar el risc potencial del molí en funció de les condicions de contorn sota les quals es troba: velocitat del vent, situació del mar de fons i grau de fatiga estructural. Per tal d'avaluar el dany potencial sobre l'estructura s'han definit tres estats possibles: servei, dany a les pales i destrucció de la torre. El procés d'*estudiar la vulnerabilitat* ha consistit en construir un model capaç de predir quina és la probabilitat de que el molí acabi en cadascun dels tres possibles estats en funció de les accions externes sota les que es troba.

Per tal d'afrontar el problema, s'ha plantejat una regressió lineal múltiple. Ara bé, aquesta regressió precisa d'unes *dades experimentals* que ajustar, dades que hem obtingut a través d'un procés de simulació de Monte Carlo. Per tant, s'han dut a terme els passos que es presenten a continuació. En primer lloc, s'ha proposat un model de comportament pel molí, tenint en compte que el molí està actiu sota la condició de velocitat del vent inferior a 25 m/s i que està inactiu per raons de seguretat una vegada es supera aquest llindar. En segon lloc, s'ha definit una simulació de Monte Carlo per obtenir les probabilitats d'estar en els tres estats per a diferents valors concrets de les accions externes, considerant que diversos dels paràmetres involucrats en el model són variables aleatòries. Finalment, a partir de les dades obtingudes a la simulació s'ha plantejat la regressió lineal múltiple a través de la qual s'ha intentat ajustar els valors de les probabilitats per tal d'arribar a un model que estimi el risc estructural sota condicions arbitràries.

En referència a la regressió, malgrat tot, hem de mencionar que donat que les probabilitats són valors acotats entre 0 i 1, no pertanyen a la recta real, de forma que no admeten un ajust a través d'un model de regressió convencional. En altres paraules, com que les variables que estem intentant predir amb la regressió no són variables el domini de les quals sigui la recta real, es necessita *un tractament apropiat que tingui en compte la seva naturalesa*. Així doncs, s'ha procedit a utilitzar el tractament composicional.

Quant als resultats, el model de regressió lineal múltiple que prediu les probabilitats d'estar en els tres estats que hem definit com a funció de les accions externes ha resultat tenir sentit i proporcionar uns resultats admissiblement acurats d'acord amb la simplicitat del model que hem plantejat. En relació a la utilitat d'un projecte d'aquestes característiques, hem d'entendre el present estudi com una eina addicional per a la presa de decisions en el context de la fase de disseny de molins de vent off-shore.

Contents

List of Figures

List of Tables

Chapter 1

Introduction

The present project is aimed to study the structural vulnerability of an off-shore windmill of the Danish Northern Sea. From the term *vulnerability*, however, it is not straightforward to infer what the actual project is about, so several comments need to be made with reference to the objectives. The main issue we have dealt with in this project is the problem to find the probabilities of collapse of the windmill under determined conditions (situation of the sea, wind speed and fatigue on the structure). In other words, the question we have tried to answer with this project is the following one: what is the probability of collapse for the windmill in case the conditions of the wind, the sea and the degree of fatigue are these ones we supply? Therefore, our main goal has been to build a model who can provide a prediction for the probability of the windmill to collapse under an arbitrary situation.

It is important to point out that these probabilities that we will be trying to predict are conditional probabilities, since they are dependent on the *external actions* that we supply (wind speed, sea conditions and fatigue of the structure). Consequently, the present project is aimed to evaluate the potential risk on the structural safety of the windmill under fixed external conditions. It is particularly relevant to focus on this point, especially when referring to the potential usefulness of the project. At the moment when a certain investment on a wind power plant is considered, several questions arise with reference to its optimal design. On the one hand, the design must ensure the long-term viability of the windmill, by providing enough strength to address the potentially dangerous situations that might appear. On the other hand, however, the design must take into consideration how the cost is incremented as the safety on the windmill is increased. For the reasons we have just set out, the definition of a wind plant brings up the following trade-off problem: finding the minimum amount of resources necessary for the windmill in order to ensure its long-term viability. Therefore, in order to optimize the design of the windmill, it is extremely important to model, somehow, the *risk* the windmill will be under.

The present project is aimed to tackle this risk evaluation. By building a model which provides the probability of collapse conditional to the external actions of the wind and the sea, we are modelling *how vulnerable the windmill becomes* when we vary the external conditions on the wind plant. Finally, once this modelling has been made, we can study how the characteristics of the windmill have to be modified in order to address successfully the potential storm conditions the windmill is expected to come across. In other words, at the preliminary stage of the definition of the windmill we can somehow think of what the storm conditions might be, but we are unable to quantify the *risk* the structure will be under, so we do not have a system which enables us to make an optimized design. However, as long as we have a model like the one presented in the this study, we definitely have more tools with respect to what the optimal design of the windmill has to be.

However, there is a second objective which can be inferred from the main aim of the project. By carrying out this study, not only will we be able to quantify the risk the windmill is under but also

we will have information about what are the most important parameters to take into consideration with reference to the structural stability. For example, we do not know *a priori* whether the most dangerous action on the windmill is the force of the wind or the forces supplied by the sea. Therefore, by carrying out this project we will also be able to determine to what extent the different forces on the windmill are relevant.

Overall, it is important to keep in mind that the present study should be understood as a further tool for the optimization of the structural design of off-shore windmills, since its primary contribution is a modelling of the risk a windmill is under. By introducing a study like the present project in the early stages of a wind plant design, we will definitely have an additional criterion to address the problem of whether the amount of resources we are using for the plant are worthwhile.

1.1 Goals and methodology

First of all, the main objective of the project is to find a model which is able to predict what the conditional probabilities of collapse will be once given the external conditions (which are the wind speed, the sea conditions and the degree of fatigue). To do so, a regression model will be considered. As it will be developed on further stages of the project, the procedure we will follow is the following one: first, we will obtain the probabilities of collapse for several sets of external actions. These probabilities will be found through Monte Carlo simulation, and will be our *experimental* data from which we will fit a regression model. Once these probabilities have been determined, we will be able to build the regression, which will try to provide an expression to estimate the probabilities of collapse for whatsoever external conditions. In the end, the result we will have is a model who provides a prediction for the probabilities of collapse for arbitrary external conditions.

As a general overview, we have to say that even though the most complex part of the project is the obtention of the simulated conditional probabilities through Monte Carlo simulation, the core problem is to actually see whether a model of the characteristics that we have thought of is meaningful, and, in case it is, to what extent the results it predicts are accurate. With respect to this idea, it is important to set out one remark. From now on, what we have called *external actions* will be also regarded as *explicative variables*. Once we have set we will be building a regression model, it is much more appropriate to treat these external conditions for the role they will have on the model, so treat them as the explicative variables of the regression model.

For the reasons exposed above, we can divide the project in two different stages. First, the *experimental* data has to be obtained. Therefore, we have to build a physical model who is able to evaluate whether the windmill breaks or not as a function of the external actions, and that can be used in the Monte Carlo simulation to obtain the conditional probabilities for fixed conditions. To do that, we have identified the most critical points of the windmill, and have defined a breaking criterion which is able to determine whether there is collapse or not. This mathematical model has been fully developed in Chapter 2, as well as it has been computed in MatLAB (see reference [38]) to carry out the calculations. The second stage is building the regression model once the data has been obtained, as it is explained in Chapter 3. However, it is also in this section where we will have to make a deep analysis on whether the results we have obtained are meaningful and consistent with previous research, and whether there are any improvements that can be proposed for future endeavors.

Once the physical model has been mentioned, we should focus a little bit more on *what we exactly mean when we talk about the conditional probabilities*. In fact, in case we were asked to define the possible states of the windmill, we would not probably think about two possible states like "service" or "collapse". Even though we could reduce our criterion to a binary possibility, in case we should make a proper description of the state of the windmill we would probably think about the following possibilities: service state, collapse at the tower, mechanical-electrical default, collapse at the blades,

collapse at the hub and erosion at the base of the tower among others. Indeed, the potential final outcome of the windmill after a storm is not an easy situation to describe. In our project we have assumed that there are three possible states: service state, blade breaking or collapse at the tower. Regarding all the possible states that we mentioned before, we have to refer to the hypothesis that we will only be studying the structural vulnerability of the windmill, so no comments will be made regarding the soil or the electrical part. It is arguable whether we could have thought of a more detailed model, but in that case the complexity of the physical model would have become significatively higher. Therefore, the fact of including more states to the model presents a trade-off between the higher accuracy provided by having multiple final states and the limitations that they generate in terms of computational cost. For further information about these three possible states we have to refer to Chapter 2. We are now able to describe what we exactly mean when talking about the conditional probabilities; for every fixed set of external actions, we will be finding the probabilities to be in the three possible states, service, blade breaking or tower collapse. In fact, these three states represent three degrees of damage, since they are indicative of a "progressively more damaged structure" (in case everything is right the state will be service, for a medium storm there will be blade breaking and under extreme conditions there will be collapse on the tower). It is important to keep in mind that these probabilities will always be *conditional* to the external actions (in fact, this is a very intuitive idea, since it seems very reasonable that the probability to break the tower is dependent on the wind speed, the sea conditions and the fatigue on the structure).

Up to now the main objective has been defined, as well as the process that we will be carrying out in order to achieve it. However, there is still a comment to make. We have set out that in order to build the multiple regression model we need to compute a Monte Carlo simulation, so that we can obtain the conditional probabilities associated to a certain set of values for the external actions. It is with these results obtained through simulation that we will fit a multiple regression model. However, the straightforward question could be *why* we have to use a Monte Carlo simulation, since as soon as the external actions are fixed the final state of the windmill could seem to be fixed as well. The explanation is that, in fact, once the external actions are fixed, *the final situation of the windmill is not fixed*. In the same way that has been done in similar vulnerability studies (for instance, see [6]), there are certain parameters involved in the computations that cannot be assumed to be known constants because they are random variables. For example, in our case, the clearest example of that is the yielding limit f_y for the steel of the tower. This parameter is the key one to evaluate whether the tower can resist the forces it is under. However, its value cannot be assumed to be constant, since there is an evident variability inherent to it. In other words, in case we fix the boundary conditions we do not know yet what the final situation for the windmill will be, since we do not know the value for these random parameters involved in the computations of the model. In fact, these parameters are random variables that can be described through a probability distribution. For example, a log-normal model could seem suitable for the yielding limit f_y we have mentioned. The distributions associated to every parameter are described in this chapter (see section 1.4), and as it can be checked they have been chosen according to the correspondent bibliography.

Once we have pointed out the presence of random variables in our physical model for the behaviour of the windmill, it is straightforward to see that once the external actions are fixed the final situation of the windmill is unknown. Here is where the Monte Carlo simulation needs to be defined; given that there are several parameters whose value is a random variable (with a known distribution), it is virtually impossible to determine what the conditional probabilities to be in the three states are, since we have no analytical methodology to take into consideration all the random parameters at the same time. Let's imagine we fix a set of values for the external actions: even though the mathematical model we have built to determine whether the windmill breaks or not can be applied, it is still dependent on the random parameters, which, by definition, are aleatory. Therefore, given the fact that there are

random parameters, depending on their value the final situation will be one or another. To address this situation, the Monte Carlo simulation is defined (see references [36] and [9]).

In order to develop the reason why we have used the Monte Carlo simulation we could use the following example. Let's imagine we have a box full of three-coloured balls. This box, however, is not transparent and we are not able to determine the percentage of balls of each colour. In order to evaluate this percentages it seems intuitive that the easiest way would be to start to take balls out of the box and counting the amount of balls of each colour. In the end, we could estimate the percentages of each colour by dividing the number of balls of each colour over the total number of balls we have taken out. That is exactly what the Monte Carlo method is about. The problem we currently have with the windmill is, in fact, the same: we have a model dependent on several random parameters, so a priori we do not know how to estimate the probabilities to be in the three states once the external actions have been fixed. In order to estimate these three probabilities, what we will be doing is simulating values for the parameters and applying the mathematical model repeatedly until we have a *high enough* number of simulations. Coming back to the example of the box, it is extremely obvious how the accuracy of the percentages will increase as we increase the number of balls we take out. Let's imagine we only take out three balls: even though we could have an idea of *what is likely to be in the box*, our results would not be accurate, whereas in case we took, let's say 1000 balls, the outcome would seem much more reliable. Moreover, as more balls are taken the resultant percentages tend to converge to the real values, so the results become gradually less dependent on the outcome of the next balls. Analogously, in the case of the windmill the more simulations are done the higher the accuracy becomes. Moreover, the results for the probabilities have to converge in the end to the real values, in the same way as in the example. However, this is where the main problem of these kind of simulations come: as we increase the number of simulations, even though the accuracy is increased, the computational cost is increased as well. According to the MatLAB code that we have built, a simulation takes approximately 0.03 seconds. Therefore, the more simulations we make, the higher the accuracy will be, but the higher the cost will be in terms of time. Moreover, given that our time is limited, the following trade-off is presented: is it better to have few sets of values of external actions with huge amount of simulations, or is it better to have more sets of values but with a smaller number of simulations? The answer to this question is that there is probably an optimal combination which provides the maximum accuracy for the final results. However, since we do not know what the optimal combination is, the following solution has been considered: for every set of values we have considered 300000 simulations. In total, we have considered 100 sets of values. With regard to the term *set of values*, we will also be calling them *points*, since each *set of fixed external actions* generates one point of the regression (which is defined with the probabilities of being in the three states we have defined). Overall, each point has taken an average computation time of 3 hours, so in the end the computation time has been approximately 13 days (300 hours).

However, one comment has to be made with reference to the Monte Carlo simulation. Again let's imagine the same example of the box with the balls, but let's imagine there is an extremely low percentage of a certain colour of balls. In that case, even if the amount of balls that we took out the box was high, the results would not be accurate. Let's imagine the percentage is, for example, 0.001%, and that the total balls that we take out is 100. It is easy to see that by no means will we be able to estimate properly this percentage, since either out of the 100 balls there will be no balls from the low-probability colour so the estimated percentage will be 0%, or either we will be "lucky" to have at least one ball of that colour so the estimated percentage will be 1%. Therefore, it is easy to see how this extremely low probability situations generate inaccurate results, which make us either have to increase the number of simulations (therefore increasing the computational cost) or either to have to deal with huge potential error. The main problem with respect to this situation is that, in fact, both probability equal to zero or one are impossible to achieve in practice, since by definition *nothing*

is impossible, only highly improbable; in other words, the values "zero" and "one" are the equivalent to the $-\infty$ and ∞ in the real scale, they are non-achievable values.

For the reasons we have just set out, there will certainly be problems in several simulations. Going back to the windmill, let's imagine we fix the following external conditions: wind speed equal to 1 m/s, no swell sea at all and extremely low fatigue of the structure. For this case, it is painfully obvious that regardless of the values of the random parameters we will not obtain collapse on the tower. In other words, it is *practically impossible* to have a complete destruction of the windmill when there is no storm at all and there is no fatigue on the structure. Therefore, even though we carry out 300000 simulations for this set of values, it is highly probable that we obtain zero "collapse at the tower" (or even though we obtained one among 300000, this result would not be accurate). It is for these situations that the *Sample Importance Re-sampling* has been used.

The *Sample Importance Re-sampling* procedure cannot be explained with the box full of balls analogy that easily. The main aim of this procedure is to *force the improbable situations to occur* in order to be able to evaluate them, but *be aware of the modifications that have been done to the model to make them appear* in order to analyze the results properly. This definition, even though it is not particularly rigorous, provides an intuitive idea of what has been done. Going back to the case of the windmill where there could be no collapse at all, the way of *making the collapse occur* could be done by modifying the yielding limit f_y of the tower. In plain words, the way to have total destruction of the windmill under very soft external actions is that the resistance of the steel is low enough. Therefore, what we will do is modify the probability distribution of the steel in order to have a balanced result on the simulations. After that, however, the results we found on the simulation will have to be modified *according to the changes that we have done on the probability distribution of the resistance of steel*. For more information about this methodology, we have to refer to [20] and [5].

With reference to the conditional probabilities and addressing the regression, the fact that the terms we are trying to predict with the regression are probabilities introduces a problem: probabilities are not real-scale-numbers, since they are bounded between zero and one. Moreover, these three conditional probabilities are not independent, since they always sum one. Therefore, according to [29], a statistical treatment will have to be applied to the experimental data in order to build the regression. In other words, a conventional regression model provides a prediction for variables that are real-scale numbers, which is not the case. Consequently, given that the probabilities are not in the real scale we have to apply a methodology, which is the compositional treatment, in order to address the regression model construction. This methodology was proposed by Aitchison in 1986 (see [21]), and consists on a transformation of the probabilities into coordinates, which are suitable variables to fit a conventional regression model.

1.2 Objectives

Once the methodology has been set out, we can set the main objectives of the present project. In fact, the ultimate objective is unique, and consists on the construction and further analysis of a vulnerability model. However, several goals have to be accomplished in order to build such model successfully.

1. First, a physical model has to be proposed for the behaviour of the model. In other words, we need to build a mathematical model based on physical equations which can evaluate the stresses on the key points of the windmill in order to quantify the damage on the structure. This model will have to take into consideration that the blades are rotating as long as the wind speed is below 25 m/s, and that the windmill is stopped for safety reasons over this wind speed threshold.

2. In the present model, several parameters will be assumed to be constant (for example the value for gravity on Earth, equal to 9.8 m/s^2), whereas there will be other ones which will be treated

as random variables (see further development of such parameters in section 1.4). These random variables will have to be characterized, so the correspondent distributions will have to be determined.

3. In order to fit a regression model, experimental data has to be obtained through Monte Carlo simulation. This simulation will be computed in MatLAB, and will provide the conditional probabilities to be in the three states we have defined for the different sets of external actions that we fix. Therefore, the third objective consists on programming the correspondent code in MatLAB so the simulation can be carried out.

4. The previous simulation will require using the Sample Importance Re-sampling methodology, according to [20] and [5]. Consequently, we will have to include in the MatLAB code such procedure in order to maximize the accuracy of the results.

5. In order to address the regression, the predicted variables and the explicative variables will have to be treated because their domain is not the real scale. Otherwise, the regression model would certainly be inaccurate because it would not be taking into consideration the nature of the data we are dealing with.

6. Finally, once the previous objectives have been reached, the regression model can be built. Such regression will address the fitting of the simulated in order to obtain a general model which can predict the probability to be in the three possible states for whatsoever external actions.

1.3 Hypotheses

According to the resources that we have and the scope of this minor thesis (TFG), several simplifications have to be made in order to end up with a *reasonable* problem. In other words, in case no simplifications were made, the cost in terms of time and computational cost would make the present project an unaffordable problem. Therefore, it is important to set out the limitations of the study in order to analyze the accuracy of the results. These hypotheses have been divided into groups according to the part of the windmill they refer to. Before setting them out, however, we have to say that during the project there will be certain details where we will make additional hypotheses.

1.3.1 Basic hypotheses regarding the project

The following hypotheses are probably the most important ones, because they define the approach we have taken to tackle the problem of the vulnerability of the windmill. As it can be seen, they can be understood as a further explanation of the terms appearing on the title.

1. First, we will be working with an off-shore windmill whose characteristics will be specified in sections 1.3.2, 1.3.3, and 1.3.4. Even though we have not focused on a particular wind plant, the present project has analyzed a windmill that could perfectly have been on the "Horns Rev I" plant in Denmark (see [1] and Figure 1.1). That means that both the geometry and environmental conditions (wind and sea) have been considered to be similar. We have assumed the windmill to be similar to a real one in order to be able to compare the outcome of the project with the actual results that have been obtained in reality. However, we have to clearly state that according to the definition of the windmill we have made at the present chapter, as well as the simplifications that have been made in addition (and which will be developed right after), our windmill is a *theoretical model of the real one*, even though their behaviour could be claimed to be similar to the real windmills at Horns Rev I. In Figure 1.2 we present an image of Horns Rev I.

Figure 1.1: Geographical location of the Horns Rev I wind farm in Denmark (*source: Google Maps, Google Inc.*).

Figure 1.2: Photograph of Horns Rev I wind farm, where we can see the type of off-shore windmill we will be considering in the present project: 3 blade off-shore windmill with a hub height of approximately 65 meters above sea level and a 2 MW power (*source: http://nortus.pinger.pl/m/2173121*).

2. Second, we have to state that the present project will focus on the structural vulnerability of the windmill, so no comments will be made about the mechanical-electrical behaviour. In case a more comprehensive study was to be made, we should certainly take into consideration all the physics associated to the operation system of the windmill. However, from our point of view the windmill will be "at service state" regardless of whether its electrical devices are working or not, since we will only be focusing on the structural stability of the structure.

3. No comments will be made about the foundation system of the windmill. As it will be developed in the next chapter, we will not consider the possibility of fracture of the soil on the foundation nor erosion at the base of the tower. In other words, we will be assuming that the soil and the foundations of the structure are able to cope with *any* force that is applied on the windmill. This hypothesis could seem odd, since it could seem that as long as the soil under the foundation is able to resist the forces of the tower it is impossible to consider its failure. However, this assumption is no longer obvious when we consider forces which may vary its direction (waves and wind), may be cyclical (waves) or may be able to generate erosion at the base of the tower (waves). The reason why we have not considered this possibility is that in case it had been included in the model the problem might have become unaffordable in terms of complexity.

4. It is important to emphasize on the term *pseudo-static* we have used in the title. The term *pseudo-static* refers to the fact that we will not be considering resonance on the windmill. In fact, resonance might be an important detail to study regarding the global vulnerability of the structure (see [31]), since as long as we are dealing with dynamic forces (wind, waves) it seems intuitive that it may play a relevant role with respect to the stability. However, this part of the study will not be carried out, so no further considerations on the dynamic component of the forces will be made.

1.3.2 Hypotheses made on the blades

1. A *stall type* of windmill has been assumed, which means that we have considered that the blades cannot regulate their torsion with respect to the directrix in order to modify their behaviour. In other words, the torsion of the blades is fixed and their orientation is always the same (see reference [31] for further information). Nowadays it is more common to find a *pitch system*, which enables the blades to change their orientation; nevertheless, by introducing that extra degree of freedom the problem would have become much more complex.

2. No *conicity* has been assumed on the blades. The term *conicity* stands for the angle between the blades and the vertical axis, according to [31], as it has been illustrated on Figure 1.3. Assuming no *conicity* is equivalent to consider that the blades are vertical, so the rotation circle defined by the blades is on a vertical plane. This *conicity* is usually introduced in order to avoid any problems regarding the interaction between the blades and the tower. However, by introducing this angle in the formulation the problem would become more difficult while its impact would have been limited. Therefore, we have neglected this little orientation of the blades towards the wind.

3. The blades have been assumed to be perfectly connected to the hub, which means that the blade's behaviour can be assimilated to a corbel (because it is perfectly fixed on one extreme and free on the other one). We haver to say that in fact the union with the hub is not usually that rigid, since by doing that the moments on the hub become more important. However, by making this assumption the structural problem becomes much simpler (even though the results will be somehow conservative because the moments we will find will be higher than the actual

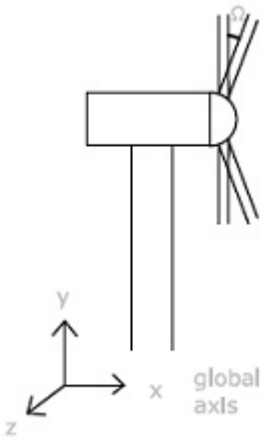

Figure 1.3: Scheme of what *conicity* means to illustrate the simplification we have made (*source: self elaboration*).

ones). For further studies it could be studied to what extent the simplification of perfectly rigid union with the hub is accurate.

4. The rotation speed of the blades, ω, will be assumed to be constant and equal to 12 rpm (values obtained from [31]) in case the windmill is working. That hypothesis is very close to reality, since most of the windmills are designed to work at a constant speed. As long as the rotation speed for the alternator is constant, the rotation speed for the blades ought to be kept as constant as possible. Moreover according to [37] and [31], by keeping the wind speed constant the energetic efficiency is maximized.

5. The blades are usually made of several materials, including steel and high resistance fibers (typically carbon fiber), according to [35] and as it can be seen in Figure 1.4 . In case we made a deep analysis on the behaviour of the blades, we should definitely quantify the aggregated resistance of the union of these different materials. However, in our study we have made the following simplification: we have used an *equivalent yielding limit*, which is to say that we have understood the blades as an element made of a single *equivalent material*. By doing this, the breaking criterion has been extremely simplified, even though we have certainly lost accuracy. However, according to the available time that we have had this solution seems admissible.

Figure 1.4: Image of the different materials involved on the blade (*source: www.evwind.com*).

6. Referring to the geometry of the blade, we have to mention that the design is usually made in order to maximize the energetic efficiency; in other words, the shape for the blades is defined so that the performance of the windmill is optimized. However, introducing this variation of the bade's shape would have limited a lot our computations. Therefore, we have made several simplifications:

   (a) When it comes to model the force of the wind on the blade, we have assumed that the exposed area to the wind is constant. In fact, the blade section at the hub is bigger than at the edge, because mass is deliberately concentrated near the hub. However, we have assumed the chord to be constant, so the modelling of the force of the wind on the blade is easier to calculate. A schematic drawing about the blade we have considered is presented in Figure 1.5.

   (b) Regarding the blade as a structural part where to compute efforts and deformations a further simplification has been made. We have already stated how difficult the shape of the blade is to model. Therefore, since the section varies along the blade, the parameters such as the weight or the inertia are not constant, and should be modelled according to this variable nature. However, we have made the simplification to study the structural behaviour of the blade as if it was a beam, so with a constant weight an inertia. As it can be seen in Figure 1.5, we have assumed a constant area exposed to the wind (which is defined with a constant value for the chord), as well as a constant section which generates a constant inertia. By doing this, the blade behaviour can be studied as a beam.

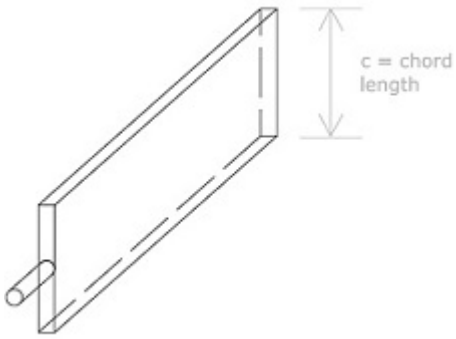

Figure 1.5: Scheme of the simplified blade we have used in the parametrisation of our model (*source: self elaboration*).

   (c) It is important to state that there are further hypotheses regarding the geometry of the blade, but they have been explained in Appendix A, where the calculation of the forces of the wind on the blade have been fully characterized. The reason why they have been included in the Annex and not in the present chapter is because they cannot be set out straight away without talking about the procedure we will be carrying out to compute the forces of the wind. Consequently, since these hypotheses are very particular details that are easier to explain in the Annex, we have thought it is more appropriate to explain them there.

7. With reference to the structural analysis, we have to set out an overview about the situation we will be dealing with. Our simplified blade, which we have assumed to behave like a beam, will be 40 meters long, according to the dimensions of the windmills at Horns Rev I plant in Denmark

(see [1]). The chord has been assumed to be constant and equal to 3.5 meters. This value is the maximal value of the chord for the blades of the Horns Rev I windmills, according again to [1]. It is arguable whether a smaller value could have been used, since by using the maximum value for all the blade will provide quite a conservative approach. This is in fact, a flaw of the model, because a deeper analysis about what the optimal chord length should be could have been done. However, according to the rest of hypotheses that have been made in the project, we believe that the present hypothesis is admissible, even though we should definitely point out that in case further studies were to be made they should consider the uncertainty associated to the value we have used. A simplified scheme of the blade we have just defined is presented in Figure 1.6.

8. The resultant force on the blades will be assumed to be on the directrix of the blade; in other words, no torsion will be assumed on the blade because the force supplied by the wind will always be on the directrix. The present hypothesis seems reasonable as long as we suppose a situation like the one illustrated in Figure 1.6.

Figure 1.6: Scheme of the blade we have used in our model, according to the simplifications that have been set out in this chapter (*source: self elaboration*).

9. We will assume that the hypotheses of the resistance of materials theory are applicable, which means we will assume that the deformations the blades will eventually have are small (so no second order analysis will be required). In fact, this hypothesis should be verified in the end. However, it seems intuitive that the deformations of the blades will not be big enough to have to consider the great deformations theory.

10. Modern windmill blades tend to concentrate the mass of the blades near the hub. By doing this, stability is improved, since as long as there is a higher amount of mass rotating far from the center of the hub the potential problems become more dangerous. However, we have assumed the blade to have a constant chord, so the weight has to be considered as an uniformly distributed force. In other words, since the blade of our model has a constant shape, the weight has to be uniformly distributed. The procedure we have followed has been the following one: we have considered the global weight of the blade, equal to 6.5 tones (according to [1]), and divided it over the 40 meters of the blade, so we have found the weight per unit of length.

11. The inertia of the blade, needed to estimate the deformed shape of the blade under wind stress, has been analyzed as if the blade was a tube. In the past hypotheses we have always drawn the blade as rectangular and massive, in terms of analyzing the behaviour when there is wind. However, even though these hypotheses are correct with respect to modelling the forces of the wind, they do not fit when considering the deformation of the blade. As it can be clearly seen in Figure 1.4, when analyzing the blade's structural behaviour, in terms of deformation, a tubular shape is the one which seems more appropriate. In fact, this hypothesis is clearly false in practice, since we have already stated how the transversal section of the blade varies along

the blade. However, since the blade has a significant hollow part, simplifying the blade as a tube it has seemed to be the most adequate solution.

1.3.3 Hypotheses made on the hub

1. With reference to the hub (which will be also regarded as nacelle), we will assume it as a *box* whose only function is to transmit the efforts from the blades to the tower. In fact, the nacelle is where the electrical devices are installed, so given that we are only focusing on the structural vulnerability we will not be interested in what may happen to it. With reference to its structural vulnerability, there are two critical points which should be at least mentioned. First, there are the junctions with the blades; these points, however, are already studied with the blade analysis, since the weakest point of the blade is at the union with the nacelle (see Chapter 2). Second, there is the junction between the nacelle and the tower. This union is usually done with screws, even though no further information has been found with respect to this detail on the references. Overall, since no regard will be made with reference to the mechanical-electrical devices, we will study the nacelle together with the tower. In other words, no comments will be made regarding the vulnerability of the nacelle itself.

2. The nacelle will be assumed to have its gravity center aligned with the directrix of the tower, that is to say that no extra moments will appear on the tower as a result of a misalignment of the nacelle. The mass of the nacelle is approximately 79 tones, according to [1], where we have to sum the mass of the 3 blades (20 tones in total). In case this hypothesis was inaccurate, it would not be difficult to introduce on the model the eccentricity of the nacelle with respect to the tower; however, since the information we count on is limited with reference to this topic, we have made this hypothesis which provides a simpler approach to the problem.

1.3.4 Hypotheses made on the tower

1. The tower has been simplified as a 5 cm thick cylinder. Nowadays it is also usual to see slightly conical towers; however, the simplification we have made is perfectly aligned with other hypotheses of the model, and provides a good result despite its simplicity. In Figure 1.7 we present a transversal section of the tubular profile of the tower, with the principal magnitudes we will use in our calculations.

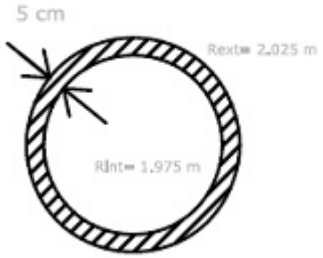

Figure 1.7: Transversal section of the tubular profile of the tower, which we have simplified as a cylinder (*source: self elaboration*).

2. The tower is 73 meters high, even though the first 12 meters are under water level. Therefore, the total height can also be expressed as 61 meters above sea level. It is important to point out

that this height level is the level of the hub, so the center of rotation of the blades. The principal magnitudes referring to the geometry have been illustrated in Figure 1.8.

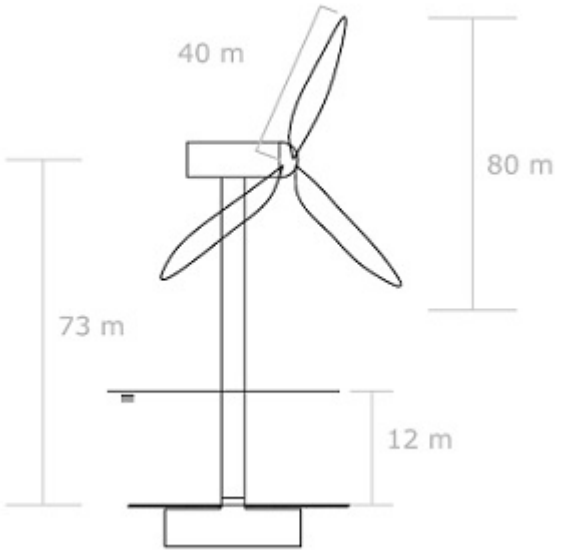

Figure 1.8: Principal magnitudes of the windmill we have studied. These magnitudes have been taken from the real dimensions of the windmills of the off-shore wind farm Horns Rev I in Denmark, according to [1] (*source: self elaboration*).

3. Since no information has been found regarding the steel used in Horns Rev, we have set a 355 MPa resistance steel. It is relevant to highlight a few comments about this topic. A vulnerability analysis, as it has been already seen, is done for a determined windmill, so no choice has to be made with reference to the steel or the resistance because it has been already fixed. Indeed, the main idea of these kind of studies is to evaluate the risk a certain designed windmill will be under, so no dimensioning choices have to be made in a project like this. Second, we have to refer to the fact that no information has been found with respect to the steel used in Horns Rev I. Therefore, we have assumed a conventional steel with a yielding limit of 355 MPa (according to the Spanish nomenclature -see [39]-, a steel S355 has been used). Finally, with an off-shore structure like the one we are analyzing, we have to say that several studies should be made in order to address the corrosion problem. However, we have not considered corrosion on the present study, so no further comments will be made regarding this topic, even though it is a detail that should be certainly studied in future endeavors. Overall, with reference to the steel, we have to say that the only data we will need is the yielding limit, so in the present section we have only focused on the justification of this particular value.

4. According to what has been stated for the nacelle, the mass of the blades and hub (20 + 79 tones) will be regarded as a punctual mass on top of the tower, and which is aligned with the directrix.

5. Just like we have presented with the blades, the theory of resistance of materials will be applied, therefore assuming little deformations on the tower. In fact, this hypothesis seems very intuitive, since it does not seem reasonable to consider extreme deformations on the windmill even though under strong storm conditions.

6. Referring to the structural analysis, the tower will be regarded as a corbel, which means that we will be considering that one extreme is perfectly fixed (so the mathematical boundary condition will be that the angle is zero on that extreme) and that the other one is free (so the mathematical condition will be that the moment is zero).

7. The tower's mass is approximately 360 tones (this result can be easily checked by considering the 5 cm thick and 73 meter high cylinder's volume and multiply it by the steel density).

8. With reference to the inertia of the tower (to calculate the deformed geometry), we have assumed that the tower is tubular, so the conventional formula for a tube has been used, according to [32].

1.3.5 Hypotheses on the wind

1. The wind speed is a monotonously growing function of height, which can be modelled with the expression proposed in [3]. By assuming this, we are accepting that the wind speed is very close to zero for low heights and that continues to grow as we increase the height. This wind speed distribution has been illustrated in Figure 1.9, and the expression is presented in equation (1.1).

$$v = v_{hub} \cdot \left(\frac{z}{z_{hub}} \right)^{0.2}, \tag{1.1}$$

where v_{hub} and z_{hub} stand for the wind speed and height at the hub and z refers to the height we are studying.

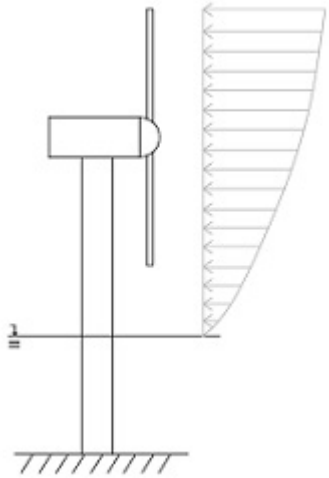

Figure 1.9: Very basic scheme of the wins speed distribution with height (*source: self elaboration*).

2. This wind speed distribution is constant for a certain fixed height. In other words, if we consider a horizontal plane at a certain height, all the points are moving at the exact same speed, which means that the wind speed distribution has been simplified significatively.

   So far, from these two first hypotheses it is important to point out that as long as v_{hub} is known (the wind speed at the hub's height), the wind speed distribution is fixed. First, from this wind speed we can obtain the vertical distribution according to [3] (first hypothesis). Furthermore, we have set that the wind speed is constant once the height has been fixed, so the wind speed field is known (second hypothesis). This proposal, though being consistent, underestimates the

potentially dangerous effect of turbulence, which is the variability in the wind speed distribution. In order to address this drawback of the past hypothesis, further considerations have to be made, because it is highly important to introduce the impact that turbulence may have on the general operativity of the windmill.

3. In order to address the turbulence problem, we will allow the position of the resultant force of the wind on the windmill to be aleatory. By doing so, we are considering that the wind speed distribution cannot be symmetric, so that it can be variable. This position of the resultant force will be defined through two random variables we have named *horizontal and vertical eccentricities*. These two variables will be characterized thoroughly in section 1.4 section, and its use will be fully developed in Chapter 2. However, it is relevant to keep in mind that turbulence will be taken into consideration.

4. As it has been illustrated in Figure A.1, the *zero wind speed* will be assumed to be at the *calm water level*, which is the level without any waves. As it will be seen in Appendix C, by considering the waves the sea level will vary. However, even when there are waves, we will stick to the hypothesis that the starting point for the wind speed is at the calm sea level.

5. The blades will be considered to behave the same way, that is to say that the force of the wind on the blades will be assumed the same on all three blades. There are a few comments to be made regarding this hypothesis. So far, we have set out how wind speed varies with height, so as long as the blades cover a 80 meter height range (see Figure 1.10), the forces on the blades should vary with the rotation, because wind speed is not constant with height. However, in order to simplify the calculations on the blades, we will assume that the wind speed at the hub is representative of the wind speed for all the rotation circle, as it has been illustrated in Figure 1.11.

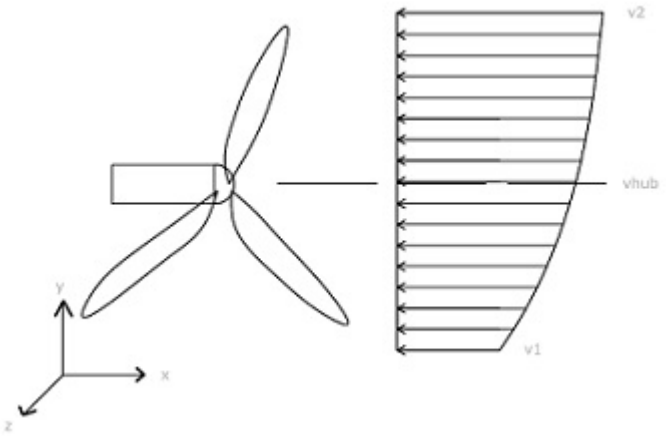

Figure 1.10: Real wind speed distribution at the rotation circle, according to the first hypotheses we have made. It is easy to see how modelling the force on the blades when they are moving becomes extremely complex (*source: self elaboration*).

6. By considering an uniform wind speed field at the rotation area of the blades, we can infer that the wind speed at every blade is the same, so that all the exposed area of the blade will be under the same wind speed conditions, as it can be seen in Figure 1.12.

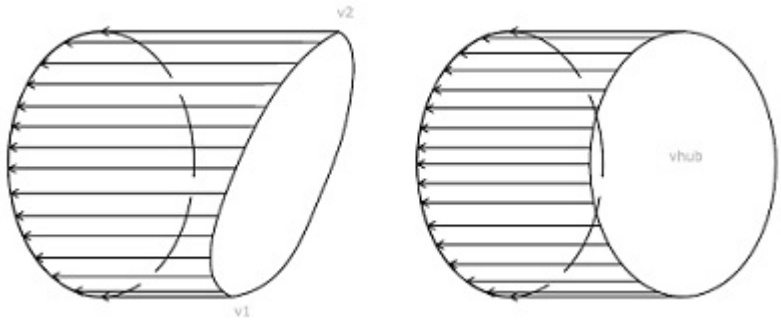

Figure 1.11: Simplification of the wind speed distribution at the rotation circle (*source: self elaboration*).

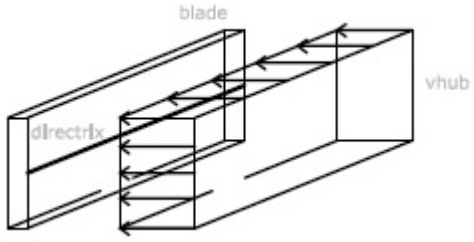

Figure 1.12: Wind speed distribution for the three blades of the windmill (*source: self elaboration*).

7. The wind speed will be assumed to be unidirectional, which would be equivalent to say that *all the wind affecting the windmill has the exact same direction*. Moreover, the windmill stays always oriented to the wind (by definition). In case further studies were to be made, they could include certain variations on this hypothesis, even though it is not unreasonable to assume that the wind speed direction is the same on the whole area of the windmill.

8. Even though we have always implicitly assumed it, we have to state that we have only focused on the horizontal component of the wind speed. It is highly intuitive that the vertical component of the wind speed is extremely smaller than the horizontal one, and that its potential effect on the vulnerability is very limited. According to [37], the vertical component will be neglected in the present study.

9. The wind is assumed to be a global mass of air which comprises all the windmill. More specifically, we are assuming that all the rotor circle is under the same wind conditions, and that the wind speed field is *infinite*, which means that it is extensive enough to assure that all the parts of the windmill are under the same wind conditions.

10. No interference of other windmills is considered. The present study is aimed to model the behaviour of an off-shore windmill that deals with a *free* wind flow. This hypothesis does not mean that the conclusions that we will obtain are incorrect when considering the windmill within a wind farm, but we have to set clear that in case other windmills were close enough to interfere on the wind speed conditions, additional calculations would be required, since neither the operativity nor the vulnerability would be the same. For more information about this topic we have to refer to [31]. To illustrate this interference situation we have presented Figure 1.13; with this photograph it seems easier to explain what windmill interference is about.

Figure 1.13: In this photograph we have tried to introduce the idea that the presence of other windmills may interfere on the activity of a particular windmill belonging to a wind farm (*source: http://nanosync.wordpress.com/*).

1.3.6 Additional hypotheses regarding the windmill

1. With reference to the orientation of the windmill, we have to say that in order to maximize the energetic production the windmill has to be oriented towards the wind. According to [31], the system to orientate the windmill can either be *mechanical* or through an engine. The term *mechanical* refers to a type of windmill which orientates by itself towards the wind because of its mass distribution. However, most of the current windmills change their orientation with an engine (for further information see [31]). With reference to our model, we will be assuming that the windmill changes its orientation with an engine, so no *bullwhip forces* can take place. The term *bullwhip situation* refers to the transient state for the wind orientation in which the hub oscillates until the stable position is found. Nowadays most of the windmills have an engine-based system, since the other system generates peak efforts which may end up damaging the windmill.

2. Corrosion has not been taken into consideration, even though it would be a good detail to consider in future studies. Since the windmill we are studying is off-shore and most of the materials have a metallic component, it seems reasonable that the corrosion on the tower should be taken into consideration. The main effect of it is that the resistance of the tower should not be assumed as uniform because the part in contact with the water is clearly under worse conditions than the rest of the tower.

3. The windmill operates normally under a wind speed below 25 m/s. Above that level, the windmill stops because operating as usual could result in serious damage on the structure. This threshold has been obtained from reference [4]. Several further comments will be made referring to the windmill operativity in Chapter 2, because it is easy to see that even though this division in active/inactive windmill seems reasonable and consistent with the references, uncertainty arises with respect to *what happens when the wind speed is exactly 25 m/s.*

4. The calculations have been made considering a V80-2.0 MW system (according to the Horns Rev I wind farm, information provided by Vestas (see reference [4]).

5. The distance to the shore is assumed to be in between 14 and 20 km, just like the Horns Rev wind farm in Denmark. In fact, this location could be different, since this exact information will not be explicitly used at any point. However, provided that we have compared our results to Horns Rev I, as well as we have considered similar wind and storm conditions (see reference [1]), the results that we obtain have to be understood to be in a location similar to the one we have assumed as a reference.

6. Finally, there are a few parameters whose value is constant (for example the blade length, blade chord, gravity on Earth, etc.). These values are presented in table 1.1. There is no reference associated to these values, since either they have been widely assumed or they have already been defined in the present chapter.

Name of the parameter	Value	Units
Gravity	9.8	m/s^2
Air density	1.225	kg/m^3
Steel specific weight γ_s	78500	N/m^3
Water depth	12	m
Hub's height above sea level	61	m
Water density	1000	kg/m^3
Blade chord	3.5	m
Blade length	40	m
Blades mass (3 blades)	20	$Tones$
Hub mass	79	$Tones$
Tower mass	360	$Tones$
Distance to the shore	$14 - 20$	km
Blade inertia (tube)	1.2568	m^4
Tower inertia (tube)	6.5918	m^4

Table 1.1: Constant values of the model.

1.4 Parameters of the model

With reference to the parameters involved in the model, we have to set clear that we have divided them into two groups. On the one hand, there is a group of constant parameters, whose value can be assumed to be constant. These values have been already set in section 1.3. The explanation for assuming its value as a constant is that either the impact of considering them as random variables on the final outcome of the model is very limited, or their dispersion with respect to the mean value is practically zero. The second group of parameters will be fully characterized right after, and contains all the parameters involved in the model that cannot be treated as constants. With regard to these values, it is important to say that it is often easy to find their average values on several references (for example, see [39] for the yielding limit for the steel). However, in these same references there are certain comments about how to *consider a security margin* that takes into consideration the potential dispersion of the actual value. It is from these comments that we can be able to estimate the dispersion of these variables.However, even though it may be inferrable from the references that several parameters are in fact random variables, it is not straightforward to obtain what the actual distribution is. If we look carefully at the parameters we are estimating, we will see that there are several features that the distributions we are looking for must have. First, they have to be unimodal, since it seems intuitive that there has to be a *most likely value for the parameter*, and that this value has to be unique. Second, this probability distribution has to *match the scale of the variable*. For example, when talking about the yielding limit for the steel we cannot use a real-scale distribution because this parameter is by definition, non-negative. Nevertheless, once this comments have been made, it is still not direct to infer a probability distribution for a certain parameter. In fact, once we have set out our probability distributions it would be arguable why there cannot be other probability functions which describe in a more accurate way the real behaviour.

In total, we have considered 11 random parameters in the model, 8 of which have a log-normal distribution, 2 a logit-normal distribution and 1 a uniform probability distribution. These distributions will be justified right after, as well as the their parameters.

1.4.1 Log-normally distributed parameters

The parameters with this distribution have in common that they are non-negative parameters. Therefore, a normal distribution cannot be considered because it would not be consistent with the natural domain of the parameters we are dealing with. However, it is important to remark that there are certain references which implicitly propose a normal distribution as appropriate, such as [39] for the yielding limit of steel: in fact, as long as the parameter we are studying is *far enough from zero*, the log-normal and normal models provide a very similar approach.

The log-normally distributed parameters of our model can be divided into two groups. First, there are the resistance parameters of the tower and the blade (yielding limits and Young modulus), which from now on will be regarded as *resistance parameters*; these are the values that have been often assumed to be normally distributed, but that since they have to be non-negative values the log-normal model seems more adequate. Second, we have the values used for the computation of the swell sea, where we have to refer to [18]. These two groups of parameters will be presented separately because the characteristics of the distributions have been found through different procedures.

Resistance parameters

The parameters we have modelled are both the yield limit for the steel of the tower and the material of the blade, as well as their Young Modulus (so 4 parameters in total). With reference to the characterization of the distributions, we have to recall that a log-normal distribution is fixed with

its parameters μ_{log} and σ_{log}, according to [17]. In the first place, we have to say that we could find estimations for both the average value and standard deviation from the bibliography (see [39] for the steel and [35] for the blade). However, since we have considered the fatigue as an explicative variable, it seems reasonable that these distributions have to be dependent on it. Let's develop a little bit more this concept: it seems intuitive that in case we are dealing with a highly fatigued structure, the average value for the resistance will be significantly lower than when the structure was built. In other words, the average resistance of the tower and the blade can be assumed to decrease as the fatigue increases. Moreover, it seems that as the structure becomes more fatigued, the uncertainty associated to the exact value increases, so the standard deviation could also be assumed to increase. However, intuitive as this hypothesis may seem, we have not found an accurate expression to model this behaviour, so a simple method has been considered. Therefore, even though the methodology we have followed provides a consistent solution, it could be improved in further studies.

The value for each parameter provided by the references (see table 1.2) can be assumed to be the median of the distribution. In fact, since no distribution has been proposed on the references we have used (see [41] and [35]), it is not clear to determine whether the value we get is the average value, the median, or the mode. Let's analyze this concept. From the definition of this value, it seems more intuitive to understand the value as the 50% percentile rather than the average value of the distribution. It would be arguable, though, whether this value could also represent the mode. However, the potential error associated to this judgement has to be put in context; since the values we are dealing with are not close to zero, the log-normal approach provides an extremely similar result to the outcome we would have obtained in case we had used a normal distribution. Therefore, even though for a log-normal distribution the average value is different from the median and the mode, these three values will be very close as long as they are far from zero. Consequently, even though we will assume the value from the references to be the median of the distribution, the results that would be obtained in case we had reached a different conclusion would be absolutely comparable. According to [17], we have to state a few important comments; first, a log-normally distributed variable is the one whose logarithm follows a normal distribution. Second, since the logarithm has a normal distribution, it is easy to verify that for that distribution it is true that the average value is equal to the median and the mode. Finally, since the logarithm is a bijective transformation, the median for the normal distribution will be the logarithm of the median of the log-normal distribution. For the reasons we just set out, we can infer that the first parameter for the log-normal distributions μ_{log} is:

$$\mu_{log} = \log X,$$

where X stands for the value we have obtained from the references. Summarizing, what we have just done is obtain the first parameter of the distribution through the data that we have from our references. Overall, we have understood the value from the references to be the median of the log-normal distribution, so once we apply the logarithm this value coincides with the average and the mode, so it is the first parameter of the associated normal distribution μ_{log}.

With reference to the deviation σ_{log}, we have even less information than the previous case. Therefore, we have assumed a reasonable methodology according to what has been taught in [41]. It is a common practice to assume a 10% reduction for the resistance in order to consider the *potential inaccuracy* of the values. The procedure we have followed is the following one: we have set a three-standard-deviation distance between the median we have obtained from the references and the 10% reduced value. According to [17], for a normal distribution more than 99% probability is within a distance of 3 standard deviations (in particular, the demonstration for this comes from Chebyshev's inequality). When in the structural analysis context we consider this reduction, the result is that *we ensure that the value we are considering generates no risk at all with respect to the variability of the value.* Therefore, this is consistent with the idea that there will be a more-than-99% probability to be

over this value. Therefore, σ_{log} is obtained by imposing that the distance between the median value and the 10% reduced value is 3 times the value σ_{log} we are looking for:

$$\log(median) - \log(0.9 \cdot median) = 3 \cdot \sigma_{log},$$

$$\sigma_{log} = \frac{\log(median) - \log(0.9 \cdot median)}{3}.$$

However, up to now we have not introduced the fatigue. In fact, the distributions according to the previous comments are considering a 0% fatigue. As we commented, these distributions can be assumed to vary as fatigue increases. The procedure we have followed is estimate how the distribution may look like for a 100% fatigue and build a linear interpolation for the cases between 0 and 100%. It is important to point out that by supposing a linear interpolation we are considering the easiest way to approximate the distributions, even though there is uncertainty about how accurate this hypothesis is. This linear interpolation method should be studied more thoroughly in case further studies were to be made.

Referring to the 100% fatigue situation, we have set that the median resistance value decreases until 90% of the initial value (we have not found this specific value on the references, so further research should be made regarding this topic in order to increase accuracy). With reference to the standard deviation, we have set that under extreme conditions the standard deviation is the double of the initial deviation (since no particular reference has been found with respect to this detail, we have assumed a reasonable value). For the reasons we just exposed, the expression for μ_{log} and σ_{log} are dependent on the fatigue, so they are different according to the state of the windmill.

Parameter	Units	median	deviation	μ_{log}	σ_{log}	reference
Steel Young Modulus	N/m^2	$2.1 \cdot 10^{11}$	10%	$\mu_{log}(median, fat)$	$\sigma_{log}(deviation, fat)$	[39]
Blade Young Modulus	N/m^2	$3.75 \cdot 10^{10}$	10%	$\mu_{log}(median, fat)$	$\sigma_{log}(deviation, fat)$	[35]
Steel yielding limit	N/m^2	$355 \cdot 10^6$	10%	$\mu_{log}(median, fat)$	$\sigma_{log}(deviation, fat)$	[39]
Blade yielding limit	N/m^2	$669 \cdot 10^6$	10%	$\mu_{log}(median, fat)$	$\sigma_{log}(deviation, fat)$	[35]

Table 1.2: Characterization of the log-normally distributed resistance parameters.

Swell sea parameters

In order to address the definition of the swell sea parameters, we have to refer to Appendix C, where the mathematical development for the forces of the sea on the windmill has been fully characterized, according to [18]. As it can be seen in table 1.3, the distributions have been already provided in [18], whereas the other two need to be explained more thoroughly so we have referred to the correspondent Annex.

Parameter	Units	μ_{log}	σ_{log}	reference
C_D drag coefficient for swell	non-dimensional	2.5	1.2	[18]
C_M massive coefficient for swell	non-dimensional	2.5	1.2	[18]
water velocity swell wave u	m/s	Appendix C	Appendix C	[18]
water acceleration swell wave a	m/s^2	Appendix C	Appendix C	[18]

Table 1.3: Characterization of the log-normally distributed swell sea parameters.

1.4.2 Logit-normally distributed parameters

The logit-normal model has been assumed for the eccentricities of the resultant force of the wind on the rotor. Ideally, in case the wind speed field was uniform, the resultant force would pass through the centre of the hub. However, even though we have made this hypothesis with regard to the computation of the forces on the blades, it would be incorrect to neglect the possible eccentricities (horizontal and vertical) of the resultant force, since in that case we would be neglecting additional moments on the tower which may not be small. Therefore, we have introduced these eccentricities as random parameters.

Regarding why we have considered these parameters to be random, it seems intuitive that their value is not a constant, since as long as the variability of the wind speed field is aleatory the position of the resultant force on the rotor is variable as well. Therefore, it seems reasonable to model these parameters as random variables. With reference to the characteristics of the probability distribution, it seems reasonable to consider a symmetric probability function with respect to the hub, since it makes sense that, on average, the resultant is applied at the center of the hub. The main point about the probability distribution is that the domain of the eccentricity is limited, since it is obvious that the resultant force of the wind on the rotor has to be somewhere *within* the area of the rotor. Therefore, both eccentricities, horizontal and vertical, have to be in between $[-R, R]$, being R the radius of the rotor. In case the domain was all the real scale, a normal distribution could be proposed. However, since we have these limitations, the logit-normal seems more appropriate. Therefore:

$$e_x \in Logit - Normal(\mu_{logit}, \sigma_{logit}),$$

$$e_y \in Logit - Normal(\mu_{logit}, \sigma_{logit}),$$

The logit-normal distributions, like the normal distributions, are described through two parameters: μ_{logit} and σ_{logit}, which are about to be justified for the parameters we have set out (for more information about this distribution see [23]). We have said that the domain of the eccentricities is $[-R, R]$, so since the radius of the rotor is 40 meters the domain is $[-40, 40]$. However, it is much easier to compute the calculations with a positive domain, so we will set the zero at the left extreme of the radius and will say that the domain is $[0, 80]$. With reference to μ_{logit}, since we have already explained that the center of the hub will be the average point of application of the force, it is straightforward to infer:

$$\mu_{logit} = \text{logit}(40).$$

With reference to the variability of the distribution, we have assumed a reasonable value, since no reference has been found with respect to the potential deviation of this parameter. To estimate the value for σ_{logit}, we have used the Chebyshev inequality (see [17]), and the logical procedure has been the following one. We currently know that the average value of the point of application is at the center of the hub, so at the position 40. Given that we do not know what the potential deviation is, we will assume a reasonable value: we will assume that *the majority of the points* are within 1.5 meters from the hub (so in the central 3 meters of the rotor, both horizontally and vertically). With respect to why we have chosen this value, we have no bibliography where we can refer to, so a reasonable estimation has been made. According to Chebyshev, the 99% of the probability in a normal distribution is within 3 times the standard deviation from the average value. Therefore, what we have done is to consider that the distance between the average value and this "admissible limit value" is 3 times the standard deviation, like what we have done for the log-normally distributed parameters. Expressed in mathematical terms:

$$\sigma_{logit} = \frac{\text{logit}(40) - \text{logit}(38.5)}{3}.$$

Even though the hypotheses we have made provide consistent results with what happens in reality, the accuracy of these distributions is limited. Therefore, it is important to remark that in case any further studies were to be done, they could try to improve the current description of these parameters.

Overall, for the reasons we have exposed above, the eccentricities have been modelled in the following way:

$$e_x, e_y \in Logit - Normal(\mu_{logit}, \sigma_{logit}),$$

where the expressions for μ_{logit} and σ_{logit} have been just set out.

1.4.3 Uniformly distributed parameters

The parameter we have modelled through this distribution needs to be explained; the rest of the parameters had a clear physical meaning, and their distribution could seem intuitive when we thought about the actual meaning of the potential dispersion. The uniformly distributed parameter is the "angle between the wind speed and the swell sea", regarded as ϵ:

$$\epsilon \in Unif[0, 360].$$

As it is fully developed in Appendix C, the presence of the wind induces the formation of waves on the sea, which have the same direction as the wind (and that we have called wind waves). However, at the time to consider the forces on the tower we have to consider the presence of the swell sea waves, which are waves that have been created far away from the windmill and that have no relation with the wind waves. Since no location has been fixed for the windmill, a priori *any* combination of directions is possible, so that is the reason why we have assumed the angle between the wind and the swell sea to have an uniform distribution between [0,360] degrees. It is important to explain the fact that we *have not fixed a specific location*: even though we have taken as a reference the Horns Rev I plant, we have been unable to reach the primary directions for the swell sea and the wind. Therefore, given the very little information we had referring this topic, we have concluded that the best available solution was the present one. By making this assumption of uniform distribution, we are implicitly admitting that in further studies more research should be done regarding this aspect, since the result we will obtain can be improved with the addition of local data from the windmill we are studying. In fact, once the location for the windmill has been fixed and the information regarding the angle between the wind and the sea has been found, this distribution can no longer be assumed to be uniform, because there will probably a dominant wind direction and a primary direction for the swell sea.

1.4.4 Summary of the random parameters considered in the model

The distributions we have considered for the random parameters of the model are summarized in table 1.4.

Name of the parameter	Distribution	Units
Steel Young Modulus	Log-Normal	N/m^2
Blade Young Modulus	Log-Normal	N/m^2
Steel yielding limit	Log-Normal	N/m^2
Blade yielding limit	Log-Normal	N/m^2
C_D drag coefficient for swell sea	Log-Normal	non-dimensional
C_M massive coefficient for swell sea	Log-Normal	non-dimensional
water velocity swell wave u	Log-Normal	m/s
water acceleration swell wave a	Log-Normal	m/s^2
Horizontal eccentricity of the resultant of the wind ε	Logit-Normal	m
Vertical eccentricity of the resultant of the wind	Logit-Normal	m
Angle between the swell sea and the wind speed	Uniform	$^{o}(degrees)$

Table 1.4: Distributions for the random parameters of the model.

Chapter 2

Physical model for the behaviour of the windmill

2.1 Blade analysis

2.1.1 Structural approach for $v_{hub} < 25$ m/s (active windmill)

First of all it is necessary to point out that we will be working with two systems of coordinate axes, the global axes and the local ones. The global axes have been defined at the bottom of the tower in such a way that the x axis is in the direction of the wind, as it can be seen in Figure 2.1. Therefore, these axes have a fixed position once the direction of the wind has been set. It is also relevant to point out that these axes remain the same regardless of whether the blades are moving or not, since even though the windmill is inactive it is still oriented towards the wind.

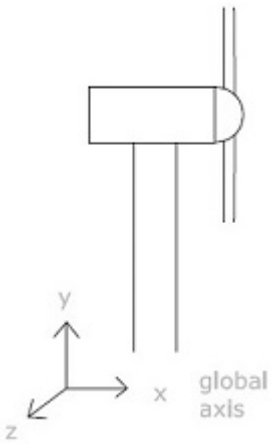

Figure 2.1: Scheme of the global axes location (*source: self elaboration*).

The local axes $\{x', y', z'\}$ have been defined for the blades. As it will be seen later on, all three blades will be assumed to behave the same way, which means that if one of them is expected to break down, the model will result in collapse for all three of them. Consequently, we will only be studying one blade, since the other two will have the exact same behaviour. Since it is much easier to study the blade if the coordinate axes are aligned with its directrix the local axes have been defined, as it can be seen in Figure 2.2. Therefore, this coordinate axes system is defined so that it moves the same way as the blade, so it always stays in the same relative position with respect to the directrix. As it

will be developed later on, it can be easily seen how this local coordinate axes system is non-inertial, bacause it has a centripetal acceleration (which is by definition the same acceleration as the blades).

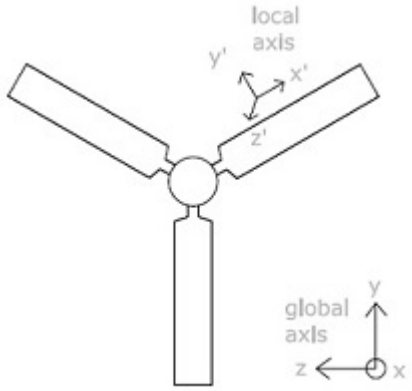

Figure 2.2: Position for the local axes, which rotate with the blade, in comparison with the global axes which are fixed (*source: self elaboration*).

In order to apply the Newton equilibrium equations we will have to define an equivalent inertial local axes system, since equilibrium equations must be written with respect to an inertial reference system. This equivalent coordinate axes system will have the same position as the local axes but will not rotate, so it will be inertial. Instead, we will add a centrifugal force to consider the fact that the blades are rotating. In other words, a non-inertial reference system can always be transformed into an inertial one by adding an *inertia* term that takes into consideration the acceleration the non-inertial system is under, according to [30]. Therefore, in fact, we will be dealing with three coordinate axes: the global ones, at the bottom of the tower, the rotating local axes (which are a non-inertial reference system because they have the same centripetal acceleration as the blades), and the inertial local axes, which are equivalent to the rotating local axes but are an inertial reference system. Referring to the notation, any inertial system will be defined as $\{x, y, z\}$, whereas the non-inertial reference system will be regarded as $\{x', y', z'\}$.

The weakest point of the blades, according to the hypotheses that have been previously made (see section 1.3), is the junction with the hub. Each blade can be understood as a beam which is perfectly fixed on one extreme and free on the other one (what in the resistance of materials's theory is regarded as a corbel), so the maximum efforts will always be on the fixed border, according to the wind characteristics assumed in the hypotheses. Therefore, the present model will try to evaluate the values for the resultant forces and moments in this critical point. These values will be referred as $F_X, F_Y, F_Z, M_X, M_Y, M_Z$, where F stands for a force and M for a moment, and where X, Y, Z stand for the three directions of the space. Consequently, the criterion we will use in order to evaluate whether there is collapse or not on the blades will only consider this critical point; in other words, there is no other possible breaking process that can take place on the blades apart from its collapse on the junction with the hub through plastic yielding (see "Breaking criterion" section)

Before setting out the equations, we have to state that as long as the blades are moving, the force of the wind will have two components, parallel and perpendicular to the blade, according to [31]. As it has been schematized in Figure 2.3, f_T stands for the *tangential* force, whereas f_N stands for the *normal* force (perpendicular to the blade). These two forces are not uniformly distributed along the blade, in fact their computation must be done through iteration, as it has been fully developed in Appendix A. However, complex as they may be to compute, once the wind speed has been fixed their calculation is straightforward. Having said that, as long as the distribution of these forces is known it

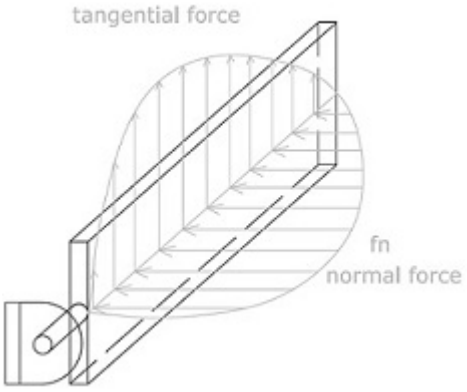

Figure 2.3: Scheme of the force of the wind on the blades (*source: self elaboration*).

is possible to compute their resultant value. Nevertheless, before continuing it is important to make a comment on the notation we will be using: f_T, f_N will stand for the distributed values, whereas F_T, F_N will stand for the resultant values (integration of f_T and f_N along the domain of the blade). In other words:

$$F_N = \int_0^R f_N dr,$$
$$F_T = \int_0^R f_T dr.$$

The equilibrium problem for the blades has been specified in Figure 2.4 and Figure 2.5. For a random position of the blade, the actuating forces are its weight, the tangential and normal forces due to the wind and the reaction forces produced at the junction. However, since the blades are moving we have to introduce F_I, the inertia force. This force does not exist in reality, but it has to be introduced in the formulation of the problem in order to consider the centripetal acceleration that the blade is suffering with its rotation. In other words, as the local axes are moving with the blades (non-inertial coordinate system) and we need to work with an inertial reference system, we have to consider an equivalent inertial reference system by adding an *inertia* term. Such inertia force is computed as the mass multiplied by an acceleration (which takes into consideration the acceleration of the local axes), where the acceleration can be expressed as it can be seen in equation (2.1) (according to [30]):

$$a = a' + a_{O'O} + \omega \times (\omega \times r) + 2 \cdot (w \times v') + (\alpha \times r). \tag{2.1}$$

The involved terms in the description of this acceleration, in this order, stand for the tangential acceleration in the local axes (zero, since the blade only rotates), the relative tangential acceleration from both coordinate systems (zero, since the tangential acceleration is always zero), the centripetal acceleration, the Coriolis term (negligible for this study) and the angular acceleration term (zero, since the angular speed is constant). In our particular case, the only non-zero term is the centripetal force. In other words, the only difference in terms of acceleration from the local axes with respect to the equivalent inertial coordinate system is that the local axes are rotating at a constant angular speed ω, solidary to the directrix of the blade:

$$a = \omega \times (\omega \times r) = a_N.$$

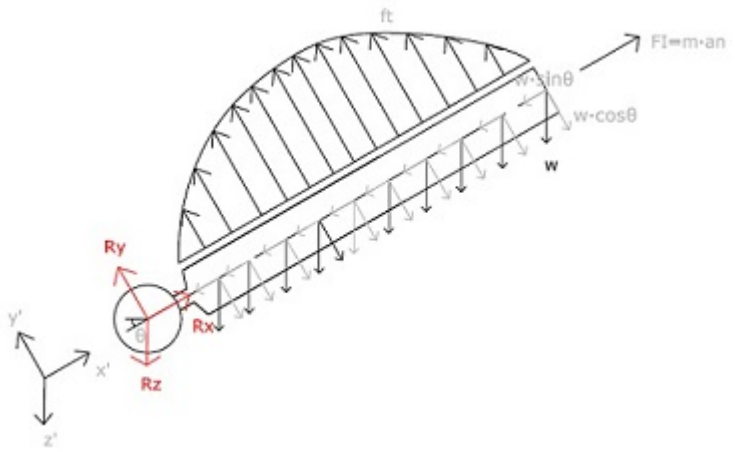

Figure 2.4: Representation of the forces actuating on the x-y plane for a randomly positioned blade. The external forces are presented in black whereas the reactions have been drawn in red (*source: self elaboration*).

The reaction forces (R_X, R_Y, R_Z) are found through applying Newton equilibrium on the blade (see Figure 2.4), as described in [30]. It is remarkable to see that the inertia term is always on the direction of the directrix, so it will only appear in the equilibrium equation on the x direction, regardless of the position of the blade. These equations are the following ones:

$$R_X - W \cdot \sin(\theta) = m \cdot a_N = m \cdot \omega^2 \cdot r,$$

$$R_X = W \cdot \sin(\theta) + m \cdot \omega^2 \cdot r,$$

where r stands for the distance from the center of gravity of the blade to the centre of rotation (centre of the hub) and θ stands for the angle between the directrix of the blade and the horizontal (see Figure 2.4) . By doing the same in the y direction:

$$F_T - W \cdot \cos(\theta) + R_Y = 0,$$

$$R_Y = W \cdot \cos(\theta) - F_T.$$

With reference to R_Z, according to Figure 2.5:

$$R_Z = F_N.$$

From the previous calculations we can set out a few conclusions. With reference to the reactions, it is clear that R_Z is independent of the position of the blades, whereas both R_X, R_Y depend on the position angle θ. As the blades rotate at a constant rate, it is straightforward to see that both R_X, R_Y will vary cyclically according to the angular velocity ω. As we are studying the most restrictive case to have collapse on the blades we will have to consider the maximum values for R_X and R_Y. From the previous equations, though, it is easy to see how these maximums cannot take place simultaneously because they depend on $\sin(\theta)$ and $\cos(\theta)$ (so when one is maximum the other is zero and viceversa). However, we will consider that the critical situation is the superposition of these two maximums. Even though we will focus on this aspect at the moment to define the breaking criterion, it is important to keep in mind that we will be interested in the maximum values of the reactions since they are the most restrictive situations, regardless they may not take place simultaneously. In fact, it could be argued that it is inconsistent to consider both maximums simultaneously, since from the previous

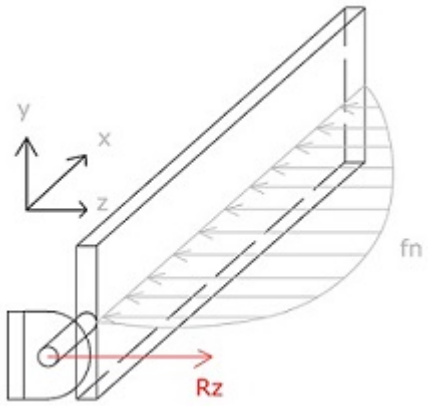

Figure 2.5: Scheme of forces actuating on the z axis (*source: self elaboration*).

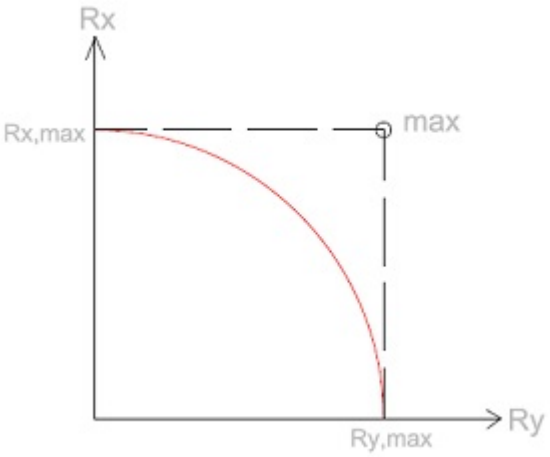

Figure 2.6: Scheme of the simplification we have made for the critical values for the reactions. (*source: self elaboration*).

equations it is easy to see that they will never coincide, by definition. The reason why we have considered both maximums at the same time is because of the breaking criterion (Von Mises). In order to decide whether there is collapse or not, the reactions in the three directions of space are taken into consideration. However, some of these reactions are cyclical, so when considering the possibility of breaking the blades we should consider all the possible combinations of reactions. In order to avoid such tedious verification, we have considered the worst case we can think of, even though it is not achievable in practice (since this combination is impossible by definition). However, by assuming both maximums at the same time we end up with a much simpler system of verifying the state of the blades, even though we are overestimating the forces on the junction. It could also be arguable whether this simplification is worthwhile, since the accuracy is reduced. However, given the fact that we are using an extremely simplified criterion to model the highly complex breaking process of a windmill blade, this assumption is aligned with the accuracy we will be able to provide at the outcome of the project. This simplification has been exemplified in Figure 2.6: according to the equilibrium equations the possible combinations are on the red circle; for our study we have considered the point marked with max, which even though is not on the circle is an upper bound of the reaction values.

Secondly, it is especially important to understand that by introducing the force F_I we have transformed our non-inertial axes to an inertial coordinate system, but we have kept the orientation of our local axes. It is not necessary to change the values the global coordinate system because as we will apply the same analysis we apply to beams it is required to have the efforts aligned with the directrix. It is remarkable to set clear the uses of the axes: as the blades are moving a non-inertial coordinate system that moves with the blades is needed. However, in order to get the real reactions on the hub we have to consider that the system has a centripetal acceleration, which is equivalent to have an inertia force applied at the directrix of the blade and consider an inertial system. By doing that we will have the reactions on an inertial system, but still oriented with the directrix of the blade.

Finally, since the values for the weight and the angular velocity are known (and fixed), as long as we know the wind speed v_{hub} we are able to compute both F_T and F_N and find the reactions on the union of the blades and the hub in a straightforward way, since even though the wind forces may be difficult to compute they only depend on the wind speed.

Up to now, the reaction forces have been found by applying the equilibrium Newton equations. Referring to the moments, it is important to state first that given that R_Z and F_N are applied on the directrix of the blade, M_X will always be null regardless of the values of the forces. In other words, as we have set in section 1.3, under any circumstances torsion will not occur on the blade, which is inferred from considering a constant wind speed for all the rotor. Therefore, we only need to compute both M_Y and M_Z.

With reference to the moment M_Y, we have to solve the problem schematized on Figure 2.7. Moreover, as we have stated in section 1.3, the blades will be assumed to behave as beams (perfectly

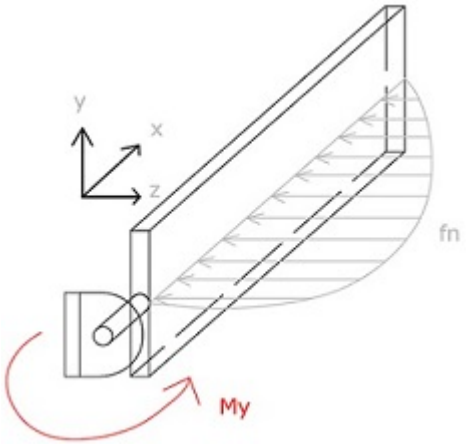

Figure 2.7: Scheme of the reaction moment on y axis (*source: self elaboration*).

fixed on one extreme and free on the other one). Therefore, the behaviour for each blade will be equivalent to a corbel (Figure 2.8).

It is important to set out that these kind of structural problems have been thoroughly studied before and have tabulated solutions. However, since the force of the wind is not uniformly distributed and it is calculated through an iterative procedure the solution for such problem has to be computed through building the differential equilibrium equations. In order to obtain M_Y, we have taken into consideration the differential part of the blade illustrated in Figure 2.9, in the same way that has been proposed in [32]. By applying equilibrium of moments on this differential part of the blade:

$$\sum M_A = 0,$$

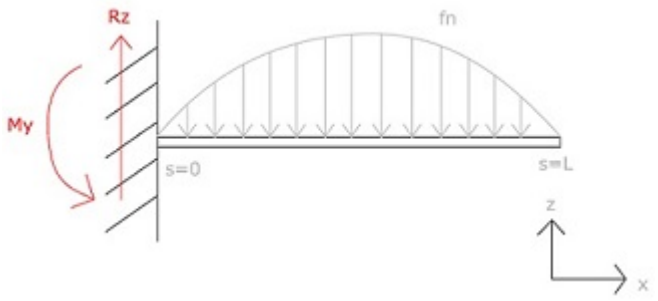

Figure 2.8: Structural approach to the blade behaviour by analyzing it as a corbel (*source: self elaboration*).

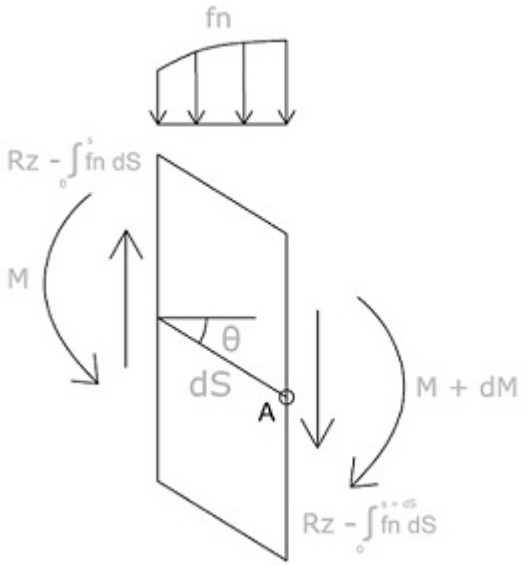

Figure 2.9: Forces applied on a differential part of the blade (*source: self elaboration*).

$$0 = -M + M - dM - \left(R_Z - \int_0^s f_N ds\right) \cdot ds \cdot \cos\theta,$$

where θ stands for the angle and s stands for the arc parameter we use to describe the position on the blade, according to the same nomenclature proposed in [32] (note that θ is a function of s). By developing that equation and imposing $R_Z = F_N$, as well as stating the trigonometrical relationship between dx, dy, and ds, we get the following differential system of equations:

$$\begin{cases} \frac{dM}{ds} = -\left(F_N - \int_0^s f_N ds\right) \cdot ds \cdot \cos\theta \\ \frac{dx}{ds} = \cos\theta \\ \frac{dz}{ds} = -\sin\theta. \end{cases}$$

Now the following equations are applied ([32]):

$$M = \chi \mathrm{EI},$$

$$\chi = \frac{d\theta}{ds},$$

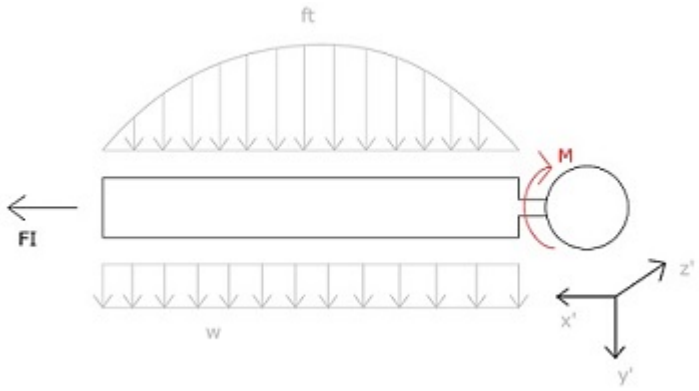

Figure 2.10: Representation of the most restrictive case with reference to M_Z (*source: self elaboration*).

where E stands for the Young Modulus, I for the inertia of the section (calculated in section 1.3) and χ for the curvature of the directrix. Therefore, the previous system of equations leads to:

$$\begin{cases} \frac{d^2\theta}{ds^2} = -\frac{1}{\mathrm{EI}} \cdot \left(F_N - \int_0^s f_N ds\right) \cdot \cos\theta \\ \frac{dx}{ds} = \cos\theta \\ \frac{dz}{ds} = -\sin\theta, \end{cases}$$

which is a non-linear system of equations with the following boundary conditions:

$$\begin{cases} x(0) = 0 & \text{local x axis centered on the beginning of the blade,} \\ z(0) = 0 & \text{local z axis centered on the beginning of the blade,} \\ \theta(0) = 0 & \text{perfectly fixed beam on one extreme,} \\ \frac{d\theta}{ds}(L) = 0 & \text{free on the other extreme.} \end{cases}$$

This non-linear system has to be solved every time in order to get the geometry of the deformed blade as well as the moment M_Y in the junction of the hub. In other words, since the forces of the wind are not uniform along the blade and have to be calculated for every wind speed we provide, in order to describe the final situation of the blade as well as the reaction moment M_Y we have to solve the previous system of differential equations for each wind speed that we consider (in fact, we could find the reaction through equilibrium, but by doing this we would not be able to find the expression of the deformed blade). In the mathematic model we have computed in MatLAB this system of equations has been solved through the shooting method (see references [34] and [19]). In particular, the mathematical problem we end up once we have developed the differential equilibrium is analogous to the problem proposed by Wang in [10].

With reference to the moment M_Z, a similar procedure has been considered. However, this case presents certain further difficulties. In the previous system of equations, once the wind speed had been fixed, the expression of f_N, f_T was fixed and constant for all the possible positions of the blade, so the moment M_Y was certainly the same regardless of the position of the blade. In the present problem, however, even though f_T behaves the same way, the direction of the weight of the blade does not rotate with the blade, so the moment M_Z varies cyclically just as R_X and R_Y did. Consequently, we have computed the most restrictive case possible, which is when f_T perfectly superposes to the weight (note that in all other cases the resultant force is below this upper level), as it can be seen in Figure 2.10 and Figure 2.11.

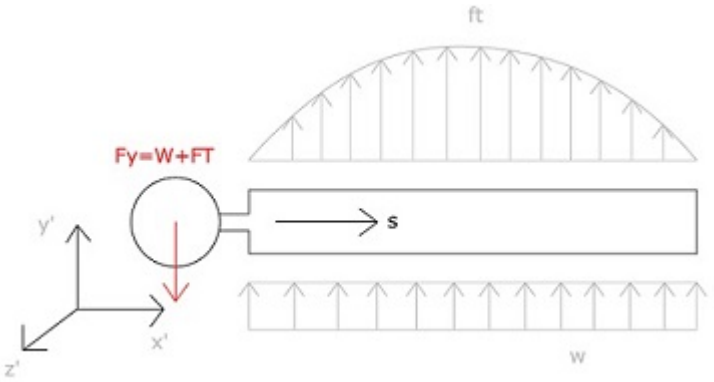

Figure 2.11: Representation of the most restrictive case with reference to M_Z with the axes in the conventional position (*source: self elaboration*).

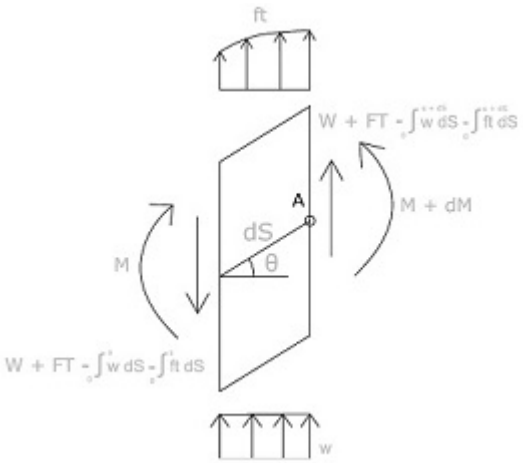

Figure 2.12: Forces applied on a differential part of the blade (*source: self elaboration*).

It is relevant to set out that it could be interesting to study the variation of the moment along all the possible positions of the blade. However, since our interest is to simply study whether the blades break down or not, it is only necessary to study the most critical position with respect to the moment, because that will be the most limitative condition for the blade to remain undamaged. Setting the axes in a conventional way, the problem is equivalent to considering the situation described in Figure 2.12. Just as we did before, equilibrium is applied to a differential part of the blade:

$$\sum M_A = 0,$$

$$0 = -M + M + dM + \left(W + F_T - \int_0^s w ds - \int_0^s f_T ds\right) \cdot ds \cdot \cos\theta,$$

$$\frac{dM}{ds} = -\left(W + F_t - \int_0^s w ds - \int_0^s f_T ds\right) \cdot \cos\theta.$$

By applying the same methodology as before, the non-linear system of differential equations is:

$$\begin{cases} \frac{d^2\theta}{ds^2} = -\frac{1}{\mathrm{EI}} \cdot \left(W + F_T - \int_0^s w ds - \int_0^s f_T ds\right) \cdot \cos\theta \\ \frac{dx}{ds} = \cos\theta \\ \frac{dy}{ds} = \sin\theta. \end{cases}$$

Moreover, the boundary conditions are:

$$\begin{cases} x(0) = 0 & \text{local x axis centered on the beginning of the blade,} \\ y(0) = 0 & \text{local y axis centered on the beginning of the blade,} \\ \theta(0) = 0 & \text{perfectly fixed beam on one extreme,} \\ \frac{d\theta}{ds}(L) = 0 & \text{free on the other extreme.} \end{cases}$$

This system is solved in a similar way as the previous one (through the shooting method, analogously to [10]).

So far the 6 reactions on the union of the blade with the hub have been calculated. Furthermore, it has been set out that many of these values vary cyclically according to the position of the blade. It has been also pointed out that we will be interested in the maximum values for these reactions, since they are the magnitudes we will be considering to evaluate whether the blades break down or stay at service state. In particular, we have seen that R_X, R_Y and M_Z are cyclical. The maximum value for R_X happens when the hub has to handle the whole weight in addition to the inertia force, as it can be checked in Figure 2.13. With reference to R_Y and M_Z, their case has been already studied

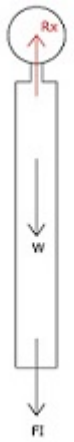

Figure 2.13: Scheme of the most restrictive case with regard to R_X (*source: self elaboration*).

previously, since the most restrictive situation is when the weight superposes to the tangential force, as it can be seen in Figure 2.14. However, as we have introduced before, the strategy we have followed is to consider that the three maximums happen simultaneously so that the values we obtain once we fix the wind speed are unique and are always over the maximum efforts of the blade.

By modelling the behaviour of the windmill with the previous proposal, we are able to get a relatively *cheap* approach to the reactions on the junction of the blade and the hub when the blades are rotating at a steady state (so their angular velocity is constant) as well as an approximation of the deformed geometry under the wind conditions we provide. It is important to set out, once again, that these results tend to overestimate the actual maximal efforts, since we have considered the superposition of all the maximum values for the reactions. It is relevant to finally remark that no

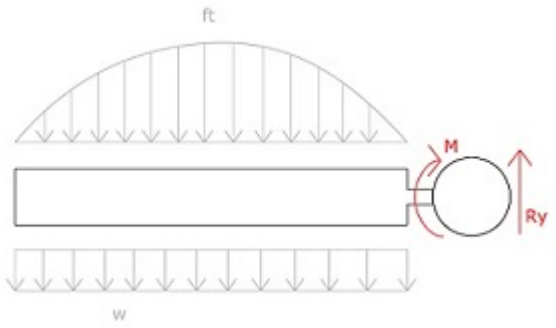

Figure 2.14: Scheme for the most restrictive case for both M_Z and R_Y (*source: self elaboration*).

distinction can be made between the fact "rupture of one blade" or "rupture of more than one blade". It is painfully obvious that these two possible states are different because their economic impact is different, but since the hypothesis that all blades behave the same way has been assumed no further conclusions can be obtained from the present model.

2.1.2 Structural approach for $v_{hub} > 25$ m/s (stopped windmill)

In case the blades do not move, the relative speed between the wind and the blades is perpendicular, since the wind is perpendicular to the blades by hypothesis. As it can be checked in Appendix A, the important parameter with reference to computing the force of the wind is not the absolute wind speed but its relative value with respect to the blades (Figure 2.15).

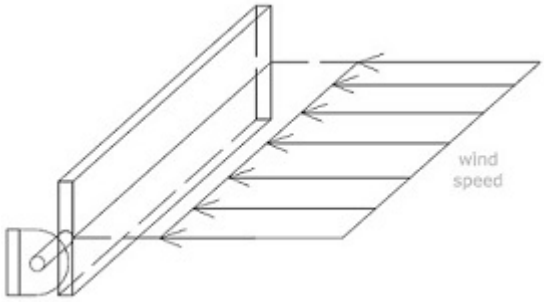

Figure 2.15: Absolute wind velocity scheme (*source: self elaboration*).

Moreover, with reference to the computation of the force through the method explained in Appendix A we have to say that for high wind speed values C_D increases while C_L decreases, according to [31]. These changes are very significative, because C_L becomes low enough to neglect the tangential force f_T while the f_N becomes much more relevant (see Figure 2.16). This fact is consistent with what we would expect: as long as the blades do not move and are under high wind speed conditions, the normal force they experiment supplied by the wind is much higher than in previous situations, whereas since there is no rotation in the rotor there is no tangential force induced by the relative velocity.

For the reasons exposed above, the problem with a stopped windmill will be different in several ways: first, there will be no f_T to be considered. Moreover, there will no longer appear an inertia force F_I to change our non-inertial coordinate system to an inertial one (since the local axes will not

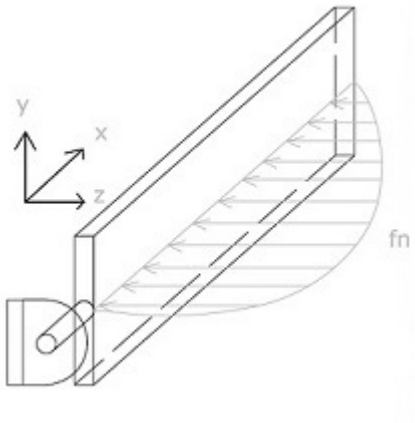

Figure 2.16: Resultant force of the wind on the blade (note that there is no tangential component, so the resultant is perpendicular to the blade (*source: self elaboration*).

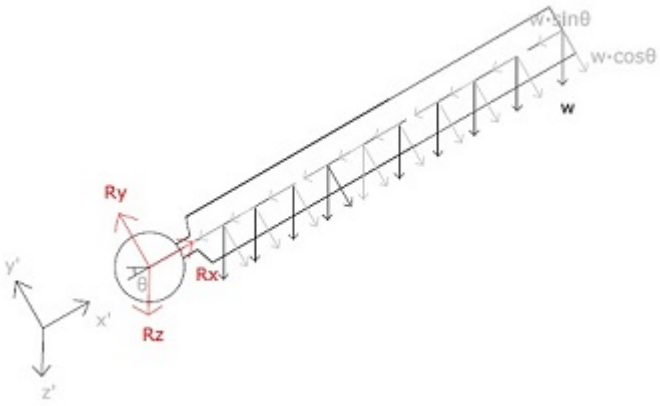

Figure 2.17: Scheme of the actuating forces on a randomly positioned blade for a stopped windmill (*source: self elaboration*).

be moving now). Finally, the values for f_N will be significantly higher and they will become the main source for blade vulnerability.

With reference to the computation of f_N, before continuing we have to state that several further hypotheses have been made with reference to the calculation of the force of the wind (see Appendix A). As a result, we have to be aware of the uncertainty associated to this computed value due to the simplifications made in addition to the initial hypotheses, as it can be verified in Appendix A.

It is especially relevant to comment on again the fact that we are not studying the transient state in which the windmill is reducing its velocity at the moment $v_{hub} = 25$ m/s, since we are either applying the "constant angular speed rotation" equations or the "stopped windmill" ones. This transient situation that happens at $v_{hub} = 25$ m/s is assumed to happen very quickly and has not been introduced in the model, though it seems reasonable that it can be a peak-effort situation. Therefore, additional uncertainty exists with respect to this particular effect, and were any further studies to try to improve this model they should certainly try to approach this drawback.

Finally, before starting to build the physical equations, we have assumed that, since all the previous hypotheses are still applicable, all the blades behave the same way so there is no specific "most

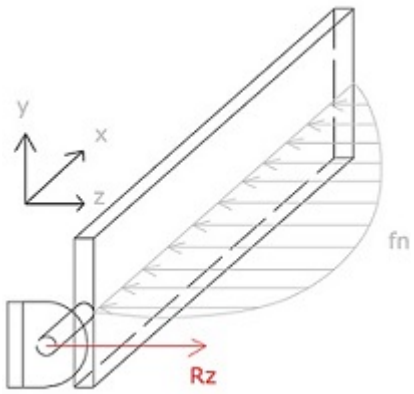

Figure 2.18: Forces applied on the z axis of the blade (*source: self elaboration*).

restrictive position of the blades". In reality it has been already demonstrated that wind speed changes with height, so the conditions on the blades do not remain the same along all the possible positions. However, as we have done in previous chapters, the final position of the windmill after being stopped does not affect its final vulnerability under any circumstances.

Having set out the further comments that must be considered, we will proceed in the same way as in the active windmill situation, even though the final results will be different. With reference to the reactions at the junction, they can be calculated through Newton equilibrium, according to [32]. Since no inertia term nor tangential forces have to be considered, the expressions are less complex, as it has been schematized in Figure 2.17:

$$R_X = W \cdot \sin(\theta),$$
$$R_Y = W \cdot \cos(\theta).$$

Referring to the reaction in the z axis (Figure 2.18):

$$R_Z = F_N = \int_0^R f_N ds.$$

Just like the case of an active windmill, both R_X and R_Y are dependent on the position θ. As we have already done before, we will be focusing in the maximum values for these forces in order to study the most restrictive cases.

With regard to the moments, it is still verified that the torsion moment is null ($M_X = 0$), since the hypothesis that wind speed is constant on all the area of the rotor is still valid (so the resultant of f_N is applied on the directrix of the blades regardless of the wind conditions). For the moments M_Y and M_Z, the same procedure as before will be applied. When it comes to study the maximum moment M_Z, we see that the most restrictive situation is the one in Figure 2.19:

As we have done in other situations, equilibrium is applied to a differential part of the blade, according to [32]:

$$\sum M_A = 0,$$
$$0 = -M + M + dM - (R_Y - \int_0^s wds) \cdot ds \cdot \cos\theta,$$

and since by equilibrium $R_Y = W$ in this situation, then:

$$\frac{dM}{ds} = (W - \int_0^s wds) \cdot \cos\theta$$

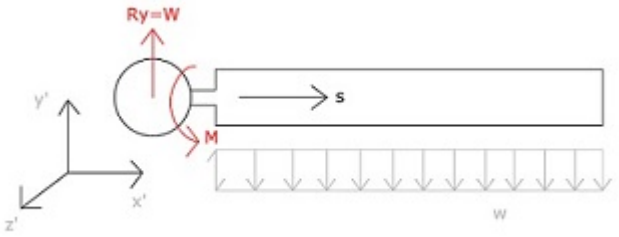

Figure 2.19: Most restrictive situation with regard to M_Y (*source: self elaboration*).

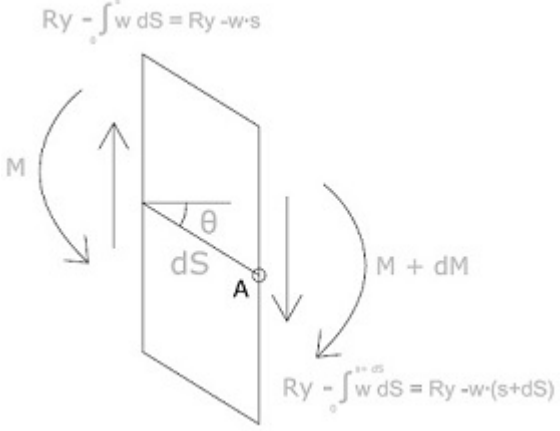

Figure 2.20: Forces applied on a differential part of the blade (*source: self elaboration*).

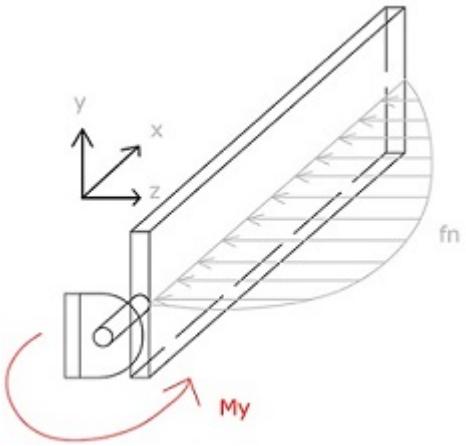

Figure 2.21: Reaction moment M_Z (*source: self elaboration*).

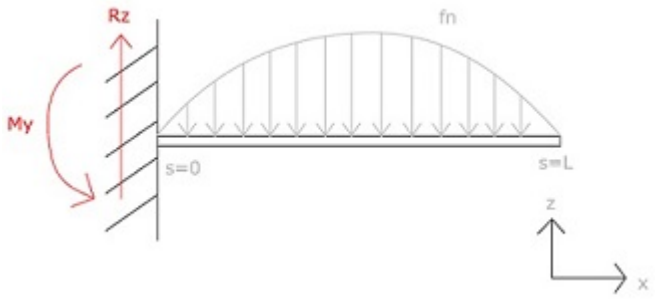

Figure 2.22: Structural approach to the blade behaviour by analyzing it as a corbel (*source: self elaboration*).

Proceeding like in previous cases, we reach the following non-linear system of differential equations:

$$\begin{cases} \frac{d^2\theta}{ds^2} = -\frac{1}{\mathrm{EI}} \cdot (W + F_T - \int_0^s w ds) \cdot \cos\theta \\ \frac{dx}{ds} = \cos\theta \\ \frac{dy}{ds} = -\sin\theta, \end{cases}$$

with the following boundary conditions:

$$\begin{cases} x(0) = 0 & \text{local x axis centered on the beginning of the blade,} \\ y(0) = 0 & \text{local y axis centered on the beginning of the blade,} \\ \theta(0) = 0 & \text{perfectly fixed beam on one extreme,} \\ \frac{d\theta}{ds}(L) = 0 & \text{free on the other extreme.} \end{cases}$$

With reference to the M_Y computation (Figure 2.21), we proceed as before. As it has been stated, the problem is equivalent to studying a corbel, as schematized in Figure 2.22. In particular, the expression for M_Y is exactly the same as before, since even though the expression of F_N may be calculated in a different way the structural response of the blade (which behaves like a corbel) is exactly the same. Therefore, the non-linear system of differential equations is the following one, which will be solved

through the shooting method (see [34]), as it has been proposed on [10]:

$$\begin{cases} \frac{d^2\theta}{ds^2} = -\frac{1}{\mathrm{EI}} \cdot \left(F_N - \int_0^s f_N ds\right) \cdot \cos\theta \\ \frac{dx}{ds} = \cos\theta \\ \frac{dz}{ds} = -\sin\theta, \end{cases}$$

with the following boundary conditions:

$$\begin{cases} x(0) = 0 & \text{local x axis centered on the beginning of the blade,} \\ z(0) = 0 & \text{local z axis centered on the beginning of the blade,} \\ \theta(0) = 0 & \text{perfectly fixed beam on one extreme,} \\ \frac{d\theta}{ds}(L) = 0 & \text{free on the other extreme.} \end{cases}$$

For the reasons exposed in this chapter, the physical equations that are to be applied to the blades are different depending on whether we are under $v_{hub} < 25$ m/s restriction or $v_{hub} > 25$ m/s. Therefore, at the moment of building the numerical model, the first operation we will make is regard in which domain we are in order to apply the correct equations. Finally, by carrying out the analysis that have been stated in this chapter, we will be eventually able to evaluate if there is collapse on the blades, according to the breaking criterion that will be set out at the end of the chapter; in that case, we will understand the final situation of the blades as "collapse", otherwise we will assume the final state for the blades to be "service".

2.2 Nacelle analysis

It has been previously mentioned that both the nacelle and the rotor will be studied together when it comes to model the vulnerability. However, when building the physical model for the behaviour it is much more clear to make several comments on the nacelle so it is much simpler to see what forces will be transmitted to the tower. As we stated in section 1.3, we will understand the nacelle as a *box* whose main structural aim is to transmit the forces from the rotor to the tower, since we have taken a purely structural approach to the vulnerability problem (so no considerations will be made regarding the mechanical-electrical behaviour of the windmill).

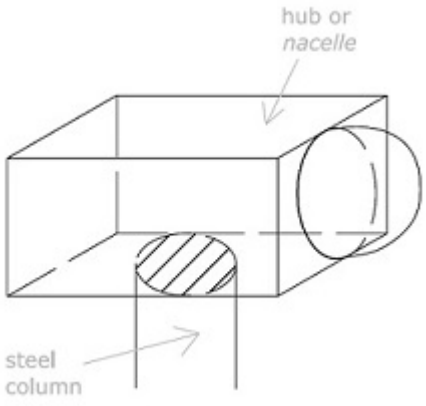

Figure 2.23: Definition of the nacelle (*source: self elaboration*).

Before building the equations, we have to set out several further hypotheses with reference to the behaviour of the nacelle. First, we will assume that the centre of gravity of the system nacelle + rotor is on the symmetry axis of the column. That is equivalent to say that there will be no extra moments on the tower because an eccentricity of the resultant vertical force. Should we consider another hypothesis, we would only have to add an extra term on the equations of the tower. Furthermore, we will assume the inertia force, whose resultant is always vertical (as it will be demonstrated later on this chapter), to be applied as well on that axis. In conclusion, we will be assuming that the resultant of all the vertical forces is always applied in a point so that it generates no moment on the tower.

With reference to the axes considered for the nacelle, they will be the same global axes that have been defined previously, but centered on the base of the nacelle (see Figure 2.24). It is important to state that the nacelle is responsible for rotating in order to make the windmill be oriented perpendicularly to the wind, so its axes, just like the global ones, will always have its x component oriented towards the wind.

With regard to the reactions on the base of the nacelle (which will be the forces transmitted to the tower), as it has been summarized in Figure 2.25:

$$R_X = F_{N,hub}$$

With reference to equilibrium in the y axis, we have to take into consideration that there may be the resultant of the F_I as well in case the blades are moving. This resultant will be, otherwise, null. It is especially important to set out a few comments about this force, since as it has been introduced to consider that the local coordinate system for the blades is accelerated and not because there is a real force it may be somehow difficult to understand whether it has to be in the nacelle formulation. In fact, it is intuitive to see that when the blades are moving there is an extra force on the nacelle due to the fact that they have centripetal acceleration, In other words, as long as the blades are

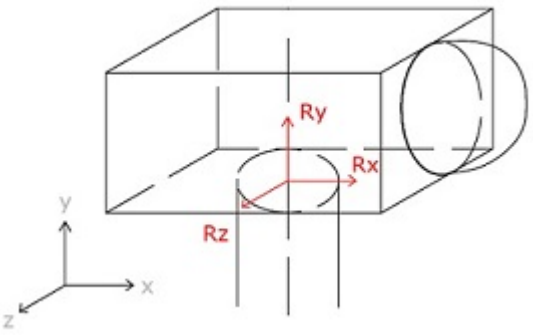

Figure 2.24: Location of the global axes we will be using (*source: self elaboration*).

Figure 2.25: Force diagram on the x axis (*source: self elaboration*).

under centripetal acceleration, the nacelle has to provide an extra force, overall, to actually take into consideration that acceleration. That is the meaning for the inertia force. It has been said that every blade has an inertia force applied on its directrix (see Figure 2.26). If we study the resultant inertia force, we will see it is constant and always pointing downwards. Intuitive as it may seem, it is not straightforward to see that regardless of the position of the blades the resultant has the same value, so we have demonstrated it below. Let's assume a certain angle Ω to be the angle between the horizontal and one of the blades ($\Omega \in [0, 2\pi)$), and F_I the inertia force applied to a single blade. As the blades form an equilateral triangle the rest of the blades have a position which is dependent on Ω as well (see Figure 2.27). Now let's compute the value for the resultant $F_{I,X}$ and $F_{I,Y}$, where X, Y stand for the

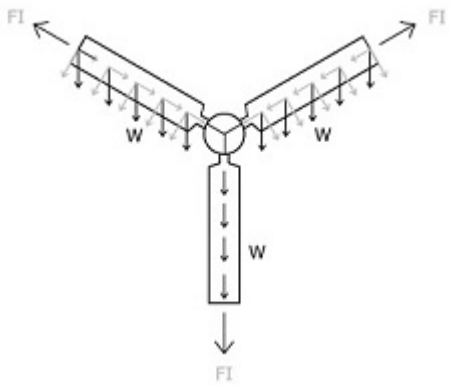

Figure 2.26: Forces actuating on the three blades of the rotor (*source: self elaboration*).

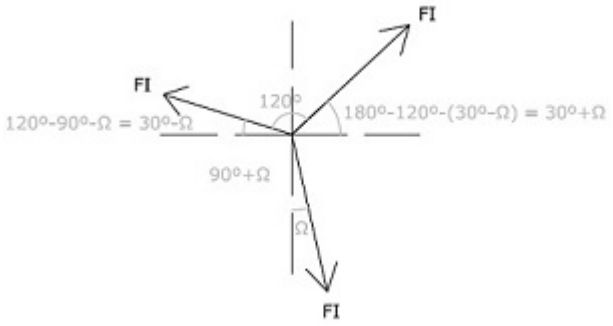

Figure 2.27: Random position of the blades to prove F_I is constant (*source: self elaboration*).

horizontal and vertical axes respectively:

$$F_{I,X} = F_I \cdot \sin\Omega - F_I \cdot \cos\left(\pi/6 - \Omega\right) + F_I \cdot \cos\left((\pi/6 + \Omega\right),$$

Now, by developing the previous expression with trigonometrical formulas to separate the angles inside sinus and cosinus and applying the equivalences between the trigonometrical values of the different quadrants:

$$F_{I,X} = F_I \cdot \left(\sin\Omega - \left(\cos\left(\pi/6\right)\cos\Omega - \sin\left(\pi/6\right)\sin\Omega\right) + \left(\cos\left(\pi/6\right)\cos\Omega + \sin\left(\pi/6\right)\sin\Omega\right)\right),$$

$$F_{I,X} = 0, \forall\Omega \in [0, 2\pi).$$

By doing the same procedure in the vertical axis:

$$F_{I,Y} = F_I \cdot \sin\left((\pi/6 - \Omega\right) - F_I \cdot \cos\Omega + F_I \cdot \sin\left((\pi/6 + \Omega\right),$$

$$F_{I,Y} = F_I \cdot \left(\left(\sin\left(\pi/6\right)\cos\Omega - \sin\Omega\cos\left(\pi/6\right)\right) - \cos\Omega + \left(\sin\left(\pi/6\right)\cos\Omega + \sin\Omega\cos\left(\pi/6\right)\right)\right),$$

$$F_{I,Y} = F_I \cdot (1 - \sqrt{3}), \forall\Omega \in [0, 2\pi).$$

Therefore, if we consider the equilibrium equation on the nacelle (Figure 2.28):

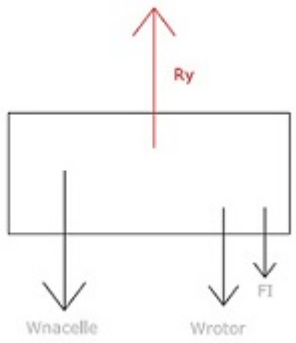

Figure 2.28: Diagram of forces on y axis (*source: self elaboration*).

$$R_Y = W_N + W_R + F_I,$$

where

$$F_I = \begin{cases} m \cdot \omega \cdot r_{cm}^2 & v_{hub} < 25 \text{ m/s, active windmill} \\ 0 & \text{otherwise, stopped windmill.} \end{cases}$$

It would be arguable to discuss whether f_T has a vertical component to be added in the previous equation. As it will be proved in this chapter, the resultant force of f_T is null on the nacelle, since its only effect is providing rotation with respect to the centre of the hub.

With regard to R_Z, no forces exist along the z axis. It is easy to see how both the inertia force and the weight have been proved to be pointing downwards. With respect to the normal force f_N, it cannot

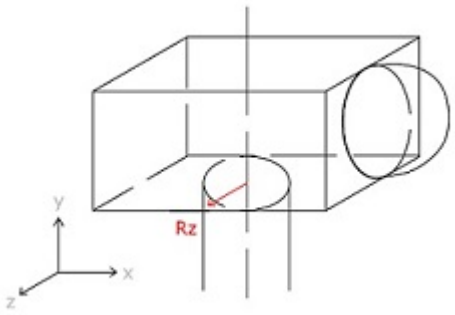

Figure 2.29: Forces on the z axis of the nacelle (*source: self elaboration*).

have a component in the direction of z by definition (because by definition is a force perpendicular to the blades). Regarding the force f_T, however, it is not direct to infer that under any circumstance there is not a component on the z direction, so we have to prove it. However, since all the blades behave the same way and are under the same force f_T, it seems intuitive that the resultant will not have a component on the z axis (by symmetry).

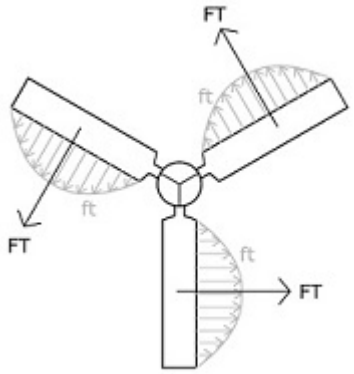

Figure 2.30: Tangential forces on the three blades (*source: self elaboration*).

Let's assume the position of the blades according to Figure 2.30 and Figure 2.31, with an arbitrary angle Ω like before. Since f_T is perpendicular to the blades, the resultant will necessarily have the same direction. We have to say that the application point is unknown because it depends on the computation of f_T, which varies when we vary the wind speed. However, this fact does not matter for the present demonstration since no matter where the application point is the resultant will keep on being perpendicular to the directrices of the blades. If we compute the value for $F_{T,Z}$:

$$F_{T,Z} = F_T \cdot \cos\Omega - F_T \cdot \sin\left((\pi/6) + \Omega\right) - F_T \cdot \sin\left((\pi/6) - \Omega\right),$$

$$= F_T \cdot \left(\cos\Omega - \sin\left(\pi/6\right)\cos\Omega - \left(\sin\Omega\cos\left(\pi/6\right)\right) - \left(\sin\left(\pi/6\right)\cos\Omega + \sin\Omega\cos\left(\pi/6\right)\right)\right) = 0,$$

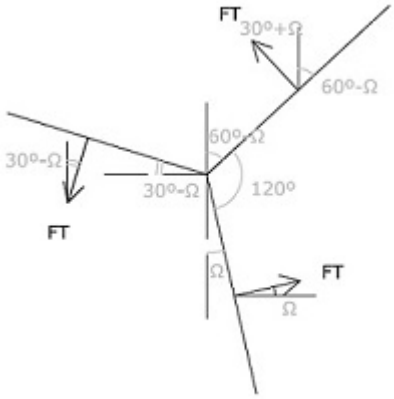

Figure 2.31: Random position of the blades to prove the resultant from F_T actuating on the three blades is always null (*source: self elaboration*).

We can also prove easily how the vertical resultant is also null:

$$F_{T,Y} = F_T \cdot \sin\Omega - F_T \cdot \cos\left((\pi/6) - \Omega\right) + F_T \cdot \cos\left((\pi/6) + \Omega\right),$$

$$F_{T,Y} = F_T \cdot \left(\sin\Omega - \left(\cos\left(\pi/6\right)\cos\Omega - \sin\left(\pi/6\right)\sin\Omega\right) + \left(\cos\left(\pi/6\right)\cos\Omega + \sin\left(\pi/6\right)\sin\Omega\right)\right) = 0,$$

$$F_{T,Y} = 0, \forall\Omega \in [0, 2\pi).$$

Therefore, we have now proved that the resultant for f_T is null, so its only effect is providing rotation with respect to the hub. Consequently, since neither f_N nor the weight nor F_I have a component on the z axis we can state:

$$R_Z = 0.$$

Finally, before computing the value for the moments on the nacelle, we should state that even though we have not explicitly mentioned it, we have applied the 3rd Newton's Law. Right after calculating the reactions on the union of the hub and the blades, we have used these values as forces applied to the nacelle. In other words, we have assumed that the external forces that the blades transmit to the nacelle are exactly the same but in the opposite sense than the force the nacelle supplies to them. The reactions found for the blades, R_X, R_Y, R_Z (we will talk about the moments later), therefore, have been directly used for the reactions of the nacelle (Figure 2.32).

With regard to the moments applied to the nacelle, their computation will certainly be more difficult than for the forces, and a lot of further hypotheses will be applied, so there is definitely an extra degree of uncertainty associated to the computations of both M_Y, M_Z (where X, Y, Z now stand for the nacelle's axes, as it was schematized in Figure 2.24. By starting with the moment M_X we have to keep in mind the 3rd Newton's law we have just talked about. In other words, the reaction moment on the nacelle will be the sum of the reaction moments on the blades but with the opposite sign. It can be easily seen that these reaction moments vary along the position of the blade because the weight does not rotate with the blades (it always points downwards), so the reactions on the nacelle from the three blades have to be necessarily different and vary cyclically. However, if we analyze the three blades at the same time, the effects of the weight have a null resultant, since the centre of gravity of the 3 blades is, by definition at the hub. That is equivalent to say that the differences in moments within all the combinations of positions of the blades are due to the weight, so at the center of the hub these differences are compensated, as it can be clearly seen in Figure 2.34. Therefore, the M_X moment, which from now on will be also referred as "torque", will only depend on the tangential force

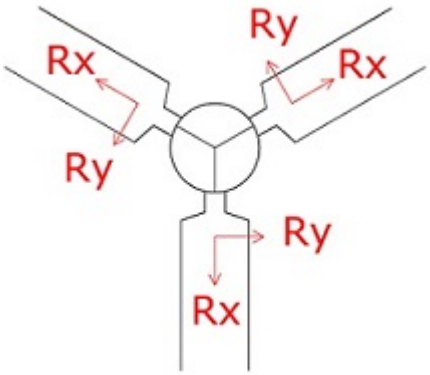

Figure 2.32: Action-reaction forces between the nacelle and the blades(*source: self elaboration*).

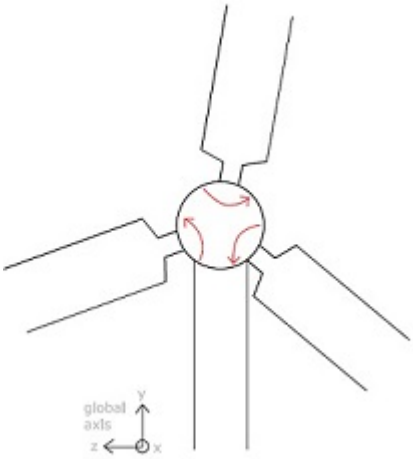

Figure 2.33: Action-reaction moments in the x direction (M_X) between the nacelle and the blades (*source: self elaboration*).

supplied by the wind, because the weight will not generate under any circumstances moment at the center (in fact, complex as it may seem to explain, it is an extremely intuitive idea that overall the weight of the blades will not induce moment on the nacelle because of symmetry). For this reason, the expression of the moment M_X can be written as in (2.2).

$$M_X = 3 \cdot F_T \cdot d_{f_T}, \tag{2.2}$$

where d_{f_T}, stands for the distance between the application point of the resultant F_T and the centre of the hub.

The moment M_Y appears due to the fact that the wind speed field has turbulence within a constant height, which means that the wind speed field is not symmetric with respect to the vertical axis passing through the centre of the hub (again, working in the nacelle's reference system, shown in Figure 2.24). This situation leads to a horizontal eccentricity of the resultant force, which generates an extra moment on the tower. However, given that the turbulence evolution is aleatory, this horizontal eccentricity is a random variable (see the Section 1.4 section for further details). This situation has been schematized in Figure 2.35. Though on average the resultant could be assumed to be applied on the center of the hub (by symmetry), we cannot treat the horizontal eccentricity as null. In order to be consistent with both the hypotheses and what happens in reality we have introduced a new variable in the model,

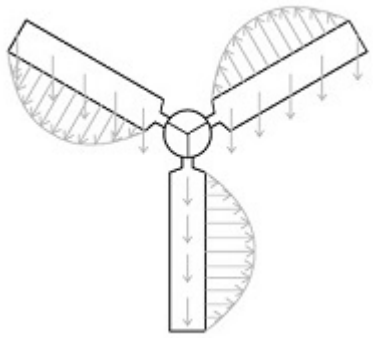

Figure 2.34: Scheme on the forces actuating on the rotor (*source: self elaboration*).

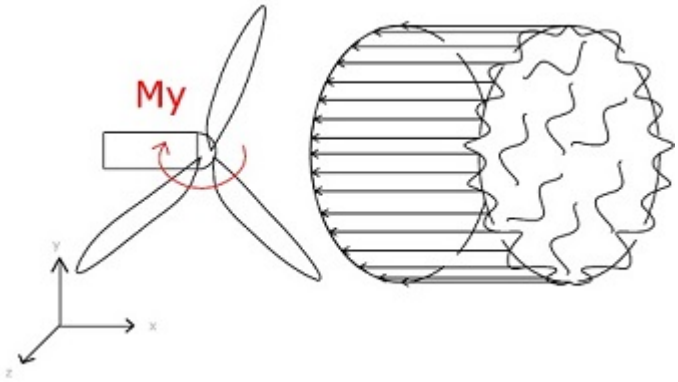

Figure 2.35: Turbulent wind speed field which generates a moment on the y axis (*source: self elaboration*).

named as e_x, which stands for the horizontal eccentricity of the force. This eccentricity has been treated as a logit-normally distributed random variable. The explanation for that assumption is that we need a symmetric and unimodal distribution whose domain is $[-R,R]$, where R stands for the radius of the rotor. In case the domain was the whole real scale, a normal distribution would have been suitable; therefore, a logit-normal distribution seems appropriate for the modelling of a variable with the previous characteristics.

By considering this variable, what we are doing is considering a random situation of the wind as an uniform field with a random position of the resultant, which is equivalent to consider a constant wind field with a random moment. A similar procedure will be carried out for the moment generated by the variation of wind speed with height (M_Z). However, with reference to this moment the situation is different because the resultant, on average, is not null (as it has been illustrated in Figure 2.36). When we stated the hypotheses, we did make an emphasis on the fact that the wind speed can be assumed to increase with height, with a function that was proposed on [3] (and which is thoroughly analyzed in [31]). Therefore, the resultant force of the wind will not be centered, on average, at the hub. However, as it can be checked in the formula, the higher the position of the hub is, the less important the variation of wind speed with height becomes. For this reason, we will proceed analogously as in the previous case and define a vertical eccentricity e_y which has the same distribution as e_x and stands for the moment generated by the turbulence and which is centered at the hub. By proceeding this way, we are able to take into consideration the possible moment due to variation of wind speed with

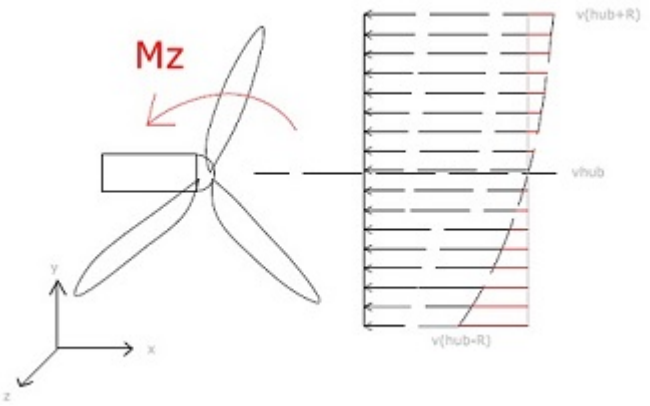

Figure 2.36: Moment on the z axis due to the variation of the wind speed with the height (*source: self elaboration*).

height, but we will be systematically underestimating this moment, since on average the resultant will always be applied at a higher point according to the non-uniformity of the wind speed with height.

Finally, to summarize what has been done we have to say that we have taken the same approach as a conventional resistance of materials' problem, by understanding an eccentrical force as a force centered on the hub with two moments that are equal to the resultant force multiplied by the eccentricity (which given the aleatory nature of the forces is a random variable. These eccentricities have been schematized in Figure 2.37. For more information the chapter number 9 of [7] can be checked; even though that problem has a completely different nature, the principle we have applied to solve the present problem is the same. This previous methodology has considered a lot of simplifications with respect to what it would be the real situation. The main aim of it has been introducing into the formulation an expression which is consistent with the hypotheses that have been made and considers an approach to what will happen in reality. For further details about the parametrization of these eccentricities please see section 1.4 .

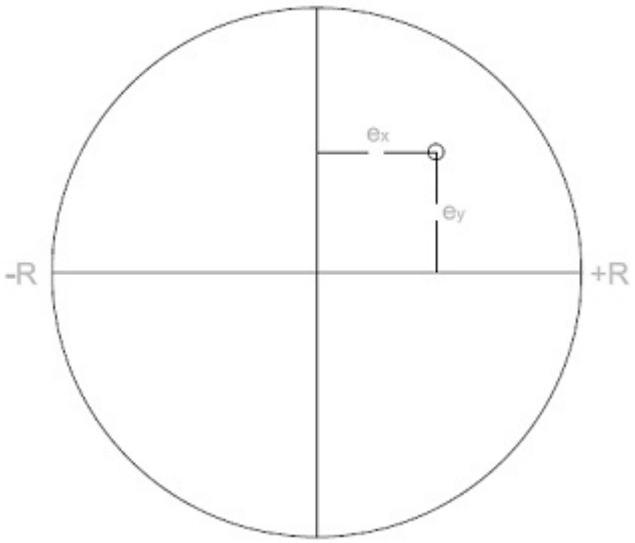

Figure 2.37: Schematization of the horizontal and vertical eccentricities of the resultant force of the wind (*source: self elaboration*).

2.3 Tower analysis

The structural problem associated to the tower is clearly the most complex one because of the large number of forces that are involved as well as the extra hypotheses that need to be assumed in order to end up with an affordable problem. In particular, the actions applied on the tower are the following ones:

- First, on the top of the tower there are the resultant forces from the system nacelle + rotor, which have been previously computed and have been named "reactions on the nacelle" (see previous section).
- Second, we have the weight of the tower, entirely made of steel, which is uniformly distributed all along the tower height (see hypotheses section).
- Moreover, we have the force of the wind actuating on the tower, This force has been proved to be proportional to the wind speed, and it has been modelled according to [3], as it has been fully explained in Appendix B).
- Finally, we have the forces caused by the sea. These forces are applied on the submerged part of the tower through waves. However, we have to set out that we have considered two types of waves. On the one hand there are the swell sea waves, which are the ones already present in the sea independently of the wind conditions; they have been created far away from the windmill and travel along the sea. The other type of waves are what we have called the wind waves, which are the ones created *because of the wind* (so they are computed from the value for v_{hub}). With reference to the sea waves, their orientation with respect to the position of the global axis is aleatory, so this force will be split into two components. The wind waves, however, have to be in the same direction of the wind (by definition of the global axis, see Figure 2.1), so no uncertainty is associated to its definition. The details about the computation of such forces are in Appendix B.

With reference to the submerged part, it is relevant to point out that the tower is under the hydrostatic pressure (Figure 2.38 and Figure 2.39). However, the force on the tower has, overall, a null resultant, so in fact it is not important.It could be arguable whether the pressure is actually hydrostatic since, in fact, there is acceleration on the water, so the situation should not be necessarily hydrostatic. Nonetheless, considering the degree of accuracy of the present model this assumption is appropriate.

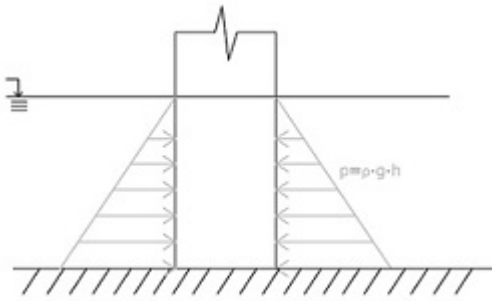

Figure 2.38: Hydrostatic pressure on the submerged part of the tower (*source: self elaboration*).

Secondly, it is important to set out a few comments on the sea forces. These forces have been estimated through the wave heights. In other words, we have computed the forces produced by the sea from the values of the amplitudes for both wind and swell waves. The value for the wave height, however, is a random variable, since not all the waves have the same height. Therefore, a representative value has been taken into consideration; this value is the so called *significant height* of the waves, which is the average value between the 33% upper values for wave heights. This value has been widely accepted to be the one to consider when dealing with wave heights, so in all formulas where we are working with a wave height we have to understand that value to be the significant height of the wave. With regard to the characterization of these waves (and the forces they produce on the tower base), it is important to state that we only need to know a value for the amplitude (significant height) and a value for the period (so, as far as we know the amplitudes and periods for both waves we will be able to estimate the forces on the tower). There is an extra comment to make about this particular topic. It seems painfully obvious how both the height and the period have to be, somehow, coupled, since it does not seem reasonable to have extremely high wave heights with short periods of time (a thorough study is proposed in [43]). However, we do not have considered a relationship

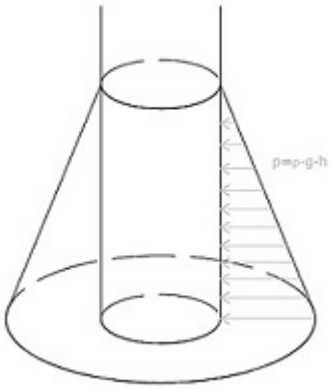

Figure 2.39: 3D representation of the hydrostatic pressure actuating on the tower (*source: self elaboration*).

Figure 2.40: Summary of the efforts transmitted from the nacelle onto the tower (*source: self elaboration*).

between them and we have assumed them to be independent. In order to see the full development of the expressions of these forces we may refer to Appendix C, where apart from modelling such forces the hypotheses that have been considered are justified. Several comments will have to be made regarding the fact we have considered the period and the wave height to be independent; they will be done in the conclusions part, where a comprehensive analysis and justification will be made.

Before building the equations, the following considerations have been made. First, we have supposed that the deformations on the tower are small enough to apply the small deformations theory, which means that the methodology from the resistance of materials is applicable ([32]). This hypothesis has been verified once the results have been obtained and has been proved to be accurate (since the deformations at the top of the tower have been checked to be small enough). Moreover, the behaviour of the tower has assumed to be like a corbel (perfectly fixed beam on one extreme and free on the other one), so the boundary conditions will be analogous to the ones of the blades. With reference to why all the forces are applied on the directrix of the tower, the explanation is because of the symmetry that there is with respect to the axis of the tower. In other words, we have assumed all the forces to be constant along the diameter of the tower (4 m long), so the resultant is consequently applied on the directrix. Once again, that hypothesis is only true "on average", since certain variability has to be expected along the diameter of the tower. However, given that the distance (4 m) is small and that these variations are aleatory, we will assume that these differences are, on average, irrelevant. Finally, we have to state that no corrosion has been considered on the tower, which means that the resistance characteristics of the tower remain uniform with time. In reality, we would expect the area of sea surface to be the most vulnerable as time goes by, but in our model the resistance parameters will evolve the same way for all the tower.

With respect to the forces transmitted from the nacelle to the tower, they are summarized in Figure 2.40; it is important to note that $R_Z = 0$, for the reasons exposed in the previous section.

With reference to the reactions forces on the floor, their value can be easily obtained from Newton equilibrium, according to Figure 2.41:

$$R_X = F_{M,X} + F_S + F_W + F_N,$$

$$R_Y = W_T + W_R + W_N + F_I,$$

$$R_Z = F_{M,Z},$$

where F_S stands for the wind wave force, $F_{M,X}$ for the x component of the swell sea force, $F_{M,Z}$ for the z component, F_W for the wind force and W_i for the weights of the different parts of the windmill (tower, rotor and nacelle).

With reference to the structural problem associated to the behaviour of the tower, we have to say that we will be dealing with the same type of differential equations as in the case of the blades

(flexion problem on two axes). However, we will have to deal in addition with a third non-zero moment which did not appear in the case of the blades: the torsion on the tower. The problem associated to torsion, nevertheless, will always be trivial to solve since we have assumed by hypothesis that all the forces actuating on the tower have their directions applied on the directrix. Therefore, the equation of equilibrium leads to:

$$M_Y = M_{Y,nacelle},$$

which means that the reaction moment at the base is constant and equal to the torsion moment applied on the nacelle as a result of the horizontal eccentricity of the force of the wind.

With reference to the main flexion problem to find M_Z, we have to refer to Figure 2.41. In this scheme we can see how there are several forces applied on the tower, but that the region where they are applied is not the same. As it can be checked in the figure, there are three relevant levels. First, we have the calm water level, which is the level of the sea under conditions of no waves at all. This is the level from which the wind force is computed, and from which all the references to the height with respect to the sea level are made. Secondly, we have the swell sea water level, which is equal to the calm water level plus the significant wave height for the swell sea. In fact, this is not a real water level, since the water oscillates with the waves (the significant height value is the amplitude of the wave). It is important to remark that since the force of the waves is cyclical we will analyse the maximum value for the force on the tower, which happens when at the maximum height, according to what is explained in Appendix C. Therefore, in our analysis we will be considering the level calm level + significant height of the swell sea. Finally, superposed to the swell sea we have defined the wind sea level, which is the swell sea level plus the significant height of the wind waves; the explanation for that is the same as for the swell sea waters, just to define the domain in which the wind wave forces will be applicable. Therefore, we can finally define 4 domains, which have been marked with different colours on the tower of Figure 2.41. These 4 domains have different equilibrium equations because they have different forces applied (for example, in the last domain there is only the force of the wind and in the first one there are the swell waves, wind waves but not wind). As it will be developed step by step, these domains are linked because of continuity boundary conditions. However, since the domains are different 4 non-linear systems of differential equations will have to be solved. Finally, we have to mention that by proceeding this way we are assuming a perfect superposition of the swell sea waves and the wind waves, since we are adding both significant heights (so we are supposing that the maximums are perfectly superposed). In fact, these two types of waves oscillate separately, and the levels we have defined vary in quite a complex way. However, by doing this hypothesis we are considering the particular case which may result in collapse of the structure, which is the most interesting one regarding the vulnerability (maximum force on the tower). It could be arguable, though, whether a less conservative approach should have been taken, because this assumption somehow overestimates the actions that are applied on the windmill.

Now we will proceed to develop the equilibrium equations for the 4 domains of the tower. In all of them the same methodology will be applied, which is equilibrium on a differential part of the tower in order to reach the differential system of equations associated to the domain, according to [32] and in the same way as proposed in [10]. Let h be the calm water level:

Case 1: $0 < s < h$ -there are $F_{M,X}$ and F_S- (purple domain)
The forces actuating on a differential part of the domain are summarized in Figure 2.42. By applying Newton's equilibrium we reach the expression of the system of differential equations.

$$\sum M_A = 0,$$

$$0 = \left(R_X - \int_0^s f_{M,X} ds - \int_0^s f_S ds\right) \cdot ds \cdot \cos\theta + (R_Y - \pi \cdot \gamma_s \cdot (R^2 - r^2) \cdot s) \cdot ds \cdot \sin\theta - M + M + dM,$$

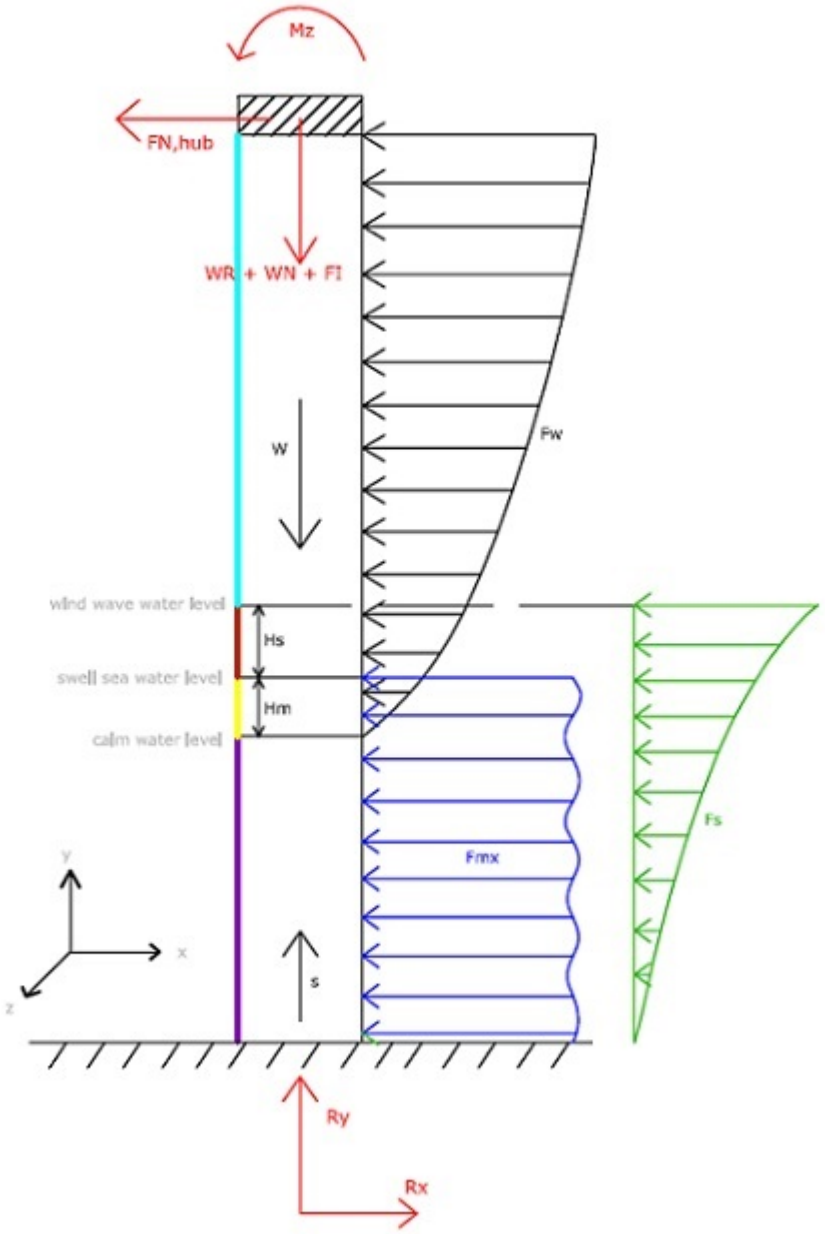

Figure 2.41: Forces and moments on the tower (*source: self elaboration*).

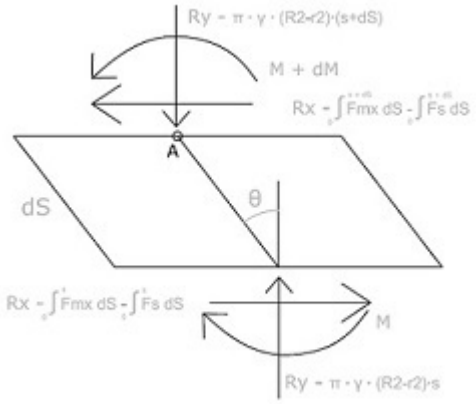

Figure 2.42: Forces applied on a differential part of the tower for case 1 (*source: self elaboration*).

$$\frac{dM}{ds} = -\left(R_X - \int_0^s f_{M,X}ds - \int_0^s f_S ds\right)\cdot\cos\theta - (R_Y - \pi\cdot\gamma_s\cdot(R^2-r^2)\cdot s)\cdot\sin\theta,$$

where γ_s stands for the specific weight of steel, R_X, R_Y, R_Z stand for the reaction forces at the base of the tower and R and r stand for the external and internal radius of the tower tube.

Now, by applying the same further equations as before (as defined in [32]):

$$M = \chi \mathrm{EI},$$
$$\chi = \frac{d\theta}{ds},$$

we reach the following non-linear system of differential equations:

$$\begin{cases} \frac{d^2\theta}{ds^2} = -\frac{1}{\mathrm{EI}}\cdot\left(\left(R_X - \int_0^s f_{M,X}ds - \int_0^s f_S ds\right)\cdot\cos\theta + (R_Y - \pi\cdot\gamma_s\cdot(R^2-r^2)\cdot s)\cdot\sin\theta\right) \\ \frac{dy}{ds} = \cos\theta \\ \frac{dx}{ds} = -\sin\theta. \end{cases}$$

With regard to the boundary conditions, they will be stated at the end.

Case 2: $h < s < h + H_m$ -there are $F_{M,X}$, F_S and F_W- (yellow domain)
By applying the exact same methodology as before we reach the following non-linear system of differential equations, according to Figure 2.43:

$$\begin{cases} \frac{d^2\theta}{ds^2} = -\frac{1}{\mathrm{EI}}\cdot\left(\left(R_X - \int_0^s f_{M,X}ds - \int_0^s f_S ds - \int_h^s f_W ds\right)\cdot\cos\theta + (R_Y - \pi\cdot\gamma_s\cdot(R^2-r^2)\cdot s)\cdot\sin\theta\right) \\ \frac{dy}{ds} = \cos\theta \\ \frac{dx}{ds} = -\sin\theta. \end{cases}$$

Case 3: $h + H_m < s < h + H_m + H_s$ -there are F_S and F_W- (red domain)

By applying the exact same methodology as before we reach the following non-linear system of differential equations, according to Figure 2.44:

$$\begin{cases} \frac{d^2\theta}{ds^2} = -\frac{1}{\mathrm{EI}}\cdot\left(\left(R_X - F_{M,X} - \int_0^s f_S ds - \int_h^s f_W ds\right)\cdot\cos\theta + (R_Y - \pi\cdot\gamma_s\cdot(R^2-r^2)\cdot s)\cdot\sin\theta\right) \\ \frac{dy}{ds} = \cos\theta \\ \frac{dx}{ds} = -\sin\theta. \end{cases}$$

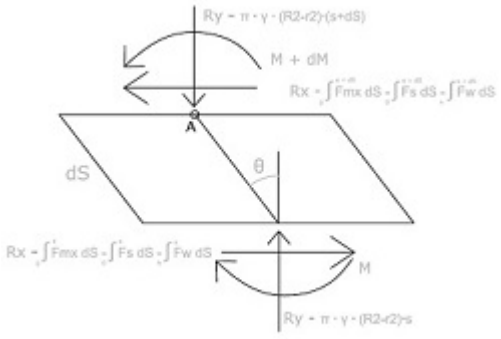

Figure 2.43: Forces applied on a differential part of the tower for case 2 (*source: self elaboration*).

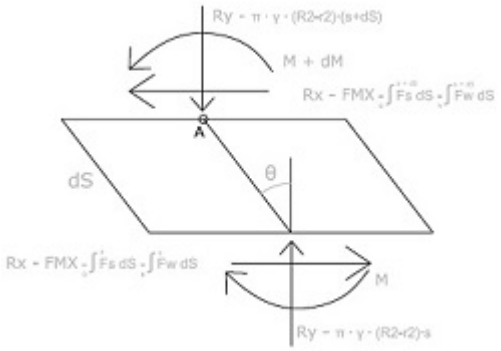

Figure 2.44: Forces applied on a differential part of the tower for case 3 (*source: self elaboration*).

Case 4: $s > h + H_m + H_s$ -there are F_S and F_W- (blue domain)

By applying the exact same methodology as before we reach the following non-linear system of differential equations:

$$\begin{cases} \frac{d^2\theta}{ds^2} = -\frac{1}{\mathrm{EI}} \cdot \left(\left(R_X - F_{M,X} - F_S - \int_h^s f_W ds \right) \cdot \cos\theta + (R_Y - \pi \cdot \gamma_s \cdot (R^2 - r^2) \cdot s) \cdot \sin\theta \right) \\ \frac{dy}{ds} = \cos\theta \\ \frac{dx}{ds} = -\sin\theta. \end{cases}$$

With reference to the boundary conditions, 4 of them are the ones we would be expecting for a corbel (two for fixing the axes, the one imposing angle equal to zero in the beginning and the one imposing moment equal to zero in the free extreme). However, since there are 4 systems of equations we still need 12 boundary conditions to get the solution we want. These 12 boundary conditions are the continuity equations for x, y, θ and $\frac{d\theta}{ds}$ at the 3 changes of domain we have defined ($s = h$, $s = h + H_m$ and $s = h + H_m + H_s$). Therefore, we now have the 16 boundary conditions that need to be set in order to get the expression of the deformed beam and the moment in the beginning. With reference to the methodology we have used to solve this problem, it is the same shooting method we applied earlier for the blades, but in a more complex problem (since the resolution of these 4 non-linear and linked systems of differential equations is more difficult to solve). Essentially, the main difficulty is that the 4 systems of equations are linked, so we have to solve them at the same time and the computational cost is higher.

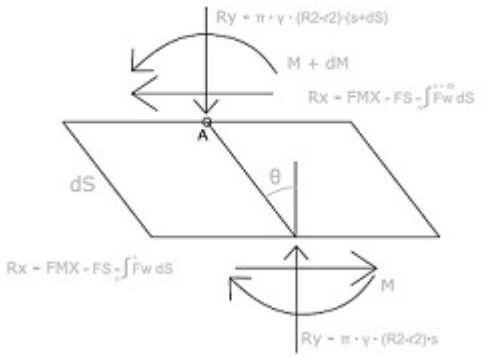

Figure 2.45: Forces applied on a differential part of the tower for case 4 (*source: self elaboration*).

Finally, before addressing the other problem of the moments on the other planes, it is important to make the following remarks. First, in the previous equations we have used implicitly the simplification $s = y$; in other words, the levels for the sea are values for y (vertical coordinate of the tower), not for s (arc parameter), which is our integration parameter. In fact, were we to strictly consider the deformation of the tower, the limits of the domains would be expressed not in the s which is our integration parameter but with y which is its projection on the vertical axis. However, since the deformations are small we have simplified $y = h$ for $s = h$. Secondly, we have to state that like the problem with the blades we are interested in the deformed geometry of the tower, so we should solve these systems of equations for example through the shooting method. However, even though we will focus on this aspect in the "Breaking criterion" section, we have to say that the process of obtaining the deformed geometry (through solving the differential systems of equations) leads to an unaffordable problem in terms of time. It is important to highlight the fact that these calculations will be done for the huge amount of simulations we will have to carry out. Therefore, as long as we need 3 million simulations, finding the deformed geometry of the tower becomes impossible (according to the limited time that we have). Consequently, we have to clearly set out that in our computations we have found the reactions through equilibrium but have not solved the differential systems of equations, so we have not obtained the final geometry and deformation of the tower. By doing that, we have accelerated the calculation process, though we have lost the possibility to take deformations into consideration for the analysis. In case further studies could afford to take them into consideration, they would only have to include the solution of the previous systems of equations.

With regard to the other moment on the floor, M_X, we have proceeded the same way as before, according to Figure 2.46. In this case, the only force that is present, apart from the reactions transmitted from the nacelle and the weight of the tower, is the z component of the swell waves force. It is important to point out that both the wind wave forces and the wind force are strictly perpendicular to the plane we are studying, because we have assumed by hypothesis they are that way. Therefore, now we only have two domains:

Case 1: $0 < s < h + H_m$

$$\sum M_A = 0,$$

$$0 = \left(R_Z - \int_0^s f_{M,Z} ds \right) \cdot ds \cdot \cos\theta + (R_Y - \pi \cdot \gamma_s \cdot (R^2 - r^2) \cdot s) \cdot ds \cdot \sin\theta - M + M + dM,$$

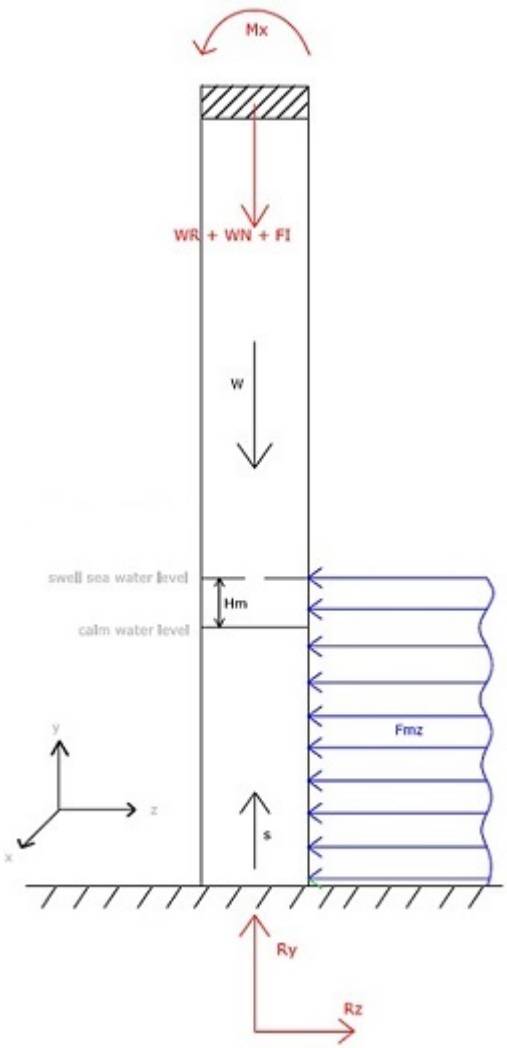

Figure 2.46: Forces and moments diagram on the perpendicular plane of the tower (*source: self elaboration*).

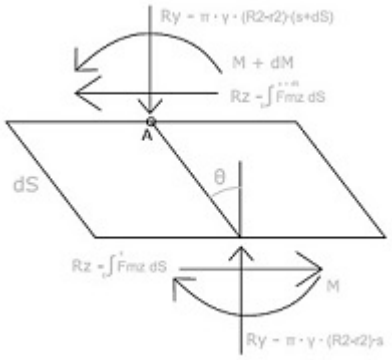

Figure 2.47: Forces applied on a differential part of the tower for case 1 (*source: self elaboration*).

$$\frac{dM}{ds} = -\left(R_Z - \int_0^s f_{M,Z} ds\right) \cdot \cos\theta - (R_Y - \pi \cdot \gamma_s \cdot (R^2 - r^2) \cdot s) \cdot \sin\theta.$$

Now, we apply the same as before:

$$M = \chi \mathrm{EI},$$
$$\chi = \frac{d\theta}{ds}.$$

The following non-linear system of differential equations is obtained:

$$\begin{cases} \frac{d^2\theta}{ds^2} = -\frac{1}{\mathrm{EI}} \cdot \left(R_Z - \int_0^s f_{M,Z} ds\right) \cdot \cos\theta - (R_Y - \pi \cdot \gamma_s \cdot (R^2 - r^2) \cdot s) \cdot \sin\theta \\ \frac{dy}{ds} = \cos\theta \\ \frac{dz}{ds} = -\sin\theta \end{cases}$$

Case 2: $s > h + H_m$

By applying the exact same methodology as before we reach the following non-linear system of differential equations:

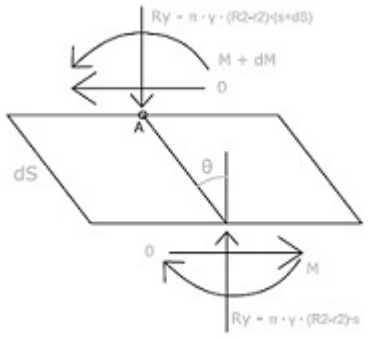

Figure 2.48: Forces applied on a differential part of the tower for case 2 (*source: self elaboration*).

$$\begin{cases} \frac{d^2\theta}{ds^2} = -\frac{1}{\mathrm{EI}} \cdot \left(R_Y - \pi \cdot \gamma_s \cdot (R^2 - r^2) \cdot s\right) \cdot \sin\theta \\ \frac{dy}{ds} = \cos\theta \\ \frac{dx}{ds} = -\sin\theta. \end{cases}$$

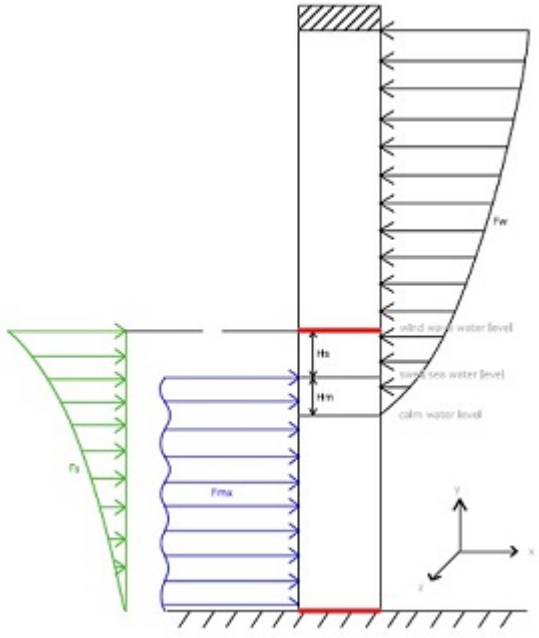

Figure 2.49: Critical points on the tower according to the loading system we have considered (*source: self elaboration*).

The boundary conditions, as we previously developed, will be the 4 ones for a corbel plus 4 continuity conditions for $s = h + H_m$.

However, with respect to the vulnerability of the tower, once the deformations and the moments on the base have been found, there are two candidate points which can be critical with reference to the stability. Unlike the previous case of the blades where all the forces had the same direction, now it is possible to get that the case summarized in Figure 2.49 is more restrictive than the union with the floor. As it is explained in Appendix B, the forces provided by the waves are cyclical, and vary between a minimum and a maximum value which are opposite; in other words, the maximum force on the tower can either be in one direction or in the opposite. When we have dealt with the main flexion problem on the tower, we have assumed a superposition of the actuating forces so that they do not compensate each other; for that case, the efforts that have been found are the maximum that can be obtained, and the most restrictive point is clearly the base of the tower. However, once the problem has been set, we have to consider the case in which the sea forces compensate the wind force. In that situation the most restrictive point is no longer at the base of the tower but at the sea surface (even though it is not clear where exactly the critical point would be). Therefore, solving the flexion problem by finding the most important efforts at the tower means having to solve the "two worst possible situations" according to the direction of the forces. It is important to keep in mind that both problems come from the same situation, since for a fixed wind speed the forces provided by the sea waves oscillate, so two *extreme* situations are possible. To solve this second problem the same methodology has been applied but with $-F_M$ instead of F_M and with$-F_S$ instead of F_S, in order to get the new reactions on the base and be able to compute the effort state at the surface of the sea.

2.4 Breaking criterion

In order to study the vulnerability of the windmill we have set up three parts which we have studied separately: blades, nacelle and tower. The aim of having made this distinction is that by studying the vulnerability of these separate components of the windmill we are able to determine with higher accuracy what the exact situation od the windmill is. In other words, by studying the blades separately of the tower we are able to evaluate whether the windmill is at the "service" state, it has "blade damage" (which means that the blades have broken down) or whether the windmill is at complete destruction (the tower has broken down). It is important to remark, once again, that we have not studied the nacelle in the same terms we have analyzed the tower or the blades (we have assumed the nacelle to transmit the forces from the blades to the tower without any possible risk to break down, which means that the windmill will either break on its blades or break down completely at the tower).

With reference to the methodology that has been applied to determine whether the blades or the tower break down we must refer to [44] and [41]. We have assumed that both the blades and the tower can only break through plastic yielding at the critical sections which have been fully characterized in the present chapter. It is arguable, though, why we have not made a further analysis on the stability of the windmill, since plastic yielding is not the only possible way to break down. The clearest example of that may be the tower case: the tower can be understood as a structure under flexion and compression. Therefore, according to [13] plastic yielding is not the only breaking possibility, since there are alternative collapses which may occur before plastic yielding takes place. It would be also arguable whether the Von Mises criterion is the most appropriate way to evaluate the stability. The explanation for that has to be made by taking into consideration the whole procedure of the present project. In fact, whatever the physical model is, the fact is that we will be using it repeatedly in order to carry out the Monte Carlo simulation. Therefore, since we will be carrying out the same calculations for a little bit more than 3 million times, we have to be very selective at the moment of defining the model. It is painfully obvious that such simplifications may generate problems with respect to the final accuracy of the results, but we have to keep in mind that in order to reach a solution for the problem with the limited resources we have (in terms of time), a very simple physical modelling is required. From this statement, obviously, we can infer that in case further studies were to be made, they could definitely achieve a more accurate outcome by improving the present physical model.

At the beginning of the project the breaking criterion had to include an evaluation of the deformed geometry; in fact, as it has just been developed, through the differential equations of equilibrium we are eventually able to define what the exact deformation at the tower and blades is. The main idea was to consider that for both blade and tower there was a limit deformation for which we considered collapse. However, as it is clear from the definition of such equations, solving all the differential systems of equations is by all means unaffordable (in terms of computational cost, the simulation with such degree of complexity in the calculations was extremely more expensive). In other words, when trying to compute the simulation we have found ourselves with the following trade-off problem: on the one hand, it would be possible to include the evaluation of the deformations on the model through finding the deformed geometry with the differential systems of equations, but by doing this we would not be able to compute as many simulations as in the case we did not consider them. Therefore, even though the introduction of the deformations in the model could seem to make the accuracy increase, in fact since we would end up with fewer simulations the results would be significatively worse. For the reason we have just set out, we made the decision to find the reactions by equilibrium but without solving the differential equilibrium equations, so no consideration about the deformation has been included in the model. By doing this simplification, the most *expensive* part of the simulation is not reduced (since it is the part of computing the forces of the wind and sea waves), but the computational

cost allows us to achieve a reasonably adequate result considering the available resources (in terms of time) that we have. However, in case any studies were to be made in the future, the deformations could be easily introduced at the model, though the computation time would be significatively higher.

2.4.1 Tower collapse

According to [41], by assuming the Von Mises criterion, once we know by equilibrium the efforts at the critical sections that we want to analyze we can build up the *comparative stress* σ_{co}:

$$\sigma_{co} = \sqrt{\sigma^2 + 3 \cdot (\tau + \tau_T)^2},$$

where the involved parameters will be defined right after. Once this value has been computed, it will be compared to the yield limit of the material (in this case, 355 MPa steel, see properties in the 6th chapter 'Materiales' from [39]). In order not to break down, it must be verified that:

$$\sigma_{co} \leq f_y,$$

otherwise, the yielding limit will be achieved and there will be collapse.

With reference to the computation of σ_{co}, we have to define the different terms which are involved. The first term, σ, stands for the tension at the section, and can be calculated as follows, according to the conventional expressions for the tension in resistance of materials [41]:

$$\sigma = \frac{N}{Area} + \frac{M}{W},$$

where N stands for the axial resultant force, M for the moments on both directions and W for the elastic modulus. In fact, there should be two moment terms in the formula, but since the tower is symmetric the elastic modulus are the same so we can work with the sum of moments. Therefore, according to the formulation we have used in MatLAB and in the present chapter:

$$\sigma = \frac{F_{Y,tower}}{Area} + \frac{M_{X,tower} + M_{Z,tower}}{W_{el}},$$

where the elastic modulus W_{el} is calculated as $\frac{I_{tower}}{D/2}$, with D being the external diameter of the tower (so D/2 is the distance from to the center to the furthest fibre).

With reference to τ_T, we have to say that the "T" stands for *torsion*, and that is computed in the following way, according to [41]:

$$\tau_T = \frac{T}{2 \cdot S \cdot t},$$

where T stands for the torsion moment on the tower, S stands for the "area contained inside the medium line of the section", and t stands for the thickness of the tower (5 cm). These parameters have been schematized in Figure 2.50. By using the nomenclature we have set out in the present project:

$$\tau_T = \frac{M_{Y,tower}}{2 \cdot S \cdot t}.$$

Finally, τ stands for the τ due to flexion, and according to [41], it can be computed:

$$\tau_{flexion} = \frac{Q}{0.5 \cdot Area},$$

where Q stands for shear force at the tower. Again, by introducing our nomenclature:

$$\tau_{flexion} = \frac{F_{X,tower} + F_{Z,tower}}{0.5 \cdot Area}.$$

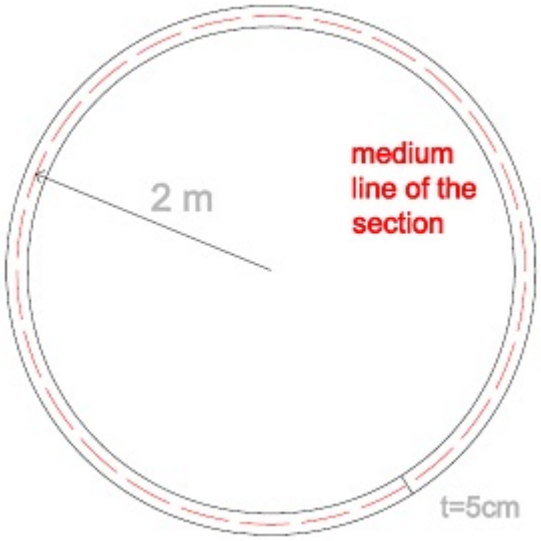

Figure 2.50: Representation of the medium line of the section and the thickness t of the base of the tower (*source: self elaboration*).

Having set out the methodology to compute σ_{co}, we must add a few remarks. First, it is easy to see that as long as we are able to provide the values for the forces and moments on the three directions of space for the critical sections, we will be able to build up σ_{co} and determine whether $\sigma_{co} \leq f_y$, so we will be able to easily evaluate whether the tower breaks or not. Second, we must say that both terms of the Von Mises equation, σ_{co} and f_y are variable, since σ_{co} is dependent on the forces on the tower and the value f_y is assumed to be a log-normally distributed parameter. Therefore, this procedure will be carried out at every simulation.

2.4.2 Blade collapse: fracture at the hub

With regard to the blade analysis, the same methodology will be applied as in the tower, even though the results we may end up getting might be less accurate than for the case of the tower. Therefore, we will be comparing the same expression for σ_{co} with the yield limit of the blade:

$$\sigma_{co} = \sqrt{\sigma^2 + 3 \cdot (\tau + \tau_T)^2} \leq f_{y,blade}$$

However, the material the blade is made of is not homogeneous, since its composition is usually made of steel and a composite (typically carbon or glass fiber). Consequently, even though we will be using an equivalent yield limit $f_{y,blade}$-which will be assumed to be a log-normally distributed parameter (see hypotheses)- the behaviour associated to the blade will not be necessarily analogous to the tower in reality. Nevertheless, the fact of using this method provides a straightforward system to evaluate the state of the blade at its base.

With reference to σ, according to [41] and proceeding analogously to tower study:

$$\sigma = \frac{N}{Area} + \frac{M}{W} = \frac{F_{X,blade}}{Area} + \frac{M_{Y,blade} + M_{Z,blade}}{W_{el}}.$$

It is important to make a few remarks on the previous calculation. First, we have to be aware of the fact that the section of the blade is not constant, so we will have to study the geometry at the union of the hub: in order to simplify the calculations, we have assumed that the section of the blade is

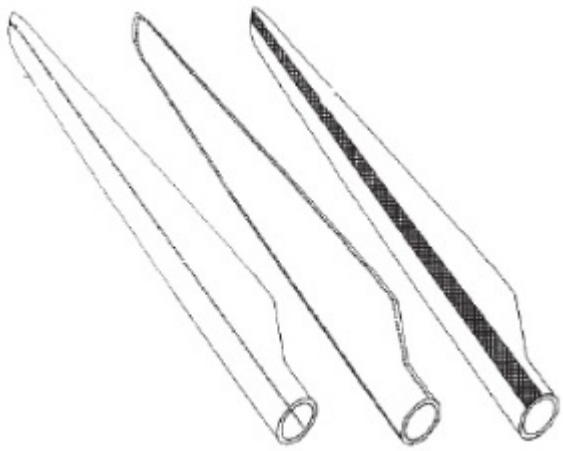

Figure 2.51: Simplified geometry of a windmill blade (*source: [35]*).

circular at the union with the hub, as it is schematized in Figure 2.51. Consequently, the value for W_{el} can be considered as equal for both directions of the moment, so the moments can be studied together.

With reference to the torsion component τ_T, we have to say that since no torsion has been considered at the blade by hypothesis, this term will necessarily be null. However, should any further study consider torsion, this term would have to be computed accordingly.

Referring to τ, its value will be computed as we have already done with the tower, and according to [41]:

$$\tau_{flexion} = \frac{Q}{0.5 \cdot Area} = \frac{F_{Y,blade} + F_{Z,blade}}{0.5 \cdot Area}.$$

2.4.3 Quantitative definition of the three possible states

Once the breaking criterion has been fixed, it is easy to characterize the different states that can take place in the windmill under any circumstances. It is important to comment, though, that in case the state is "total collapse" (state 2) it does not matter whether the blades are broken or not, since the "total collapse" state is more restrictive. The *logical path* to determine the final state of the windmill has been schematized in Figure 2.52.

As a final comment, it is important to keep in mind the reason why we have used this criterion: the purpose of the present project is to build a Monte Carlo simulation to approach the structural problem of the vulnerability of an off-shore windmill. Therefore, an extremely simple method is needed in order to be able to compute as many simulations as possible. As we already commented in this chapter, by simplifying the breaking criterion we are certainly losing accuracy as well, so the problem to maximize the accuracy of the results with the very limited resources that we have is a trade-off between the number of simulations and the thoroughness of the structural analysis. However, with regard to this idea we have to say that the problem of studying the breaking process of the blade could have been a single project by itself, so by approaching this process with a conventional resistance of materials' point of view seems to be a reasonable solution.

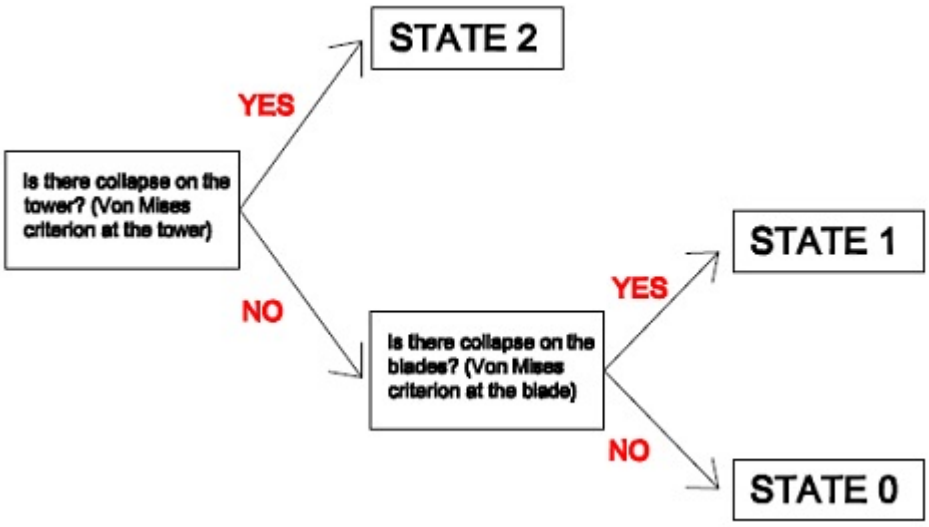

Figure 2.52: Possible states of the windmill according to the results of the breaking criterion (*source: self elaboration*).

2.5 Comments on the behaviour model of the windmill and proposal on the possible improvements for future studies

2.5.1 Comments on the blade analysis

1. Regarding the forces on the windmill when it is operating, we have to say that we have overestimated its value, so the results we may have obtained may provide a slightly more *vulnerable* windmill than the real one; the explanation for that is that since the forces are cyclical we have had to figure out a simple and consistent solution, so a little additional uncertainty has been generated (see Figure 2.6). This solution has been to consider the "worst case we can think of", which means considering all the maximum values of the reactions at the same time, even though that is an impossible situation in practice.

2. With reference to the physical approach, we have to say that we have not studied the deceleration which takes place at the cut-off wind speed; as we commented when setting out the equations for the behaviour, we have assumed that the windmill is stopped in case $v_{hub} > 25$ and operating at a constant speed in case $v_{hub} < 25$. However, in between these two situations there is a transient state where the efforts on the windmill may be very important, which is the case when the windmill is about to stop. The study of this transient state is by far more complex than the other two situations, and involves considering the turbulence which happens at the blades and makes them reduce their velocity, according to [31]. In case any further studies where to be made, this would certainly be an important detail to consider since it is very probable that the efforts at this particular time are very significative.

3. In the same way we have talked about the cut-off wind speed transient state, we should refer as well to the *initialization wind speed* or cut-in wind speed, which is the wind speed threshold in which the blades start moving. Even though we have not introduced it in our model, it seems pretty obvious that for certain extremely low values of wind speed the system is not able to operate normally, since the force provided by the wind is unable to maintain the windmill at

the "operating state" (according to [4], this cut-in wind speed is around 4 m/s, even though it varies along different types of turbine). The reason why we have not introduced it in our model is because it implied considering a transient acceleration state which would not probably be significative. Therefore, we have made the simplification that the windmill can operate under the cut-in wind speed, even though that does not happen in practice. However, these simplification does not seem to be problematic, since it seems intuitive that in case there is no wind at all the windmill is much more stable that under stronger wind conditions, so whatsoever problems which may arise for that wind speed are far less important than the potential problems generated by higher wind speeds.

4. With reference to the torsion, we have to say that even though by considering an uniform wind speed field we have been able to simplify the calculations, a few remarks have to be made. First, even though it can seem reasonable to assume that the force of the wind is applied on the directrix of the blade so no torsion is induced on the rotor, it is arguable whether we should have considered a general case and included the torsional term (which would have resulted in a more complex σ_{co} expression. Therefore, even though the results we have obtained are consistent with what was stated in [31], a deeper analysis could be made in case this project was to be progressed to a further study. Second, we have to make an important comment regarding the structural analysis: since the section of the blade is not symmetric, as long as there is a flexion effort there will appear torsion on the blade, so it will be under a flexion-torsion state, according to [13]. The explanation why we have not considered this phenomenon is that the geometry of the blade is very complex so it would have certainly been difficult to take the torsional term induced by the non-symmetry of the blade section. However, this detail should be addressed in case a more accurate result was required in future endeavors.

5. Regarding the structural analysis of the blade, we do have to refer to the hypothesis of treating it as a corbel (beam perfectly fixed on one extreme and free on the other one). In fact, since the length of the blade is approximately 40 meters long and 3.5 meters "wide" it seems reasonable to study it as a beam . However, since its geometry is not constant, it could be arguable whether a deeper analysis should have been made. However, according to the results we have found this hypothesis seems to have been validated.

6. Regarding the structural approach we have taken to tackle the structural problem of the blades we should mention the simplification we have made of the *conicity*, according to [31]. The *conicity* term refers to the inclination of the blades "towards" the wind in order to improve the structural stability as well as ensuring that under no circumstances the blades touch the tower when rotating. This *conicity* is described through the angle between the blades and the vertical axis and its structural impact is limited. However, even though the assumption of treating the blades as vertical (so assuming zero *conicity*) has worked very well with the present model, we should say that in further studies this detail could be taken into consideration.

7. With regard to the geometry of the blade, we have to say that the results we have obtained have somehow overestimated the vulnerability of the windmill for the following reason. In order to simplify the calculations, we have assumed the blade as a beam, so we have assumed its weight to be an uniform force along the radius. However, according to [35] the blades tend to concentrate its mass at the junction with the hub, so by assuming an uniform repartition of the weight force we are overestimating the inertial terms due to rotation.

8. With reference to the stopped windmill situation, we have to comment on the fact of considering that all the positions of the blade are equivalent. Even though that is a hypothesis which is

aligned with the degree of accuracy that we can expect to have according to the assumptions that have been made, we should clearly state that *not all positions are equivalent*, since the wind speed increases with height.

9. According to the initial hypotheses, we have considered no turbulence occurring at the blades, apart from the turbulence associated to the cut-off wind speed (turbulence which explains that the windmill stops). However, since air is a continuous media, we have to say that the model we have presented has considered the wind to be one-dimensional and at ideal conditions (so by definition we have assumed a non-turbulent flow). In case turbulence was about to be included in the model, the expressions of the equations would definitely become much more complex, since according to [31] they would have to include a stochastic component.

10. Finally, regarding to the blade analysis we have to highlight the fact that no resonance has been considered in the project. In fact, neglecting the potential effects of resonance can be extremely dangerous. However, the fact of introducing this topic on the model would have generated a problem by itself which could have easily become a *treball de final de grau* by itself, so we have taken this part of the study out of the model. Nevertheless, the potential vulnerability due to resonance should be definitely taken into consideration in case any further analysis were to be made, and a possible approach to the problem could be the one proposed in [31].

2.5.2 Comments on the nacelle analysis

To start with, we should remind that we have not considered collapse in the nacelle, since we have assumed it transmits without any problems the forces from the rotor to the tower. However, in fact, collapse on the union with the tower could certainly be a problem. Therefore, before commenting on further hypotheses we have to state that the vulnerability study of the nacelle has not been thorough. The reason why there is this additional uncertainty associated to the nacelle is double. First, a proper nacelle analysis should take into consideration mechanical details (associated to the natural operating features of the windmill): since no mechanical issues have been considered on the present project the study of the nacelle has to become inaccurate. In addition, no information has been found about the actual system to connect the hub to the tower. From [31] we have obtained a general overview on the construction process, but no technical information has been found regarding the number of bolts that are used to have join the hub with the tower. Therefore, the nacelle problem should definitely be improved in further analysis. Regarding the modelling of the transmitted forces to the tower, we should make a few comments:

1. First, we have assumed that the resultant of the vertical forces of the nacelle and rotor are aligned with the directrix of the tower. Since we have not defined thoroughly the nacelle, we have to say that we are not able to determine whether there is an additional eccentricity of this force generating additional flexion on the tower. This problem should be addressed by determining in more detail the exact point of application of the weights (with a deeper study of the system nacelle + rotor). In fact, in the present project we have assumed the nacelle to be *like a point with all the mass concentrated on it*, so no possible eccentricity has been considered with respect to the gravitational forces applied on it. In case this part was to be improved in further analysis, [4] could be a reliable source of geometric data for the nacelle.

2. Regarding the transient state at the cut-off wind speed, we should also point out the possible uncertainty associated to the behaviour of the nacelle. Moreover, the same concerns about the potential peak efforts on the blades at that point are still applicable for the nacelle, so the same comment about the possible future studies has to be made.

3. With reference to the horizontal forces we have to say that the introduction of the horizontal and vertical eccentricities has allowed us to take into consideration the potential effects of a misalignment of the resultant force on the windmill with respect to the hub. However, even though this approach has been successful in terms of being able to model the potential additional moments due to the position of the resultant force of the wind, we have to say that the logit-normal distributions might not be the most appropriate to describe these eccentricities. In other words, it is painfully obvious that these eccentricities exist, and that there are extra moments on the tower due to their presence, but it is not straightforward to infer that the logit-normal model is the best system to take them into consideration. Consequently, any subsequent study should consider a deeper research concerning this topic.

2.5.3 Comments on the tower analysis

1. First, and analogously to the blade comments, we have to state that the fact of treating the tower as a corbel has been proven to provide acceptable results, according to what we have eventually obtained and what we expected from [31]. Therefore, the principles applied from the resistance of materials theory could be assumed as well for further studies.

2. The main problem associated to the structural analysis of the tower is certainly the treatment of the sea forces, especially the different sea levels that have been used to compute the sea forces. In fact, there are a few comments to make with regard to this topic. First, we have to say that the sea force has a swell component, independent of the wind conditions, as well as a wind wave sea force associated to the waves induced by the presence of the wind. Therefore, no matter what approach we take to tackle this situation we will have to deal with two types of waves that may superpose and generate a variable resultant force. Moreover, several hypotheses have been made in order to end up with a *reasonable* problem (for more information see Appendix C). For the reasons exposed above, even though we have taken a conservative approach by considering the force of the waves as the superposition of the maximums of the forces, we have to say that there is certainly uncertainty associated to the results, not because the methodology is wrong but because the amount of additional hypotheses that have had to be made to reach an affordable problem.

3. With reference to the waves we have to make a remark on the approach we have taken to address the problem of the direction of the forces. Even though there is a full explanation on Appendix C, it is important to keep in mind the methodology we have carried out. In the present project we have assumed the wind speed to have an arbitrary direction; it is this direction which fixes the coordinate system, because the windmill is designed to stay always towards the wind. Once this direction has been fixed, it is easy to assume that the waves induced by the wind will have this direction. However, the swell sea can have any direction with respect to the wind, so that is the reason why we have created the uniformly distributed parameter ϵ. However, with reference to this parameter we have to say that, in fact, once the windmill has been placed somewhere in the Earth, the distribution can no longer be assumed to be uniform. In other words, once the windmill has been placed there will be a *usual* angle between the wind and the swell sea, since there will be a primary direction for the wind and a primary direction for the swell sea (so the value for ϵ will no longer be a uniformly distributed parameter). Therefore, when setting out the conclusions we have to clearly point out that the aim of introducing the parameter ϵ is that, a priori, since there is not an explicit location for the windmill, all possibilities with reference to the angle between the swell sea and the wind are plausible. However, in case any further studies were to be carried out, they should consider whether there is more information about

the location of the windmill and therefore the potential relation between the directions of the wind and the swell sea.

4. With regard to the shape of the tower, we have to say that there are certain windmills whose tower is not cylindrical (since the radius of the section decreases with height). With respect to this fact we have to say that the methodology we have applied would be no longer applicable, since the study at the base of the tower would not be the same as at the sea level because the sections would be different. Therefore, in case any other studies considered a non-cylindrical shape of the tower the methodology should be slightly adapted.

5. It is important to remark the fact that no corrosion has been taken into consideration. In fact, it has been somehow included in the "fatigue" term, because fatigue has been assumed to decrease the resistance of all materials of the windmill. However, it seems extremely obvious that the part of the tower which is partially exposed to sea water and air can develop a more intense fatigue condition than the rest of the tower. Therefore, subsequent studies could take this fact into consideration and therefore consider the potential negative effects of corrosion on the tower.

2.5.4 Comments on the breaking criterion and general comments on the physical model

1. With respect to the breaking criterion we have used (Von Mises criterion, according to [41] and [44]), we have to point out that it has worked considerably well; first, it is a very simple criterion which has reduced the computational cost associated to the simulation, so its utilisation has enabled us to be more accurate in the probabilities found through simulation with the Monte Carlo method. In addition, according to the consistent results that we have found it seems to have modelled the behaviour of both the tower and the blade admissibly well. Still, the hypothesis that this criterion is enough to describe the rupture of both the tower and the blade seems inaccurate, and even though it provides consistent results, should any further research was to be made about the topic, there should certainly be a more thorough study of the structure behaviour.

2. With reference to the fatigue on the structure, which has been treated as an explicative variable, we have to say that it has reasonably well solved the problem we had to deal with. In other words, with the introduction of this variable fat we have been able to take into consideration the fatigue of the windmill on its conditional probabilities to survive certain external actions (wind and sea conditions). In addition, its cost, in terms of modelling complexity and computational cost has been very low. However, it could be arguable whether the fatigue can be assumed to have an uniform effect on all parts of the windmill. In other words, the present model has considered the fatigue as a percentage, which determines *to what extent the resistance parameters have to be modified*. However, it seems reasonable that not all the parts of the windmill evolve the same way (in terms of fatigue), so it could seem insufficient to model the effects of fatigue with only a percentage. Therefore, any subsequent study could try to improve the modelling of fatigue, even though that would implicitly lead to a higher computational cost.

3. As a general comment, we should say that the majority of the forces that have been computed are not uniform along their domain. Moreover, some of them have been built through iterative processes (see Appendix A, B, C). In other words, all the forces involved in the computation of the calculations have been built through numerical integration of expressions that are not uniform (1st order Newton-Cotes quadrature). Therefore, there is certainly an error associated to this computations. Moreover, and especially focusing on the forces of the wind on the tower

(see Appendix A), we have to say that several forces have been found by points, so there is an additional uncertainty to the ulterior integration. Thus, the point we are trying to make is that there is an additional uncertainty we have not talked about and linked to the computations of the forces on the windmill.

Chapter 3

Regression model

The objective of the present project is to build a linear regression model on the conditional probability of being in the three states we have initially defined as a function of the explicative variables we have set up. In fact, the predicted variables will be the probabilities to be in the three possible states we have defined for the windmill, and the explicative variables will be the external actions we have provided (wind speed, swell sea conditions and structural fatigue). This regression will be computed with *R software* (see reference [45]).

3.1 Compositional treatment of the predicted variables

With reference to the conditional probabilities, we have to emphasize on two details which will be highly important with relation to the construction of the model. These three probabilities, by definition, are non-negative values between zero and one. Furthermore, their sum is constant and equal to one, since the final state of the windmill will always be either one of these three states. The fact that they always sum a constant implies that these three states are "a part of a whole", so that they are somehow related. Consequently, we can infer that the values of the probabilities cannot be understood as independent, since once two of them have been fixed the other one will be fixed as well (because the sum has to be always one). Therefore, even though there are three probabilities there are only two degrees of freedom.

Having said that, the main characteristic of the values we are trying to predict, probabilities, is that they are always bounded between zero and one. Therefore, we cannot assume them to be numbers belonging to the real scale and try to build a regression model directly since their scale is not the conventional euclidian one going from $-\infty$ to ∞. If we think about the concept of a probability itself, it is straightforward to see how a probability exactly equal to zero or equal to one is equivalent to the $-\infty$ or the ∞ of the real scale, since they are values at the extreme of the domain which are never achieved in practice. Therefore, the previous reasoning clearly motivates the idea that the probabilities have to be treated somehow in order to take into consideration the fact that they are not actual real-scale-numbers with whom we can build a regression model straight away.

The treatment that we will be applying to the predicted variables is the compositional one, proposed by Aitchison in 1986 (see reference [21]). Essentially, this treatment is aimed to transform the non-real-scale data that we currently have so that the new data that we obtain is in an euclidian space where we can build the regression. Using the same terminology as Aitchison, the values of the probabilities are in fact 3-component vectors, which are defined in a non-euclidian space called *Simplex* (for a complete description of such space see [22]). This space, by definition, will contain all the 3-component vectors whose components sum 1, but will have only two dimensions, since there are

only two degrees of freedom. For our case we have 100 points, which means we have 100 vectors which belong to the *Simplex*. Moreover, it is easy to see how we can represent all the vectors in a ternary diagram. A ternary diagram is a triangle inside of which we can represent 3-component vectors. Each point inside the triangle is defined by its three distances to the vertices, distances whose sum can be proved to be constant (due to geometrical properties of the triangle). It is relevant to point out how a point inside the triangle is fixed only with two known distances to the vertices: that is an extremely visual example of the fact that even though we have 3-component vectors we only have two degrees of freedom. In Figure 3.1 we have set all the 100 vectors we have got from our simulation in a ternary diagram.

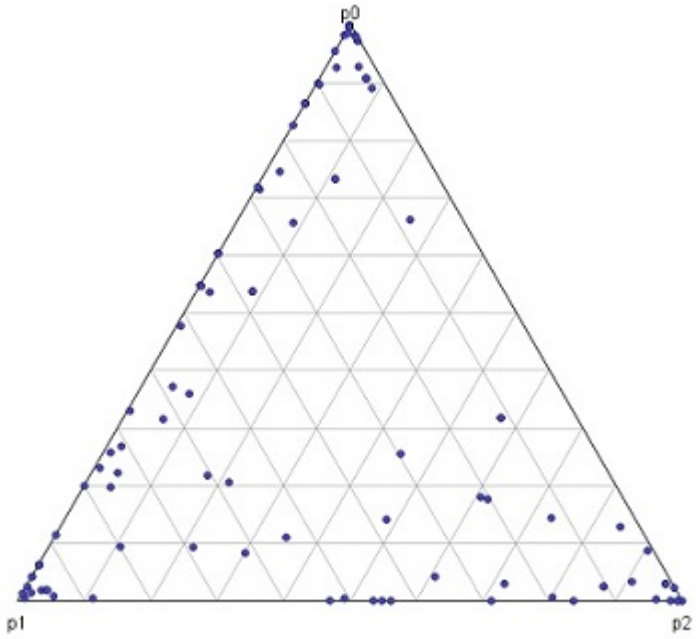

Figure 3.1: Ternary diagram representation of the probabilities obtained in the simulation.

Once the *Simplex* has been defined, and the vectors from the simulation have been proved to belong to a space of such characteristics (they are always vectors containing non-negative components and whose sum is always 1), we must refer to the transformation we need to make in order to get real-scale variables. That procedure is called coordinate transformation (see [29] for further information). From this transformation we will be obtaining a 2-component vector from every 3-component vector of the *Simplex* (which seems intuitive since we have already seen how though having 3 components these vectors have only 2 degrees of freedom). In fact, there are several coordinate transformations we can make to the data of the *Simplex*: CLR coordinates, ALR coordinates or ILR coordinates, among others. However, we will be using the ILR coordinate transformation, because these coordinates are orthogonal. The underlying idea of these transformations is that the *Simplex* space is bijectively related to an euclidian space (where therefore there is a defined euclidian distance). The values of the probabilities and the ILR coordinates are specified in Appendix D. As it can be checked, we have named this variables $UD1$ and $UD2$.

Once the ILR coordinates have been obtained, the regression model can be built. In case we had not done this transformation, as it has been demonstrated, we would not have been consistent with the nature of the data we are trying to forecast. Therefore, the model we would have obtained would have been less accurate.

It is especially relevant to focus a little bit on *what we actually mean by ILR coordinates*. Before going to the mathematical approach, it is highly important to keep in mind that the present transformation is bijective, so that in fact, talking about the vector of probabilities is exactly equivalent to considering the associated ILR coordinates. However, we are extremely interested in carrying out this transformation because by doing that we end with two orthogonal components who are in the real scale, so they admit to be fitted by a conventional regression model. It is especially relevant to understand that the model we will be building will predict ILR coordinates, but this result will be bijectively linked to a unique vector of probabilities.

The ILR coordinates are always defined trough what is called a *sequential binary partition*, according to [28]. The definition of such *partition* leads to a mathematical expression for the coordinates. In table 3.1 we have presented the partition we have considered.

Order	service state (state 0)	blade damage (state 1)	tower destruction (state 2)
1	1	-1	-1
2	0	1	-1

Table 3.1: Sequential binary partition to build the ILR coordinates.

Once the *sequential binary partition* has been defined, we can build the ILR coordinate transformation, according to [28]. As we have introduced earlier, for a 3-component probability vector we will obtain a 2-component coordinate vector, which will be built in the following way, according to the partition we have defined. Let x be the 3-component probability vector, then the ILR coordinate transformation can be expressed as follows:

$$ILR(x) = \left(\sqrt{\frac{2}{3}} \cdot \log \left(\frac{p_0}{(p_1 \cdot p_2)^{1/2}} \right), \sqrt{\frac{1}{2}} \cdot \log \left(\frac{p_1}{p_2} \right) \right).$$

In the present project the compositional treatment has been done through the *CoDapack software* (for further information, see [12]).

3.2 Treatment of the explicative variables

We have set out that we would like to study the behaviour of the windmill, in terms of describing the conditional probabilities to be in a certain state as a function of several conditions such as the wind speed, the swell sea conditions or the fatigue state of the structure. However, if we analyze the nature of these values we will conclude that it is highly probable that the suitable variable to use in the regression model may not be the explicative variable itself but a modified variable, according to whether the explicative variable is a real-scale number or not.

First, the wind speed is by definition a non-negative value, so its domain is $v_{hub} \in [0, +\infty]$ (in fact, it would be arguable whether there is a limit for wind speed, but in the present project we will assume it as a theoretically unbounded variable). Therefore, a logarithmic transformation seems to be more suitable for the regression, since the fact that it is only defined in the positive real scale leads to consider that its scale is relative. Consequently, the variable which will be used in the regression model will be $\log(v_{hub})$ instead of v_{hub}.

When referring to the significant height of the swell sea wave H_m and the period associated to the wave T_m, we have to say that they are both non-negative values, which are apparently unbounded (even though there are in fact physical limits to both variables). Therefore, a logarithmic transformation could seem to be adequate, since the scale appears to be relative. However, an additional comment

has to be made. These two variables usually appear together, since at the moment to compute the force of the sea on the tower both parameters are needed. Therefore, it would not be unreasonable to think of an *interaction* variable which was more appropriate for the regression; for instance, the variables $\frac{H_m}{T_m}$ and $H_m \cdot T_m$ could be taken into consideration. Moreover, when thinking about these alternative possible variables, we should keep in mind that their domains will still be $[0,\infty]$, so we should also consider their logarithms as potential explicative variables. Consequently, with reference to these parameters, we do not know so far whether they will be both significative or if we will have to define a new variable.

Before moving on to the last explicative variable, we should analyze a little bit further the relationship between H_m and T_m. It is important to remark that in the present model we have assumed the previous two variables to be independent, even though they seem to be closely related (see [43]). By doing this, we are assuming that for every value of H_m all the values for T_m are possible, whereas in fact this is not correct. Nevertheless, it is irrelevant for the following reason: with this project we are trying to compute the conditional probabilities to be in three states. These probabilities are, by definition, *conditional* to the probability of having a certain combination of explicative variables. The point we are trying to make can be exemplified with the following explanation. Let us consider the conditional probability theorem (see [17]):

$$\mathrm{P}[A] = \mathrm{P}[A|B] \cdot \mathrm{P}[B].$$

In case $\mathrm{P}[B]$ was equal to zero, then $\mathrm{P}[A]$ would become zero as well, *regardless* of the value of $\mathrm{P}[A|B]$. That is exactly what is happening when we are considering an impossible combination of the explicative variables. In case we provide an impossible combination of H_m and T_m, the model we have built will give us a value for the conditional probabilities to be in the three states. However, since the probability of having this combination of explicative variables will be zero, the probability to be in all three states will be zero as well because this combination is impossible. In other words, because the external conditions that we provide are impossible to happen at the same time, the probability to be in all states $0, 1, 2$ will be zero regardless of whatever the conditional probabilities are. For the reason exposed above, the idea of considering the explicative variables as independent and therefore considering "impossible combinations" in our model will not be relevant with reference to the computation of the conditional probabilities. In case an impossible combination was considered, the probability of this combination would be zero so the probability to be in any state would be zero as well *regardless* of the conditional probability the model had given us. Consequently, there is no conflict at all with the fact of considering H_m and T_m as independent to calculate the conditional probability since the final results will always be consistent.

With reference to the fatigue, its value is a percentage ($fat \in [0, 100]$), so a logistical transformation could initially seem more appropriate rather than using the fatigue value itself (see [22] for further information about transformations of compositional data). However, the logistical transformation will not be used for the following reason. The resistance of the materials, especially the steel of the tower and the materials the blades are made of, decreases because of the fatigue. Nevertheless, the limit values for the resistance, according to [41], are not zero; in fact, the resistance has been proved to decrease until reaching a stationary limit. Therefore, having a 100% fatigue on the structure does not mean that the structure is about to collapse, it only means that the resistance of its materials has reached the maximum reduction. In fact, a 100% fatigue implies that since the structure has significantly less resistance it will be more vulnerable to the external conditions. However, the simple fact of being "under strong fatigue conditions" is not equivalent to collapse. The logistical transformation is typically used with percentage variables, where the 0% and 100% stand for limit situations, for example infinite resistance and zero resistance, which is not the case. Still, since the value is a percentage, a logarithmic transformation could be more suitable than the fatigue value itself. This hypothesis will

have to be verified, since it is not straightforward from the inner definition of the variable.

3.3 Construction of the regression model and results

The regression model will try to forecast the values of the probabilities (vectors of the *Simplex*), expressed through coordinates (which are vectors with real-scale-components) as a function of the explicative variables. Indeed, we will be estimating the coefficients β_i associated to the following multiple linear regressions:

$$UD1 = \beta_{1,0} + \sum_{i=1}^{i=n} \beta_{1,i} \cdot x_{1,i},$$

$$UD2 = \beta_{2,0} + \sum_{j=1}^{j=m} \beta_{2,j} \cdot x_{2,j},$$

where $UD1$ and $UD2$ stand for the compositional coordinates (see [22]) associated to the probabilities and the values of $x_{1,i}$ and $x_{2,j}$ stand for the explicative variables in their suitable scale. It is important to remark, once again, that since there are only 2 degrees of freedom a 3-component probability vector of the *Simplex* will only have 2 coordinates.

3.3.1 Regression on the first coordinate $UD1$

With reference to the first coordinate ($UD1$) estimated model, the result has been presented in equation (3.1).

$$UD1 = 79.6017 - 18.4992 \cdot \log(v_{hub}) - 0.0266 \cdot T_m - 0.2216 \cdot fat - 0.3486 \cdot (class), \tag{3.1}$$

where as we have initially defined, v_{hub} stands for the wind speed at the hub's height, T_m stands for the period of the swell sea wave, fat stands for the percentage of fatigue, and the variable *class* is the product between a binary variable depending on whether the wind speed is above or under 25 m/s and the value of the wind speed itself.

Once the regression model has been built, several analysis have to be made, in order to evaluate the reliability and appropriateness of the model. First, we can build the Q-Q plot of the residuals of the model to get more information about whether they can be assumed to be normally distributed or not. It is important to carry out this verification because at the moment we have built the regression we have implicitly assumed normality on the residuals; in case this hypothesis was not true, there would be uncertainty about the p-values we have obtained. The Q-Q plot is presented in Figure 3.2.

From Figure 3.2 we cannot reach an unquestionable conclusion, since the tails seem to not be well fitted by the normal model. Therefore, we will carry out several normality tests such as the Kolmogorov-Smirnov test to help us reach a more accurate conclusion. However, before continuing with the analysis we should point out a few comments about these tails. These residuals which seem to not be well fitted by the normal model correspond to *extreme situations*. By extreme situations we mean that the vector of probabilities is not balanced; for example, it seems obvious that when there is no storm at all, no swell sea and no fatigue on the structure, the probability of service will be *very* close to 1 whereas the probability of total destruction will be close to zero. Therefore, even though we have used the Sample Importance Re-sampling procedure (see references [20] and [5]) to estimate more accurately these probabilities, there may be an additional error due to the fact that these probabilities are very close to the extremes of the domain (0 and 1). Consequently, even though we will check the normality of the residuals through additional statistical tests, we should certainly be aware of the potential problems that may have arisen from the presence of *extreme points*.

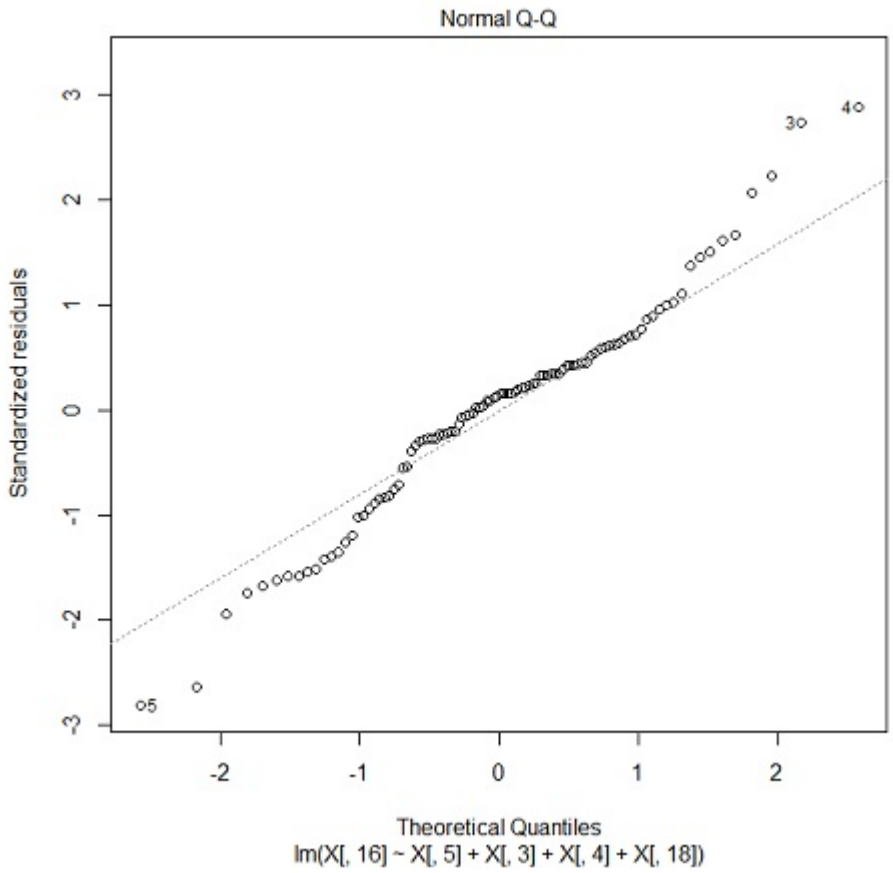

Figure 3.2: Q-Q plot to verify the normality of the residuals for the regression on the first coordinate $UD1$.

We have carried out three tests to evaluate the normality of the residuals (Kolmogorov-Smirnov test, according to [14], Anderson-Darling test, according to [47], and Shapiro-Wilk test, according to [42]). All three of them evaluate the hypothesis "normality on the residuals is acceptable". The results we have obtained, in terms of p-value are presented in table 3.2. From the results we have obtained in table 3.2, we can reject the hypothesis on the normality of the residuals, so the implicit hypothesis we have made when building the regression is incorrect. In case the residuals cannot be assumed to be normally distributed, the p-values for the T-tests on the coefficients have to be seen as inaccurate, since they rely on the hypothesis that the residuals have a normal distribution. However, by looking at the results of the p-values of these tests, we can clearly state that even though the p-values might be inaccurate, there is no doubt that the variables we have found to be significative are meaningful. For this reason, even though normality on the residuals may not be verified, there will be no effect on the results we have obtained.

Regarding the statistical results for the whole model, we can also verify that the linear model is appropriate, as it is summarized in table 3.3. According to the p-value we obtain (lower than 2.2e-16), it seems that the linear model we have proposed is appropriate, though further studies need to be made. Moreover, provided that we have obtained a R^2 of 0.825, the results seem to fit considerably well. In fact, we have found a very simple model who can explain the 82% of the variance on the first coordinate, so the outcome is more than admissible.

With respect to the R^2, it is arguable whether with 100 points 0.825 for a multiple linear regression

Name of the test	p-value	conclusion
Kolmogorov-Smirnov test	0.0001406	inadmissible (according to a conventional limit of 0.05)
Anderson-Darling test	0.006882	inadmissible (according to a conventional limit of 0.05)
Shapiro-Wilk test	0.06113	inadmissible (according to [42] the limit should be 0.10)

Table 3.2: Results in terms of p-values of the normality tests on the residuals of the first coordinate $UD1$.

Residual standard error	2.893 on 95 degrees of freedom
Multiple R-squared	0.8321
Adjusted R-squared	0.825
F-statistic	117.7 on 4 and 95 degrees of freedom
p-value	2.2e-16

Table 3.3: Principal results of the regression model as well as F contrast to evaluate whether the model is meaningful (coordinate $UD1$).

is a low value. However, achieving this degree of adjustment only with 4 significative variables is, from our point of view, accurate enough, especially if we consider the high complexity of the physical model that has been proposed to study the behaviour of the windmill. It could also be arguable whether 100 points are actually enough to fit the coefficients, since when considering a multiple linear regression the required points to fit the parameters properly increases considerably. To deal with that question, we have assumed that a minimum of 10 points per coefficient are needed to reach a reasonably accurate model. According to that general idea, there are about 25 points per coefficient, which even though is a low value, it seems enough to give a response to the problem we are dealing with. It has to be said, though, that no more points have been considered because of the computational cost (in terms of time), associated to the simulation. However, should any further analysis were to be carried out in the future, they should certainly generate a higher database of simulations in order to increase the accuracy of the fitted coefficients.

Regarding the heteroscedasticity of the residuals, we have to refer to Figure 3.3, which plots the residuals versus the fitted values. In this analysis, we would expect to find a cloud of points, centered on the zero and which completely lacked of organization. The obtention of such result would reinforce the idea that the residuals *can be assumed to be aleatory and independent of the fitted data*. By looking at the plot we have obtained several comments can be made. First, we could agree on the fact that the average value for the results is zero. However, it is also clear that a linear pattern seems to appear on the plot (in fact, there is a red line which helps to see that trend). That is undeniably explicative of a flaw of the model. For example, this could be indicative that either we have missed one explicative variable (which has been used in the physical model and discarded in the regression) or that the dependence of the predicted value on one or more variables is not linear.

With regard to the significance of the parameters, the results are presented in the following table 3.4. All the parameters with a p-value over 0.05 have been taken out from the model, so the remaining ones are significative. With reference to the physical meaning of the results, for this coordinate we have found four significative variables. Regarding the wind speed, the $\log(v_{hub})$ has been proved to be more appropriate, as we expected. With reference to the fatigue, the most significative variable has been proved to be fat itself (without the logarithm). With respect to the swell sea parameters, however, only T_m has been proved to be significative.

We should take into consideration whether there is correlation between the predictive variables.

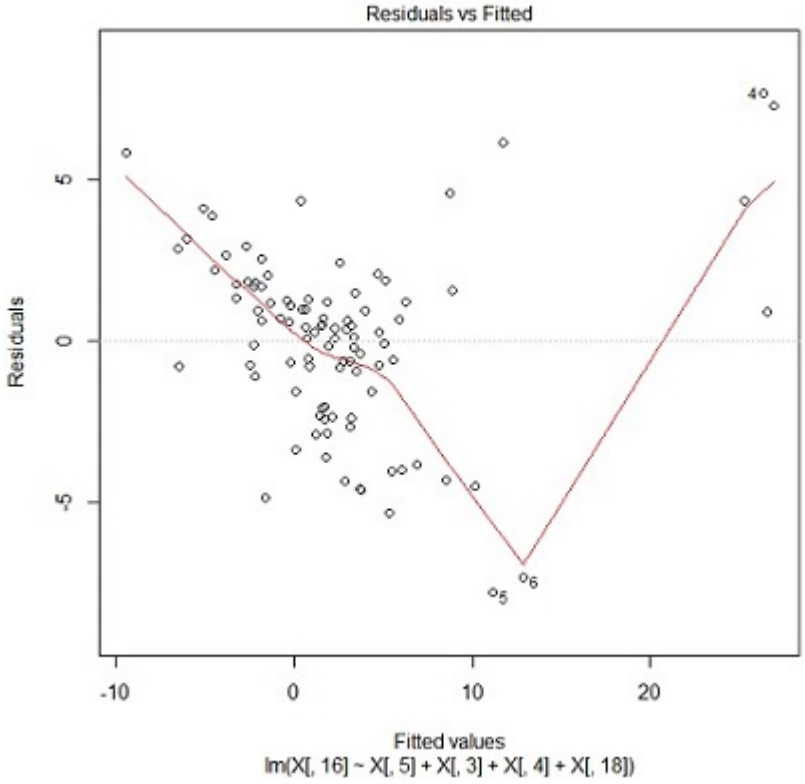

Figure 3.3: Fitted values versus residuals plot to verify the heteroscedasticity on the regression of the first coordinate $UD1$.

Name of the variables	Value of β_i	Standard error	Value for the estimator t	p-value
$Intercept$	79.601792	3.952877	20.138	2e-16
$\log(v_{hub})$	-18.499295	0.964084	-19.188	2e-16
T_m	-0.026670	0.007421	-3.594	0.000519
fat	-0.221618	0.016678	-13.288	2e-16
$class$	-0.348604	0.055949	-6.231	1.26e-08

Table 3.4: Values for the coefficients for every explicative variable as well as T contrast made to the model in order to determine whether the explicative variables are significative (coordinate $UD1$).

	$\log(v_{hub})$	T_m	fat	$class$
$\log(v_{hub})$	1.0000	-0.0006	-0.53024	-0.72713
T_m	-0.0006	1.0000	0.0378	-0.1949
fat	-0.5302	0.0378	1.0000	0.3831
$class$	-0.7271	-0.1949	0.3831	1.0000

Table 3.5: Correlation matrix to analyze whether there is collinearity on the explicative variables proposed on the model (coordinate $UD1$).

In fact, the most important impact is that in case there is collinearity the results are not trustable. Therefore, we must carry out the correlation analysis as a proxy to detect the presence of collinearity, which consists on studying whether any variable from the model can be expressed as a linear combination of the other ones. This information is summarized in the correlation matrix, which has been presented in table 3.5. The components of this matrix are the correlation parameters (usually regarded as ρ) between the variables. Logically, these parameters have to be 1 at the diagonal; moreover, this matrix has to be symmetric by definition. In fact, the interesting values are the ones outside the diagonal. The closer they are to one, the more chance there is to have a linear correlation between the variables. According to what we can see in the matrix (table 3.5), no problems of collinearity seem to be present amongst the explicative variables. It is relevant to highlight that the variable *class* is the result of the interaction between $\log(v_{hub})$ and the restriction of whether the windmill is active or inactive ($v_{hub} < 25$ m/s or $v_{hub} > 25$ m/s), so it is logical to obtain a higher value for the correspondent correlation parameter.

With regard to the robustness of the model, we should analyze the potential leverage effects that the points can have on the final expression of the regression model. In other words, we have to check *how sensitive the model is on the experimental points we have used for its construction.* In order to see whether a point modifies significatively the expression of the model, we compute the same regression model without it and compare the results. This comparison is made through computing the so called *Cook distance* (see reference [46]). The results for the leverage analysis have been presented in Figure 3.4. In this graphic we can observe how all the points stand in the area below the 0.5 Cook's distance. According to [8], and to the conventional analysis that are carried out for regressions like the one we have proposed, no problems with respect to leverage can be expected from the data we have used.

Finally, we should address the autocorrelation issue with respect to the residuals. The term *autocorrelation* stands for the situation in which the residuals from a regression have any sort of relationship. The most commonly used test to evaluate whether there is any correlation on the residuals is the Durbin-Watson test, which was proposed by James Durbin and Geoffrey Watson in references [24] and [25]. This test contrasts the hypothesis "errors are serially uncorrelated" against the alternative that "they follow a first order autoregressive process". This test has resulted in a p-value equal to 0.01062; therefore, by assuming a conventional significance of 0.05 we can conclude that no autocorrelation can be expected on the residuals of the regression on the first coordinate.

For the reasons we have just set out, we must say that according to the results we have obtained, the linear model to predict the first coordinate $UD1$ is meaningful and it is able to explain more than 82% of the variance on the data. However, it should be checked in further analysis whether the dependence of the predicted variable on the 4 explicative variables we have found can be *more* than linear (quadratic, for example).

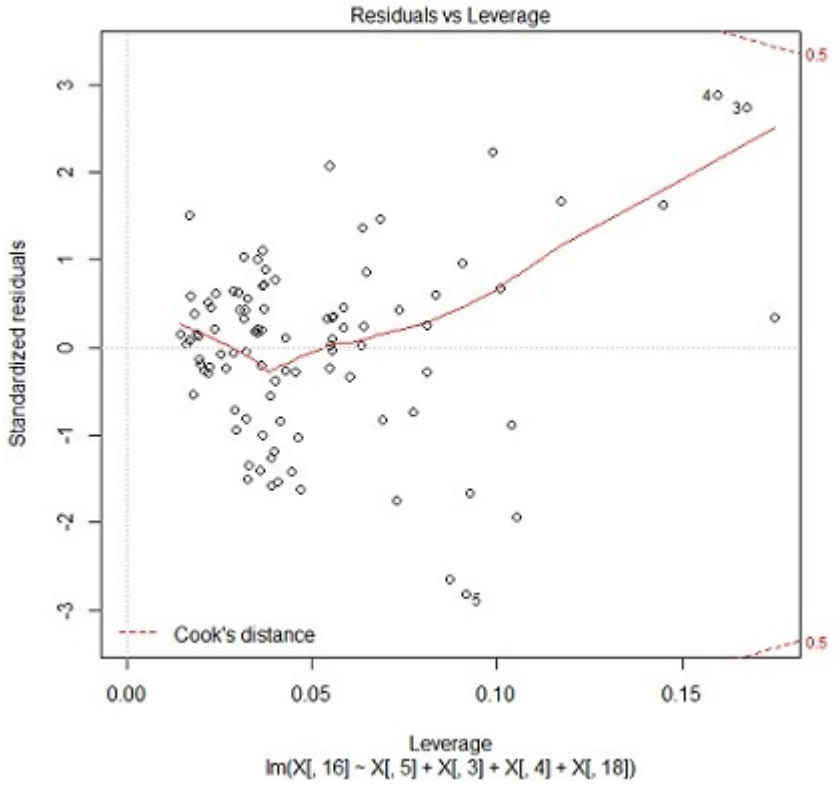

Figure 3.4: Leverage effect of the points of the simulation on the regression model for the first coordinate $UD1$.

3.3.2 Regression on the second coordinate $UD2$

The model that has been applied for the first coordinate is the same that has been applied for the second coordinate $UD2$. The results have been presented in equation (3.2).

$$UD2 = 63.4179 - 13.7458 \cdot \log(v_{hub}) - 0.0199 \cdot T_m - 0.2534 \cdot \log(fat) - 0.3856 \cdot (class). \quad (3.2)$$

First of all, we can see that the explicative variables that have been found for the regression on this second coordinate are the same ones as in the first coordinate $UD1$. In fact, intuitive as this may seem, the explicative variables for one regression do not necessarily have to be explicative as well for the second coordinate. However, these 4 variables are the only ones who have an admissible p-value

In the same way we have done for the first coordinate, normality on the residuals has to be verified. The Q-Q plot has been presented in Figure 3.5. According to what we can see in this plot, normality seems very difficult to assume since the tails seem to not be fitted properly. However, the same tests

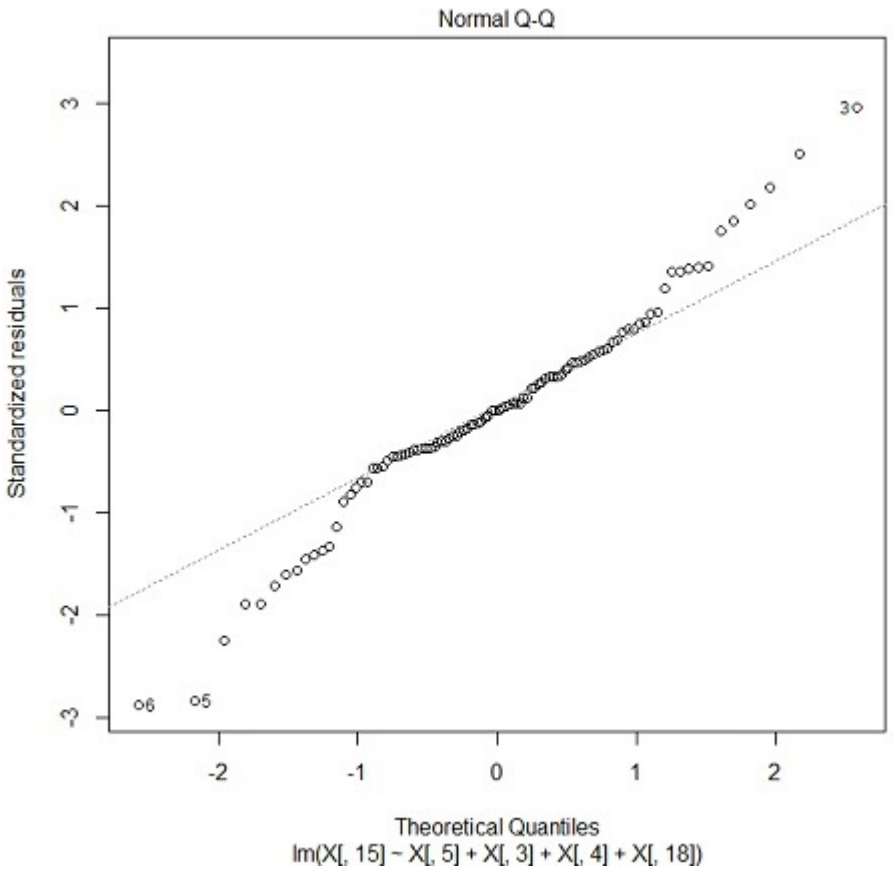

Figure 3.5: Q-Q plot to verify the normality of the residuals for the regression on the second coordinate $UD2$.

we presented before will be carried out for this regression. The results are presented in table 3.6. As it can be seen, only the Kolmogorov-Smirnov test does not reject the hypothesis of normality on the residuals. Therefore, since normality cannot be assured with forcefulness, we should be aware of the additional comments that we have already made in the first regression: since the underlying assumption of normality on the residuals is not clear, the p-values of the T-tests for the coefficients have additional uncertainty. However, according to the actual value for these p-values, this uncertainty is unimportant, since their significance in the model is extremely clear.

Name of the test	p-value	conclusion
Kolmogorov-Smirnov test	0.07203	admissible (according to a conventional limit of 0.05)
Anderson-Darling test	0.01176	inadmissible (according to a conventional limit of 0.05)
Shapiro-Wilk test	0.05869	inadmissible (according to [42] the limit should be 0.10)

Table 3.6: Results in terms of p-values of the normality tests on the residuals of the first coordinate $UD1$.

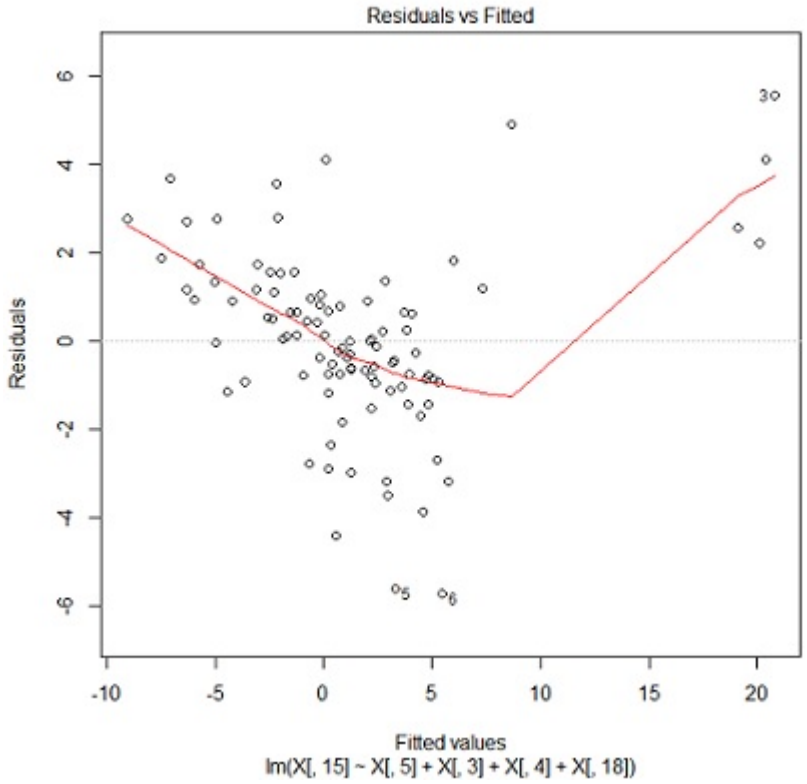

Figure 3.6: Fitted values versus residuals plot to verify the heteroscedasticity on the regression of the second coordinate $UD2$.

With respect to the heteroscedasticity of the residuals the same analysis will be made according to Figure 3.6. It is especially relevant to highlight the same pattern we saw for the regression on the first coordinate; in the plot of the figure we can see the same linear pattern on the residuals, which motivates the idea that the dependency of the predicted variable may not be linear on at least one of the explicative variables. It would be arguable whether it is possible that we have missed a variable on the regression, but at the present stage of the project it seems more probable that there may be a problem on the linear dependency suppositions.

With reference to the statistical results for the whole model, they are presented in table 3.7. Like in the previous case, the p-value for the linear model we have proposed is low enough to assume it is meaningful. In addition, regarding the R^2 equal to 0.86, we have to say that the results are very good according to the simplicity of the model we have used. Therefore, a linear regression model for the second coordinate $UD2$ seems appropriate.

Regarding the T-tests for the coefficients, the results have been set in table 3.8. We have already

Residual standard error	2.071 on 95 degrees of freedom
Multiple R-squared	0.8668
Adjusted R-squared	0.8612
F-statistic	154.5 on 4 and 95 degrees of freedom
p-value	2.2e-16

Table 3.7: Principal results of the regression model as well as F contrast to evaluate whether the model is meaningful (coordinate $UD2$).

Name of the variables	Value of β_i	Standard error	Value for the estimator t	p-value
$Intercept$	63.417996	2.830022	22.409	2e-16
$\log(v_{hub})$	-13.745840	0.690226	-19.915	2e-16
T_m	-0.019924	0.005313	-3.750	0.000304
fat	-0.253477	0.011941	-21.228	2e-16
$class$	-0.385689	0.040056	-9.629	1.03e-15

Table 3.8: Values for the coefficients for every explicative variable as well as T contrast made to the model in order to determine whether the explicative variables are significative (coordinate $UD2$).

talked about the potential uncertainty associated to the exact values for the p-values. However, it is clear from this table that the coefficients which have been found to be significative are without any doubt meaningful.

With reference to the potential collinearity of the variables we are under the same situation as for the first regression. Since we have ended up with a model whose explicative variables are the same than for the regression on the first coordinate, it is unnecessary to make another correlation analysis since the outcome will be the same. The results for the collinearity analysis have been presented in table 3.5.

With regard to the leverage effect of the data (Figure 3.7), the results are very similar to the previous regression; since there is no point beyond the 0.5 Cook's distance threshold, we can conclude according to [8] that no problems due to leverage can be expected from the data we have used in our model (so the regression model is robust).

Finally, we have carried the Durbin-Watson test in order to address the potential autocorrelation of the residuals. The same comments that were made on the first regression are applicable for the present case, so they will not be repeated. The p-value for the test is 0.001331, so we can conclude that no autocorrelation is expected to appear on the residuals we have obtained.

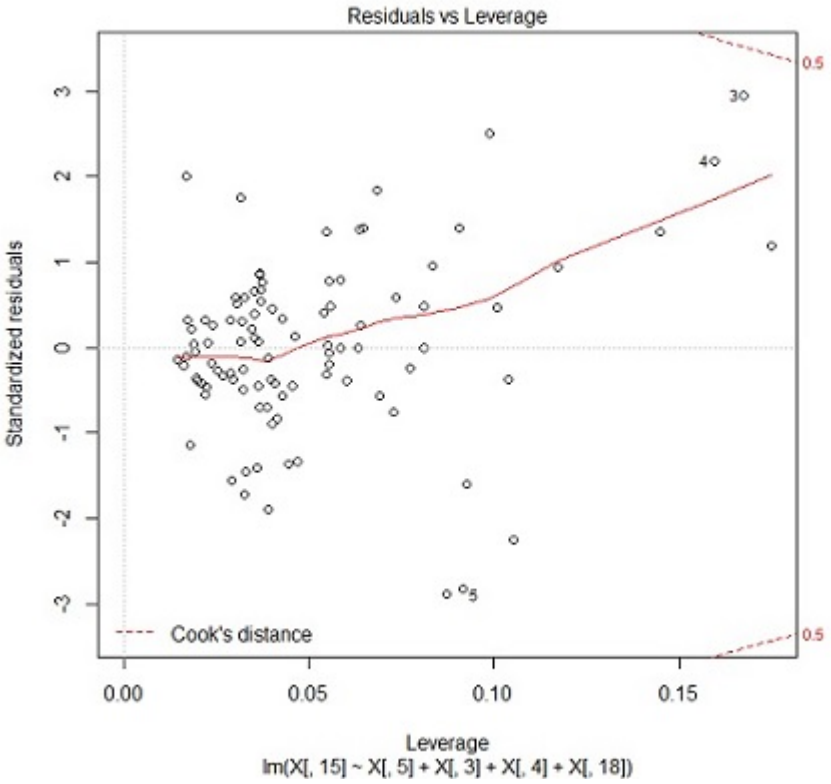

Figure 3.7: Leverage effect of the points of the simulation on the regression model for the second coordinate $UD2$.

Chapter 4

Conclusions

4.1 Conclusions on the regression model

With reference to the regression model itself and the results we have obtained, we could state the following conclusions:

1. Firstly, the compositional approach has provided a very good result, and has been proved to address the problem we were dealing with more accurately. Since the nature of the data we wanted to forecast were probabilities, a specific treatment to the data has had to be considered in order to build a traditional euclidian multiple regression. In other words, the regression would have not been adequate if we had not considered this statistical treatment and had just proposed three multiple linear regressions on the three probabilities: in fact, that would have been wrong because of two reasons: first the domain of the predicted variables is not the real scale, and second, the three probabilities are not independent because they all are "parts of a whole" (their sum is a always 1).

2. With reference to the model we had thought of, we have to say that the results we have obtained are extremely positive according to the simplicity of the model we have proposed. In fact, we have been able to explain more than 80% of the variance of the coordinates with two linear models only dependent on 4 explicative variables. We have to say, though, that even though the p-values for the linear models suggest that they are definitely meaningful, the linear pattern on the residuals brings up the idea that the dependency on at least one of the explicative variables may not be linear. Therefore, we can conclude that even though the two regression models have been proved to address successfully the problem we are working on, they can be improved in the future.

3. Regarding the explicative variables, we have to say that in the same way as for the predicted variables their domains are not the real scale; for instance, the wind speed is a non-negative variable, just like the swell wave period or its significant height. Therefore, we have defined *transformations* on these variables in order to work with real-scale variables in the regression. According to the outcome (in terms of p-values), the results with the transformed values were significatively better than the ones with the raw variables. In fact, this seems consistent because as long as the domain of a variable is not the real scale, its magnitude becomes somehow relative, so it is inaccurate to use the raw value for the regression.

4. By analyzing the variables which have been proved to be significative in the model, we have found that the wind speed, the fatigue and the swell sea conditions are meaningful. However,

referring to the swell sea conditions, we have to point out that only the period T_m is significative. This result must be commented, since even though the significant height of the swell sea wave has been discarded of the model because its p-value is over the admissible significance of 0.05, it may not be that straightforward to infer that it is meaningless with reference to the vulnerability of the windmill. In fact, according to [43], the period and the significant wave height can be assumed to be related. Therefore, we have to make a few comments on the methodology we have used in order to understand the final outcome we have reached. In our project, we have assumed the wave significant height to be independent from the period, so we have taken into consideration *more possible cases than what is actually possible*. In other words, our model includes combinations of height and period which are not achievable in practice (for example 5 meter high wave and 5 second period). Within this hypothesis, our regression model has resulted in that only the period is significative with respect to the vulnerability. However, in fact these two variables are related, so before discarding completely the effect of the significant height further analyses should be made.

5. With regard to the significance of the explicative variables, we have found for all the cases that the conclusion obtained from the p-value criterion is unquestionable. For most of the cases, this value has been found to be under 2e-16, so even though the hypothesis on the normality of the results may not be verified, the fact that these variables are meaningful to the model seems indubitable.

6. Referring to the accuracy of the results, we have to take into consideration all the hypotheses that have been made. Overall, we have made several simplifications on the behaviour of the windmill, as well as we have used approximate integration processes. Moreover, even though 300000 simulations have been made for each point, that leads to an accuracy that cannot be assumed to be higher than 5 significant digits. Therefore, we should keep in mind the limitations of the present project, so even though it provides consistent results with the references (for example, [31]), it may have uncertainty due to the limited resources we have counted on (in terms of time). In fact, the main point to justify the potential inaccuracy is that we have built a *multiple* regression model, so a huge amount of data is needed in order to adjust properly the coefficients.

7. Once the accuracy issue has been brought up, we have to refer to the Monte Carlo simulation, which has been used to find the *experimental* data to build the regression. The Monte Carlo method (see [36] and [9]) has been proved to address very successfully the problem we were dealing with. In fact, the present problem would have been impossible to solve through a *strictly analytical* procedure, since the complexity of both the physical model involved or the randomness of several parameters would have made the problem unsolvable. Therefore, and linking to the analogy of the *box full of balls* we used in the early introduction, the Monte Carlo simulation has enabled us to tackle an extremely challenging problem with a reasonable cost. We should mention as a final remark about this topic the especially useful help of the Sample Importance Re-sampling procedure (see [20] and [5]). The use of this tool has allowed us to reach a level of accuracy much higher than the one we had obtained in case we had not considered it.

4.2 Conclusions regarding the project

Once the conclusions for the regression model have been set out, we have to address the potential usefulness of the results, as well all the questions that may have arisen with respect to the vulnerability of the windmill in the first place. We have intentionally separated this global conclusion from the

previous comments because this analysis ought to be done subsequently to the regression model discussion.

According to the meaningfulness of the model we have built, we can say we have addressed the problem of quantifying the potential risk an off-shore windmill is under as a function of the external actions it comes across. At the present time, therefore, in case we are able to find local data about the external actions that will take place at the specific location of the windmill we will be able to determine whether the definition of the windmill is appropriate for this specific location. After carrying out the analysis we can end up with two possibilities. On the one hand, the present model can enable us evaluate whether the windmill is *too vulnerable* to the external actions; that would mean that it is a sensible idea to strengthen the windmill, otherwise we are dealing with a high risk of ending with a damaged structure. However, on the other hand the model will also be able to inform us whether the windmill is *too strong* for the conditions it will be under. In fact, *overinvesting resources* is as inadmissible as defining a too vulnerable structure. It is important to highlight that no comments are being made regarding *what the exact threshold of risk is*, since this is not the purpose of the project. Indeed, it is important to keep in mind the limitations of this study: our main aim has been no other to provide an indicator to evaluate the risk on the structural safety of the windmill. Consequently, the present model should be seen as a tool which could be taken into consideration at the time of evaluating whether a proposed design is optimal.

Finally, by taking into consideration the conclusions we have reached, we could say that the primary objective of the project has been achieved, since we have eventually been able to model the risk on an off-shore windmill with a relatively simple approach and with very limited resources. However, positive as these results can be, the conclusions of the present project set as well the point of start for further analysis, since even though the model has been proved to be useful, its accuracy can certainly be improved by tackling all the simplifications that have been made during this study.

Chapter 5

Acknowledgements

In the present section I would like to express my gratitude to many people who have been directly or indirectly involved in the project. In fact, it is probable that without their help the outcome of this *treball de final de grau* would have been unsuccessful. Moreover, their support has been extremely valuable especially in the most difficult situations.

First, I would like to thank my two co-advisors, professors Juan José Egozcue and Maribel Ortego. I would like to mention them in the first place because their support has gone beyond the strictly academical domain of the project. Therefore, I would like to highlight their indubitable role not only in this project but also in my academic endeavor. Perhaps the most relevant piece of advice I would like to point out is how relentless our attitude must be with respect to inaccuracy.

Secondly, I would like to express my gratitude towards all the professors from *Universitat Politècnica de Catalunya* who have contributed in the construction of the project. Rather than a strictly statistical project, this project has eventually involved plenty of additional domains of what we understand as Civil Engineering, so I would like to mention the invaluable help of Climent Molins, Joan Pau Sierra and Esther Real. Without the slightest doubt, carrying out the project without their help would have been extremely harder. Therefore, I would like to publicly express how grateful I am with regard to the time they have invested in helping me.

Regarding the statistical part, I would like to point out that this project would not have been possible if it was not for the help of the lecturer professors from *Universitat de Girona* in the CoDaCourse2013. Therefore, I would like to mention professors Vera Pawlowsky-Glahn, Josep Antoni Martín-Fernández and Carles Barceló-Vidal for their undeniable role in the Compositional Data analysis teaching.

Finally, I would like to thank my family and friends for their support. I would especially like to mention the endless support of my colleague and friend Marina Monserrat, without whom not only this project but my whole bachelor's degree would have been completely different.
Again, my deepest gratitude,

Robert Ortells Sesé

Bibliography

[1] LORC Knowledge webpage, 2011. `http://www.lorc.dk/offshore-wind-farms-map/horns-rev-1`, consulted on October 2013.

[2] Airfoil Tools, `http://airfoiltools.com/airfoil/details?airfoil=n0012-il`, consulted on October 2013.

[3] EN-61400 Norm, Technical Comitee AEN/CTN 206, UNESA, February 2004. Technical report.

[4] Product brochure, Vestas Wind Systems A/S, `http://nozebra.ipapercms.dk/Vestas/Communication/Productbrochure/2MWbrochure/2MWProductBrochure/`.

[5] Gelman A., Carlin J.B., Stern H.S., and Rubin D.B. *Bayesian Data Analysis*. Chapman and Hall/CRC Press, 2003.

[6] Musolas A.M. Vulnerability analysis in a pwr nuclear power plant containment building. Tesina final de carrera. Enginyeria de Camins, Canals i Ports, Escola Tècnica Superior d'Enginyeria de Camins, Canals i Ports de Barcelona (ETSECCPB) - Universitat Politècnica de Catalunya, Barcelona, 2013. Advisors: Egozcue J.J. and Crusells M.

[7] Massicotte B. *Calcul des structures en béton armé - Concepts de base*. Éditions da Vinci, 2013.

[8] Kim C. and Storer B.E. Reference values for Cook's distance. *Communications in Statistics - Simulation and Computation*, 25:691–708, 1996.

[9] Robert C. and Casella G. *Monte Carlo Statistical Methods*. Springer, 2004.

[10] Wang C. Lifting Horizontal Elastic Beam at Two Points. *Journal of Engineering Mechanics*, 116:141–151, 1990.

[11] Coastal Engineering Research Centre, Department of the Army US Corps of Engineers. *Shore Protection Manual. Volume I*. US Government Printing Office, 4th edition, 1984.

[12] Marc Comas-Cufí and Santi Thió-Henestrosa. CoDaPack 2.0: a stand-alone, multi-platform compositional software. In Egozcue J.J., Tolosana-Delgado R., and Ortego M.I, editors, *CoDaWork'11: 4th International Workshop on Compositional Data Analysis*, Sant Feliu de Guíxols, 2011.

[13] Beaulieu D., Picard A., Tremblay R., Grondin G., and Massicotte B. *Calcul des charpentes d'acier, tome I*. Lakeside Group, 2008.

[14] Massey F.J. The Kolmogorov-Smirnov test for Goodness of Fit. *Journal of the American Statistical Association*, 46(253):68–78, 1951.

[15] White F.M. *Fluid Mechanics*. McGraw Hill, 2003.

[16] Ingram G. Wind Turbine Blade Analysis using the Blade Element Momentum Method. Version 1.1. Durham University, 2011. `https://community.dur.ac.uk/g.l.ingram/download/wind_turbine_design.pdf`, consulted on october 2013.

[17] Canavos G.C. *Probabilidad y Estadística. Aplicaciones y métodos*. McGraw Hill / Interamericana de México, 2003.

[18] Schueller G.I. and Shah H.C. A probabilistic approach to determine wave forces on ocean pile structures, Proceedings of 13th Conference on Coastal Engineering, Vancouver, Canada, 1683-1701, *ASCE*. 1972.

[19] Recktenwald G.W. *Numerical methods with MATLAB. Implementations and Applications*. Prentice Hall, 2000.

[20] Aitchison J. The statistical analysis of compositional data (with discussion). *Journal of the Royal Statistical Society, Series B (Statistical Methodology)*, 44(2):139–177, 1982.

[21] Aitchison J. The statistical analysis of compositional data. Monographs on statistics and applied Probability. *Chapman and Hall Limited (reprinted in 2003 with additional material by the Blackburn Press)*, 1986.

[22] Aitchison J., Barceló Vidal C., Egozcue J.J., and Pawlowsky-Glahn V. A concise guide for the algebraic-geometric structure of the simplex, the sample space for compositional data analysis, In Proceedings of IAMG'02, the eighth annual conference of the International Association for Mathematical Geology. 2002.

[23] Aitchison J. and Shen S. M. Logistic-normal distributions. Some properties and uses. *Biometrika*, 67(2):261–272, 1980.

[24] Durbin J. and Watson G. S. Testing for serial correlation in least squares regression, I. *Biometrika*, 37:409–428, 1950.

[25] Durbin J. and Watson G. S. Testing for serial correlation in least squares regression, II. *Biometrika*, 38:159–179, 1951.

[26] Morison J., O'Brien M., Johnson J., and Schaaf S.A. The force exerted by surface waves on piles. *Petroleum Transactions - American Institute of Mining Engineers*, 189:149–154, 1950.

[27] Stoer J. and Bulirsch R. *Introduction to numerical analysis*. Springer-Verlag, 1980.

[28] Egozcue J.J. and Pawlowsky-Glahn V. Groups of parts and their balances in compositional data analysis. *Mathematical Geology*, 37,7:799–832, 2005.

[29] Egozcue J.J., Pawlowsky-Glahn V., Mateu-Figueras G., and Barceló-Vidal C. Isometric logratio transformations for compositional data analysis. *Mathematical Geology*, 35,3:279–300, 2003.

[30] Martínez Benjamín J.J. *Mecánica newtoniana*. Universitat Politècnica de Catalunya. Iniciativa Digital Politécnica, 2004.

[31] Rodríguez Amenedo J.L., Burgos Díaz J.C., and Arnalte Gómez S. *Sistemas eólicos de producción de energía eléctrica*. Editorial Rueda, 2003.

[32] Canet J.M. *Cálculo de estructuras I. Fundamento y estudio de secciones.* Universitat Politècnica de Catalunya. Iniciativa Digital Politécnica, 2004.

[33] Sorensen J.N. Aerodynamic aspects of wind energy conversion. *Annual Review of Fluid Mechanics*, 43:427–448, 2011.

[34] Shampine L.W. *Numerical solution of ordinary differential equations.* Chapman and Hall, 1994.

[35] González M., Jiménez A., Rodríguez A.B., Martín L., and Lind O. Palas de aerogenerador. Master's thesis, Escola Tècnica Superior d'Enginyeria Industrial de Barcelona (ETSEIB) - Universitat Politècnica de Catalunya, Barcelona, 17/06/2010.

[36] Hammersley J. M. and Handscomb D. C. *Monte Carlo Methods.* Wiley, 1964.

[37] Villarrubia López M. *Ingeniería de la Energía Eólica.* Ediciones Marcombo, 2012.

[38] MATLAB. *version 7.10.0 (R2010a).* The MathWorks Inc., Natick, Massachusetts, 2010.

[39] Ministerio de Fomento. *Instrucción de Acero Estructural (EAE).* Ministerio de Fomento, 2011.

[40] Ochi M.K. *Ocean Waves. The Strochastic Approach.* Cambridge University Press, 1998.

[41] Trahair N.S, Bradford M.A., Nethercot D.A., and Gardner L. *The behaviour and design of steel structures to EC3. Fourth edition.* Taylor and Francis, 2008.

[42] Royston P. Algorithm AS 181: The W test for normality. *Applied Statistics*, 31:176–180, 1982.

[43] Ventayol Fresno P. Modelització de la dependència període-altura d'ona mitjançant còpules. Treball final de carrera. Enginyeria tècnica d'obres públiques, Escola Tècnica Superior d'Enginyeria de Camins, Canals i Ports de Barcelona (ETSECCPB) - Universitat Politècnica de Catalunya, Barcelona, 21/07/2011 2011. Advisors: Ortego M.I. and Tolosana-Delgado R.

[44] Von Mises R. Mechanik der festen Korper in plastisch-deformablen Zustand. *Nachrichten von der Gesellschaft der Wissenschaften zu Gottingen, Mathematisch-Physikalische Klasse*, 1913.

[45] R Development Core Team. *R: A Language and Environment for Statistical Computing.* R Foundation for Statistical Computing, Vienna, Austria, 2008. ISBN 3-900051-07-0.

[46] Cook R.D. Detection of influential observations in linear regression. *Technometrics (American Statistical Association)*, 19:15–18, 1977.

[47] Anderson T.W. and Darling D.A. Asymptotic theory of certain goodness-of-fit criteria based on stochastic processes. *Annals of Mathematical Statistics*, 23:193–212, 1952.

Appendix A

Computation of the force of the wind on the blades

A.1 Computations for an active windmill (rotating blades)

When the model for the behaviour of the windmill has been set out, it has been stated that wind speed grows with height with a function provided by the EN-61400 Norm (see reference [3]), as it has been exemplified in Figure A.1. This wind speed, however, has been assumed to be constant at all the area of the rotor so then the behaviour of the blades is the same and the further calculations become easier, as it has been stated in section 1.3. It is important to keep this hypothesis in mind because all the following calculations will be done according to the principle that the position of the blades do not matter since they all three behave the same way everywhere, even though according to [3] this assumption is false.

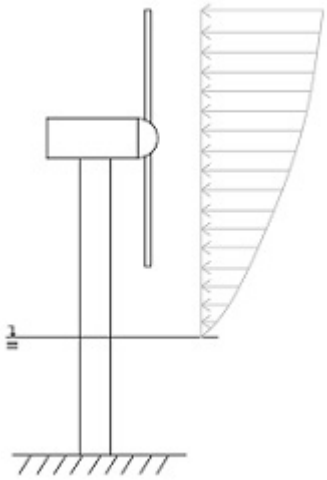

Figure A.1: Evolution of wind speed with height according to EN-61400 (*source: self elaboration*) .

The key concept to understand the nature of the force induced by the wind is that it depends on the relative velocity of the wind with respect to the blades. In order to compute the forces of the wind we will follow the same methodology as the one proposed in [31]; therefore, in case no further reference documentation is added, all the information has been taken from this reference.

In case the blades are not moving, the relative wind speed is the same as the absolute one. However, as long as they are rotating these two magnitudes are different. By looking at (Figure A.2) we can

define v as the absolute wind speed, assumed constant for all the rotor area, $\omega \cdot r$ as the velocity due to rotation (ω stands for the angular velocity and r for the radius), and W as the vectorial sum of these two velocities or relative velocity of the wind with respect to a certain point of the blade. It is important to highlight that as we approach the extremes of the blades, the linear velocity due to rotation increases, so the relative velocity W is not constant. Moreover, we can define the angles φ and β, which are the angle between W with the vertical and its complementary angle.

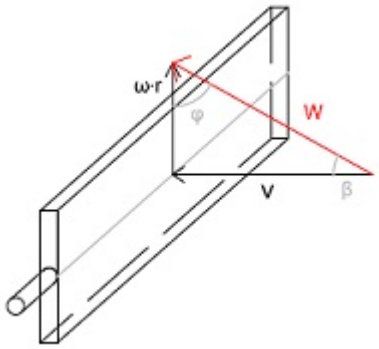

Figure A.2: Components of the relative velocity of the wind (*source: self elaboration*).

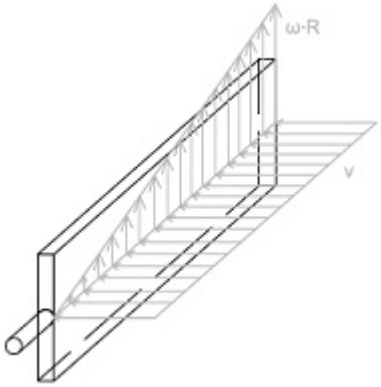

Figure A.3: Components of the relative velocity of the wind along the blade (*source: self elaboration*).

As it has been said, the vertical component of W increases with the radius, so it is therefore proved that, as long as the horizontal component remains constant the value for W increases as we approach the blades extremes (Figure A.3). Furthermore, it can also be easily seen how φ decreases as we separate from the centre of rotation. In other words, both the value and angle of the relative velocity of the wind with respect to the blades change along the blade. However, not all the angles between the wind and the blade are admissible, since turbulence has to be avoided in order to maximize the energetic efficiency. In fact, according to [31], the energy production is optimized as long as the *angle of attack* i kept constant. This angle of attack i stands for the angle between the blade and the relative wind speed, and in case there was not torsion on the blade it would be equal to the angle φ. Torsion has been illustrated in Figure A.4, and it is defined as the angle between the blade and the vertical axis. The reason to consider torsion is to address the differences in terms of angle of attack on the points of the blade; since φ is not the same for all the points of the blade, we have to introduce an additional angle to keep constant the angle between the relative wind speed and the surface of the

blade. In fact,

$$\varphi = i + \theta.$$

In other words, the main aim of introducing torsion on the blades is to somehow compensate the variation of the angle of the relative wind velocity, in order to get a value of i relatively constant. Since the angular velocity is a fixed value (the blades always move at the same velocity), an expression for the torsion angle θ can be found in order to optimize the behaviour of the blades with respect to the wind.

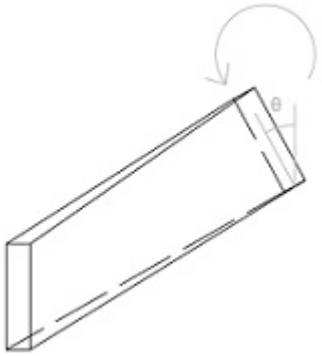

Figure A.4: Approximate shape of the blade due to torsion (*source: self elaboration*).

Therefore, if we now consider a blade with torsion, the main scheme for the relative wind speed changes a little bit, as it can be seen in Figure A.5. Essentially, the idea is that in order to optimize the efficiency the blades have to vary their inclination with respect to the vertical axis in such a way to avoid significative variations on the angle of attack i.

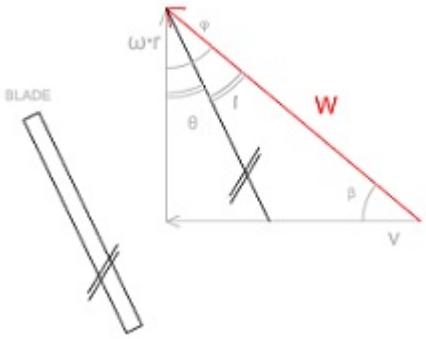

Figure A.5: Main magnitudes defined with reference to the relative wins velocity with respect to the blade (*source: self elaboration*).

With reference to the optimal expression for θ, it has been proved to be dependent on the radius r (which means that the variation of θ along the blade must not be constant). In reality, in order to maximize the energetic efficiency, several tests are made in the laboratory so as to find an empirical expression for the optimal torsion for the blades. Therefore, the real expression for the torsion is not an analytical function but a curve defined through laboratory iterations. However, this expression has usually an hyperbolic shape, like Figure A.6. In the present project we have made the simplification of assuming a single expression for the torsion:

$$\theta(r) = \frac{60}{r^{0.7}}.$$

This expression has been proposed by the present project with the numerical model we have built in MatLAB. According to what happens in reality, we have created this expression which provides consistent results at the outcome of the numerical calculations. It is important to remark that the present solution for the torsion angle is not the optimal expression, but it provides an extremely simple description which, while being consistent with what happens in reality, provides a correct approach to the modelling of the force of the wind.

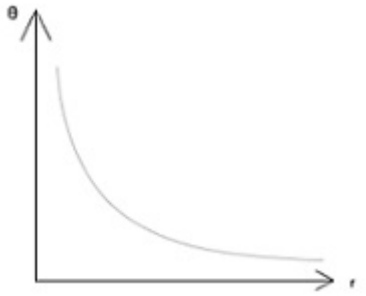

Figure A.6: Approximate shape of a hyperbolical torsion law along the blade (*source: self elaboration*).

With reference to the rotation velocity, we have previously stated that it has been fixed in section 1.3. In particular, $\omega = 12rpm$. The decision for ω is not arbitrary. In order to maximize the energetic production, the value for λ has to be near 7, according to [31]:

$$\lambda = \frac{\omega \cdot R}{v_{hub}} \sim 7,$$

where R here stands for the radius of the rotor, v_{hub} for the wind speed at the height of the hub and ω has to be considered in rad/s. Therefore, when taking a conventional value for $v_{hub} = 10m/s$, we obtain an angular velocity of around 12 rpm. It is remarkable to highlight that according to this principle, the bigger the rotor is, the slower the rotation has to be in order to get an optimal λ.

In order to be able to set out the computation for the force of the wind, a brief introduction on the basic concepts of a windmill has to be made. A windmill is aimed to extract energy from the constantly moving wind mass. Its activity and impact on the wind speed field can be summarized in Figure A.7.

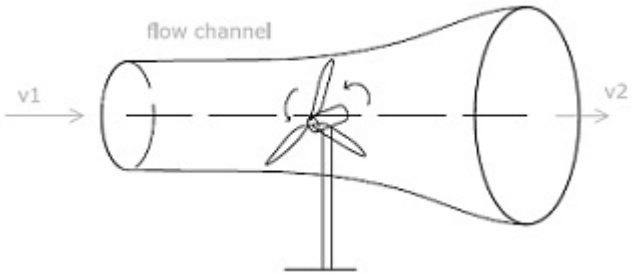

Figure A.7: Wind flow channel with the initial and final wind speeds, according to [31] (*source: self elaboration*).

Once a windmill starts operating, the rotor defines a flow tube (or flow channel), which is a volume of moving air involved in the interaction with the blades of the windmill. As a result to the windmills

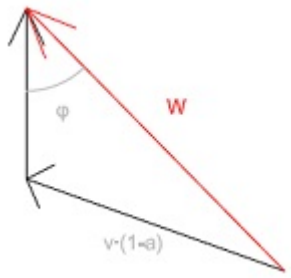

Figure A.8: Horizontal component for the wind speed considering the blocking effect of the windmill (*source: self elaboration*).

operation, there is a loss of energy in the mass of wind due to the extracted energy from the blades. This loss of energy implies a reduction on the wind speed. This reduction in the velocity of the wind can be expressed in terms of the parameter a, which is defined as the "blocking parameter" of the windmill (see [31]). In other words, this parameter is explicative of the impact that the windmill has on the movement of the air contained in the flow tube. According to the terminology of Figure A.7:

$$v_2 = v_1 \cdot (1 - 2 \cdot a),$$

where v_1 and v_2 stand for the initial and final wind speeds (steady wind speeds for the situation when the windmill is far enough). By applying conservation of the momentum, it can be proved that the wind speed at the windmill can be expressed as:

$$v_{windmill} = \frac{v_1 + v_2}{2},$$

which is equivalent to say that the wind speed reduces linearly because of the presence of the windmill.

Before continuing we have to make a comment on the notation we are using. In all previous chapters we have named v_1 as v_{hub} (or simply v), since v_{hub} stood for the wind speed at the hub's height "without the interference of the windmill". In fact, what we were talking about was v_1 and not the wind speed at the hub itself, because as we have just said the wind speed close to the hub has already been reduced due to the blocking effect of the blades. In other words, the name v_{hub} was not particularly appropriate for v_1 since the wind speed at the hub itself is not v_{hub}. The explanation for that is that, in fact, we will not need the wind speed at the hub for our equations because the only significative variables will be the wind speed at the hub height with no interference of the windmill and the "blocking parameter" a. By naming $v_1 = v_{hub}$ and by combining the last two equations, the velocity at the windmill can be expressed:

$$v_{windmill} = \frac{v_{hub} + v_{hub} \cdot (1 - 2a)}{2} = v_{hub} \cdot (1 - a).$$

In the same way we have exposed that there is a reduction of wind speed in the flow channel as a result of the activity of the windmill, there is another impact on the wind speed field due to the rotation of the blades. As it can be seen in Figure A.9, the fact that the blades are rotating induces a rotation component to the mass of wind moving on the flow channel. By applying conservation of angular momentum, we reach a similar expression in which we can see that there is a linear progression from the wind speed of v_1 where there is no rotation component until the v_2 state in which there is a rotation component $2 \cdot \omega \cdot r \cdot a'$, being a' the induced rotation velocity coefficient:

$$\omega_{windmill} = \frac{2 \cdot \omega \cdot r \cdot a' - 0}{2} = \omega \cdot r \cdot a'.$$

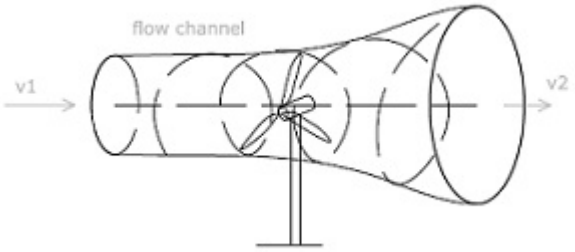

Figure A.9: Circular velocity induced to the wind flow channel due to the activity of the windmill (*source: self elaboration*).

Therefore, it has now been proved how the relative velocity has to take into consideration both the blocking coefficient a which stands for the reduction of wind speed due to the "blocking impact" that the windmill has on the flow channel and the induced rotation component generated by the rotation of the blades and considered through a'. The final expression of W is summarized in Figure A.10.

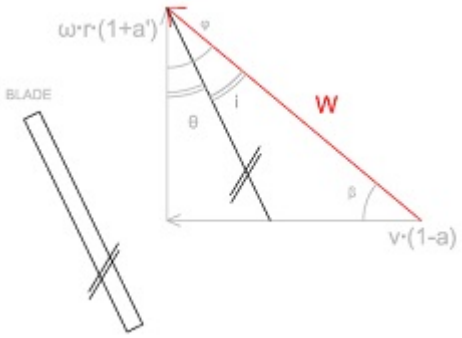

Figure A.10: Real components and magnitudes relevant to the relative velocity of the wind considering the blocking effect and the induced rotation (*source: self elaboration*).

Consequently, we can obtain the following expressions, according to [31]:

$$\varphi = \text{arctg}\frac{v_{hub} \cdot (1-a)}{\omega \cdot r \cdot (1+a')},$$

$$W = v_{hub} \cdot \frac{1-a}{\sin\varphi}.$$

It is highly important to know that the values for both a and a' are different for every radius of the blade; that means that they are not constants to be found for every windmill, they are a function of the radius r, and vary in case we change the wind speed conditions.

Once the previous parameters have been defined, the formulation for the force of the wind on the blades can be set out. As summarized in Figure A.11, the force on the blades is dependent on the vector "relative wind velocity" W. Due to this velocity, the blades experiment a resultant force that can be separated in two components: a drag component, which has the same direction as W and a lift component, which is in the perpendicular plane. These two forces will be referred as f_D and f_L, respectively. It is important to know that, since W, a, a' and φ vary with the radius, the values for f_D and f_L cannot be constant along the blade. In other words, for every value of the radius a value for a, a', W and φ have to be calculated, and from those values we can obtain the value for f_D and

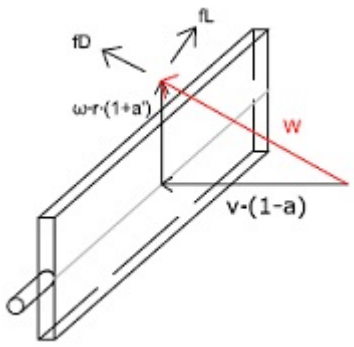

Figure A.11: Relative wind velocity components and scheme of the drag and lift forces (*source: self elaboration*).

f_L. The forces f_D and f_L have been proved to be dependent on the variables we have previously set out. The analytical expression to compute them is the following one, according to the application of momentum conservation:

$$f_L = \frac{1}{2} \cdot \rho_{air} \cdot W^2 \cdot c \cdot C_L,$$

$$f_D = \frac{1}{2} \cdot \rho_{air} \cdot W^2 \cdot c \cdot C_D,$$

where C_L and C_D stand for the lift and drag coefficients, ρ_{air} stands for the air density (equal to $1.225 kg/m^3$, according to [37]) and c for the chord of the blade. From the results obtained from these expressions, therefore, we are able to compute the force for every value of the radius of the blade. These forces will be integrated along all the blade in order to find the resultant force of the wind in the drag and lift directions. As it is schematized in Figure A.12, f_L is the force applied on a differential area (whose width is a differential radius:

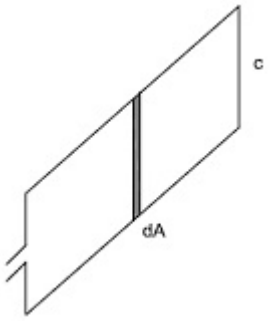

Figure A.12: Scheme of the differential part of the blade we consider to compute the forces (*source: self elaboration*).

$$f_L = dF_L = \frac{1}{2} \cdot \rho_{air} \cdot W^2 \cdot dA \cdot C_L = \frac{1}{2} \cdot \rho_{air} \cdot W^2 \cdot c \cdot dr \cdot C_L,$$

$$\frac{dF_L}{dr} = \frac{1}{2} \cdot \rho_{air} \cdot W^2 \cdot c \cdot C_L.$$

By applying the same principle on the drag component:

$$\frac{dF_D}{dr} = \frac{1}{2} \cdot \rho_{air} \cdot W^2 \cdot c \cdot C_D.$$

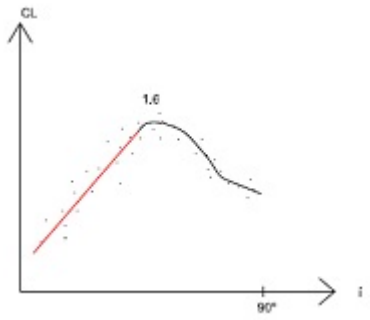

Figure A.13: Approximate behaviour of the C_L coefficient with respect to the angle of attack i (*source: self elaboration*).

However, even though it might seem that as long as we know the value for W the value for the wind force is known, in fact we do not, because both components C_L and C_D are not constant. In particular, these two coefficients depend on the angle of attack i, which depends on the angle φ, the torsion of the blade at that point θ and the parameters a and a' at that point. The dependence of these two parameters on the angle of attack i has been schematized in Figure A.13 and Figure A.14. However, this dependence is not the same for all blades; in fact, it depends on the section of the blade. In the present project we have assumed that our blades have a section NACA0012 (which is a conventional profile, whose description is detailed in [2]). With reference to how to estimate the parameters once the value for i has been determined, there is no explicit function to use, since this relationships have been found empirically (in the proposed bibliography they provide tabulated values for both coefficients as a function of the angle of attack i). In the present project, since we need an analytic (and bijective) function for these coefficients, we have approximated a straight line and a 2nd grade parabola by least squares in order to have a bijective dependence of the parameters on the angle. Otherwise, the numerical model to compute the force of the wind for a random situation would not have been possible. The explanation for that is the following one: in the present model we will be studying the forces of the wind from a finite element method approach, which means that we will discretize the domain of the blade. For an arbitrary wind speed, we will find the values for i, a, a', W, φ for every element of the blade. Afterwards, from the value of i, we will find the values for the coefficients C_D and C_L, with whom we will finally be able to estimate the values for f_L and f_D. Therefore, we need an analytical expression which gives the values for the coefficients for whatsoever value of i. From the information obtained at [31], we have created the following expressions in MatLAB, found through applying the least square approximation method to the tabulated values obtained from [2]:

$$C_L = -0.000170245604856 + 0.087355233274046 \cdot i + 0.000003740746465 \cdot i^2,$$

$$C_D = -0.003690994009938 - 0.000001039689548 \cdot i + 0.000243324124506 \cdot i^2.$$

From the previous approximation, we have obtained an interpolation function which provides a consistent solution to the problem of needing a functional relationship between the angle of attack and the coefficients However, we have to state that these relationships are only valid for the red domain from Figure A.13 and Figure A.14, since once we exceed the limit values the behaviour of the coefficients is different (in fact, the explanation is that turbulence starts to happen, as it has been developed in [31] and will be developed later on this chapter). It is extremely important to keep in mind that the procedure of finding i, W, φ, a, a' has to be carried out for every element of the blade because as long as it has been proved that W is variable with radius, then $a, a', \varphi, \theta, i, C_D$ and C_L have to be variable as well, so the value for f_L and f_D is not the same for all the points of the blade.

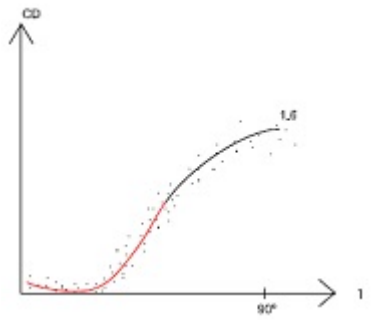

Figure A.14: Approximate behaviour of the C_D coefficient with respect to the angle of attack i (*source: self elaboration*).

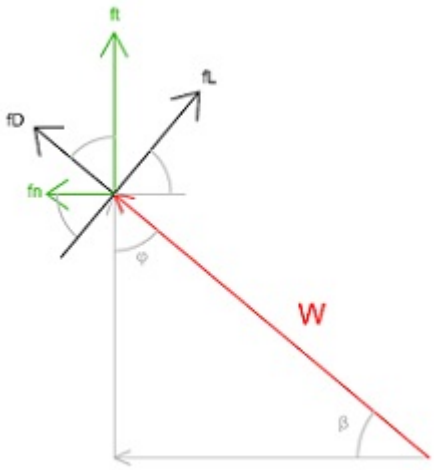

Figure A.15: Relationship between f_D, f_L and f_T, f_N (*source: self elaboration*).

Once the concepts of f_L and f_D have been calculated, the force of the wind on the blades is known, and by integration we can obtain the resultant forces F_L and F_D (since f_L and f_D have been described through finite elements this integration will have to be a numeric approach and will certainly be an approximation):

$$F_L = \int_0^R f_L dr,$$

$$F_D = \int_0^R f_D dr.$$

However, the forces we will be interested in will be the normal and tangential force with respect to the axis of the blade, referred as f_N and f_T respectively. In fact, as we will be studying the blade as a beam , we will be extremely interested to separate in a tangential force that makes the blade rotate from the normal force which appears as a result of the fact that the blade somehow blocks the air flow. These two forces, as it can be checked in Figure A.15, can be expressed as (trigonometric relationship):

$$f_N = -f_L \cdot \cos\varphi + f_D \cdot \sin\varphi,$$

$$f_T = f_L \cdot \sin\varphi + f_D \cdot \cos\varphi.$$

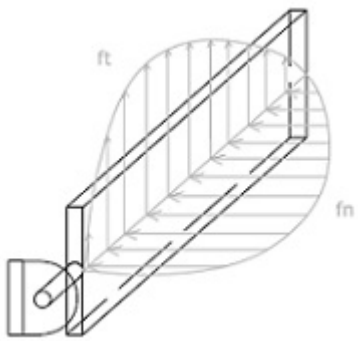

Figure A.16: Simplified scheme of the normal and tangential forces (*source: self elaboration*).

It is important to comment on a linguistical detail. Since the blade has torsion, the normal force f_N is not strictly perpendicular to the blade. In fact, what the words normal and tangential refer to is to the plane of rotation of the rotor, that by definition is independent from torsion on the blades.

Finally, once the values for f_N and f_T are known, the resultant values for the three blades can be calculated, as well as the total torque (T) supplied to the hub axis to produce the energy we have designed the windmill for (Figure A.16):

$$F_N = 3 \cdot \int_0^R f_N dr,$$

$$F_T = 3 \cdot \int_0^R f_T dr,$$

$$T = 3 \cdot \int_0^R f_T \cdot r dr,$$

where all the values have been multiplied by 3 because there are three blades.

However, as it has been previously said the values for the forces have to be computed for every value of the radius, since neither f_T nor f_N are constant along the blade (because they depend on a, a', φ, W and i. In order to compute the values along the blade the Blade Element Momentum Theory (BEM) is applied (see [16] and [33]). This method is based on the conservation of the momentum, and provides an accurate approach to the problem of finding the evolution of f_T and f_N along the blade. In particular, as it can be checked in the references, the BEM method is based on combining the 4 following equations: first, two equations for conservation of the linear and angular momentum. Second, two other equations which provide the analytical expression for f_D and f_L as a function of C_L, C_D, a, a'. By its combination we obtain the following two equations, which must be satisfied simultaneously:

$$\frac{a}{1-a} = \frac{\sigma' \cdot (-C_L \cdot \sin\beta + C_D \cdot \cos\beta)}{4 \cdot \cos^2\beta},$$

$$\frac{a'}{1-a'} = \frac{\sigma' \cdot (C_L \cdot \cos\beta + C_D \cdot \sin\beta)}{4 \cdot \lambda \cos^2\beta},$$

where β is the complementary angle of φ and $\sigma' = \frac{3c}{2\pi r}$ is a parameter called solidity. These equations have to be solved iteratively, as it is explained in the already mentioned references [16].

With regard to how we have computed those forces on MatLAB, we have discretized the domain into 40 elements (Figure A.17). After that, we have carried out the previously explained procedure

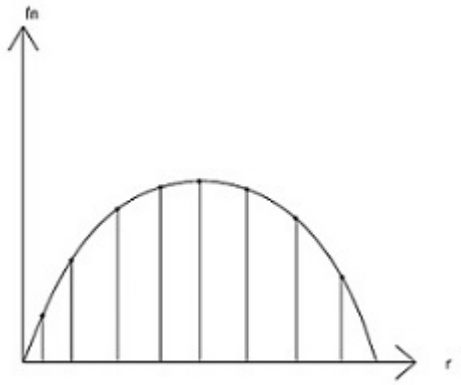

Figure A.17: Simplified shape of the wind forces in order to exemplify the integration (*source: self elaboration*).

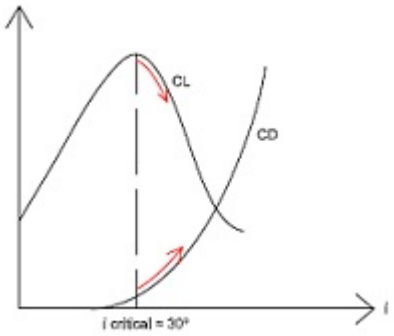

Figure A.18: Evolution of both C_L and C_D with the angle of attack once turbulence takes place (*source: self elaboration*).

so we have reached a discrete expression for both f_N and f_T. It could be arguable whether taking more points would have been better, in spite of increasing the computational cost. However, since other simplifications have been made with respect to the global vulnerability of the windmill there is no point in trying to increase the accuracy of the values of these two forces. With reference to the computation of the resultant for these forces, we have carried out the integral, which is an extremely easy process since we have simplified the expression of the function for a function defined by points. The computation of the integral has been done through a 1st order quadrature (see references [27] and [19]).

The optimal situation in a windmill activity is when C_L is maximum and C_D is minimum. In fact, a lot of times the efficiency of the energetic production is measured through the ratio $\frac{C_L}{C_D}$, which is aimed to be maximized. For conventional wind speeds, as the wind speed increaes both C_L and C_D increase, even though C_L does it much faster (Figure A.18). Therefore, for not-very-high wind speeds the higher the wind speed is the more efficient the energy production is. However, for a certain threshold of wind speed, around 25 m/s, the windmill ought to be stopped for safety reasons. In order to do that, the blades are designed so that turbulence starts to occur at this level of wind speed and the blades are stopped. In addition, further control devices are installed to keep the windmill active as long as the wind speed is reasonable.

Just to give an approach to the explanation for the behaviour of both coefficients, by regarding at

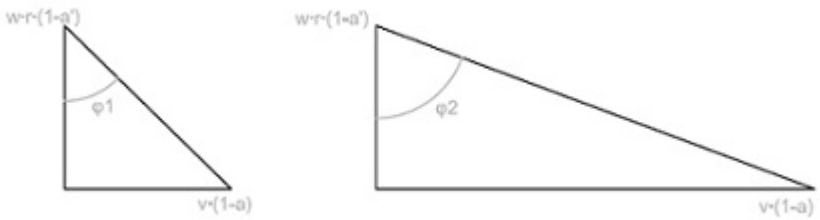

Figure A.19: Examples of relative wind velocities and its magnitudes (*source: self elaboration*).

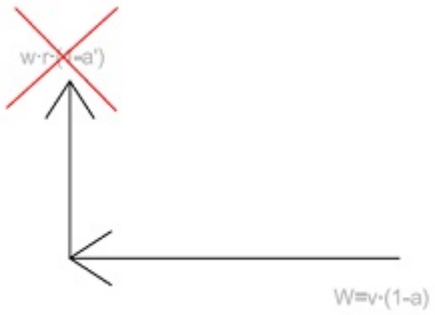

Figure A.20: Expression for the relative and absolute wind speeds (*source: self elaboration*).

Figure A.19 we can see how in case the wind speed is increased, φ increases, so the angle of attack i increases. Consequently, since it has been proved that the higher the velocity is the higher the angle of attack becomes (for a fixed value of torsion), it is straightforward to infer the behaviour of C_L and C_D with the wind speed.

A.2 Computations for a stopped windmill

In case the blades are not rotating, the relative wind speed coincides with the absolute one. Furthermore, no rotation on the flow tube air is induced ($a' = 0$), so the equations will be much more simplified. As it can be inferred from Figure A.20:

$$f_L = f_T,$$

$$f_D = f_N.$$

Furthermore, as we are now in the high-wind-speed situation, C_L can be considered as null, because turbulence is high enough to allow us to neglect the tangential force (see [31]). Therefore, we will assume:

$$f_L = 0.$$

With reference to C_D, it will be very important in the present state to consider it, since according to Figure A.19 its value will be much higher, In fact, that is what we would intuitively expect: as long as the windmill does not move any longer, the blocking effect it makes on the wind can be reasonably higher. However, with regard to how C_D has to be calculated, we have to say that the previous procedure is no longer applicable (since as we already set out the relationship between the angle of attack and the coefficients was only valid for a certain domain where there was no turbulence).

According to [31], we will assume $C_D = 1.7$ as a constant value for all the points of the blade (it seems reasonable to assume a constant value because in the present situation W is uniform in the whole area of the rotor).

According to the BEM equations obtained from [16] we have set out before (conservation of linear momentum) we can find a:

$$a = \frac{\frac{10.5}{8\pi r}}{1 + \frac{10.5}{8\pi r}},$$

where we have considered $c = 3.5$ (see the description of the windmill in section 1.3), $C_D = 1.7$, $\beta = 90^{\text{o}}$ and $C_L = 0$. It is important to note that C_D is constant along the blade directrix but the blocking coefficient a is not, since it depends on the radius r.

For the reasons exposed above,

$$f_N = f_D = \frac{1}{2} \cdot C_D \cdot \rho_{air} \cdot W^2 \cdot c \cdot dr,$$

where $C_D = 1.7$ and $W = v_{hub} \cdot (1 - a) = W(r)$. Moreover,

$$f_L = f_T = 0.$$

Once we have arrived to the final expressions for f_T and f_N, the same 1st quadrature integration os proposed (see [27]), so the resultant forces on the blades are found (note that in this case there will only be the perpendicular component, by construction).

A.3 Final comments about the computation of the wind force

Several comments have to be made with reference to the further simplifications we have carried out in our model. First, according to the BEM theory, the forces on the blades are zero in the extremes. In fact, as we approach the extreme both f_T and f_N decrease, as we have implicitly drawn in all the schemes we have used. The explanation for that is the so called "tip effect". This phenomenon consists on the presence of turbulence at the extreme of the blades, which induces all the forces to decrease as we approach the end of the blade. Actually, this is a quite intuitive situation, since it seems reasonable that the fact that the blade stops and does not continue has an impact on the forces of the wind on the blades.

However, the fact of introducing the tip effect on the formulation adds an extra degree of freedom to the equations presented above, and the computational cost increases very significatively. For this reason, we have not introduced the tip effect on our model. The direct consequence is that, by not introducing that the forces have to decrease as we approach the extremes, they keep on increasing with the radius as if the blade was continuous (Figure A.21). This is, in fact, a drawback of the model due to simplification. However, the computational cost associated to the simulation without this simplification would have been, by all means, unaffordable.

Secondly, as we have used an approximated torsion expression, as well as assumed several simplifications on the blade, the results we will be obtaining for the force of the wind are necessarily inexact. Moreover, since we have used simple approximations for the coefficients C_L and C_D, the results lose accuracy as we approach the cut-off wind speed. This fact can be easily observed in Figure A.22, where we can see that the accuracy of the functional approximation of the coefficients decreases as we arrive to the limit angle corresponding to the cut-off threshold. For these reasons, we have to say that when imposing situations near the limit the obtained results may not be entirely consistent with the initial assumptions (even though they will not be contradictory we may end up with values that are not accurate with regard to the real situation).

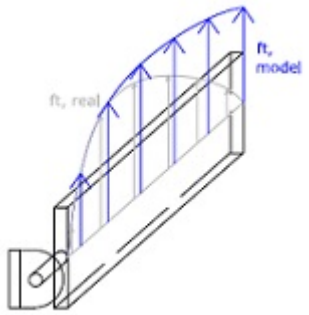

Figure A.21: Differences between the real wind force and the one used in our model due to not considering the tip effect (*source: self elaboration*).

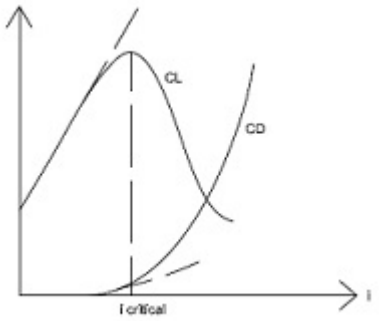

Figure A.22: Error induced in the calculations after the critical angle due to considering the expression fitted for low values for i (*source: self elaboration*).

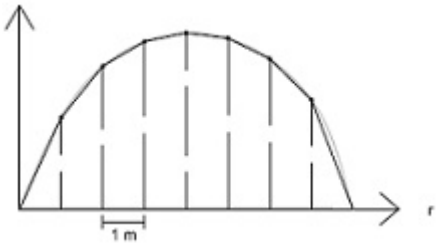

Figure A.23: Simplification of the wind forces and error committed in the integration process (*source: self elaboration*).

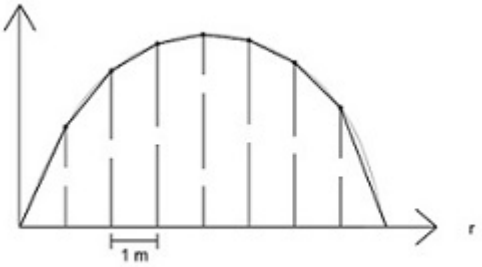

Figure A.24: Relationship between f_D, f_L and f_T, f_N (*source: self elaboration*).

Furthermore, we also have to comment on the accuracy of the integration of the forces. Since the expressions of f_T and f_N have to be found iteratively point by point, the integration that we have done afterwards has propagated the errors committed when discretizing the domain of the blade (Figure A.23). Consequently, we have to be aware of the uncertainty associated to the previous calculations, that even though they provide a correct approach by incurring on a reasonable computational cost they may be, at some point, inexact.

Finally, it is important to point out a detail that may not have been intuitive a priori. In the case where the blades are rotating, we have commented how in a correct situation the lift force f_L will be much higher than the drag component f_D. Therefore, as it can be seen in Figure A.24 it is possible that f_N, which is the normal force with respect to the directrix, has the opposite sign to the wind. In other words, according to what has been seen, it is mathematically possible that the resultant normal force of the wind on the blade in the horizontal axis is negative, so opposite to the wind.

However, this situation is no longer possible in case the windmill is not active. As long as the blades are not rotating, the force of the wind on the blades has to have necessarily the direction of the wind, according to Figure A.25.

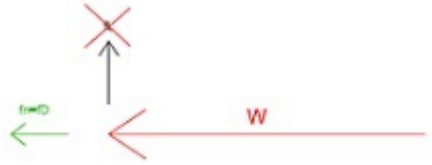

Figure A.25: Relative wind speed for a stopped windmill (*source: self elaboration*).

Appendix B

Computation of the force of the wind on the tower F_W

The force on the tower will be necessarily variable with height, since the wind speed has been assumed to grow with height according to [3] (Figure B.1). Moreover, given that we have assumed no turbulence (uniform wind speed field) on the x axis, the force will be constant all along the exposed surface of the tower.

As it has been summarized in Figure B.2, the force on the exposed semicircle of the tower will be equivalent to the force that would experiment the diameter in case the exposed zone was a rectangle. Moreover, because of symmetry the resultant will clearly be passing through the directrix of the tower and will have the same direction as the wind.

The force on the tower has a similar expression to the one used for the blades. However, obviously $C_L = 0$ since the tower does not move under any circumstance, so the relative velocity of the wind is the same as the absolute one. With reference to the value for C_D, according to [15], it will depend on the ratio height-diameter L/D (by height we understand the exposed height, so the submerged part does not count). In our particular case:

$$\frac{L}{D} = \frac{61}{4} = 15.25.$$

The reference document we have got the information from, reference [15], provides certain values for C_D for different ratios L/D. By linear interpolation, we obtain a value of $C_D = 0.867$. Therefore, the

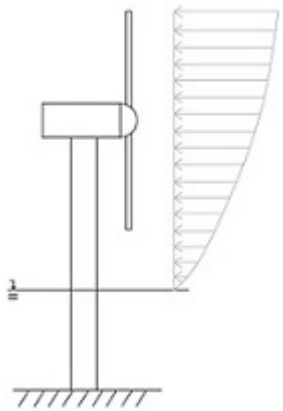

Figure B.1: Variation of wind speed with height (*source: self elaboration*).

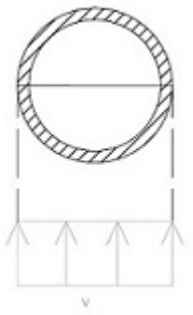

Figure B.2: Transversal section of the windmill with the according uniform wind speed (*source: self elaboration*).

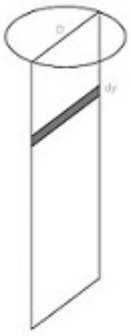

Figure B.3: Expression of the differential part of the tower used for the integration of the force of the wind (*source: self elaboration*).

expression of the force of the wind on a differential part of the tower is:

$$dF = \frac{1}{2} \cdot C_D \cdot \rho_{air} \cdot v^2 \cdot D \cdot dy.$$

The value for dF we have just found is the expression for a differential part of the tower, which will need to be integrated along height in order to obtain the final resultant, as schematized in Figure B.3.

Overall, if we integrate the previous expression:

$$F_W = \int_0^{61} \frac{dF}{dy} dy = \int_0^{61} \frac{1}{2} \cdot C_D \cdot \rho_{air} \cdot v^2 \cdot D dy,$$

where it is important to note that the integration domain is only the zone in which there is air (so the submerged part does not contribute with a wind force, obviously). A global summarize of the previous procedure can be seen in Figure B.4.

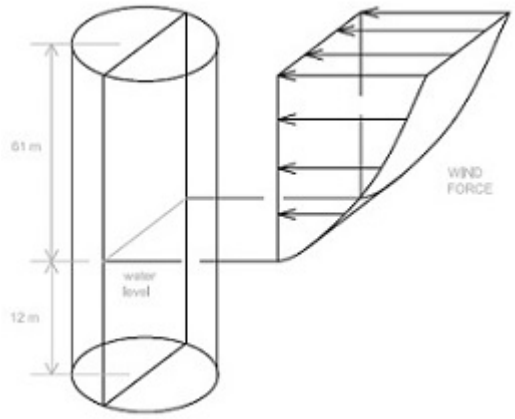

Figure B.4: Simplification of the wind speed field on the tower, according to [3] (*source: self elaboration*).

Appendix C

Computation of the sea forces

When we have considered the sea force, overall, we have divided the waves into two groups. On the one hand, there is the swell sea, whose waves are the ones which have been originated far from the windmill area, and come from a remote place. These waves are therefore independent of the wind situation at the area where the windmill is located. On the other hand there are the wind waves, which are waves generated from the presence of wind in the area. Consequently, these waves are extremely dependent on the wind conditions; in particular, the stronger the wind is, the higher these waves will be. Moreover, they will necessarily have the same direction as the primary direction of the wind. However, since we have assumed that the direction of the wind is one-dimensional, so will be the direction of the waves.

C.1 Computation of the swell sea wave force F_M

The swell sea force does not have to have the same direction of the wind, so we will assume there is angle ε between the force of the wind and the resultant swell force, as it can be seen in Figure C.1. This angle will be computed as a random variable with a uniform distribution, as it has been set out in the parameters chapter. By assuming that, we are assuming that once the wind speed has been fixed, the swell waves can be in any possible angle. In fact, that is not, in reality, true. As long as the area for the windmill is fixed, there is a dominant direction for the wind. Moreover, there will also be a dominant direction for the swell sea waves. However, this assumption has been made because no explicit location has been fixed for the windmill (we have only assumed an area from which to take orders of magnitude for the parameters, but there is no explicit location on the map).

The swell force will be divided into two components: one component in the plane of the wind force and the other in the perpendicular direction, as in Figure C.2. By definition, the x axis is in the direction of the wind, so according to the previous definition for ε:

$$f_{M,X} = F_M \cdot \cos\varepsilon,$$

$$f_{M,Z} = F_M \cdot \sin\varepsilon.$$

However, once the strategy for how this force will be divided has been set out, the main problem is how its value evolves with depth, since this force cannot be assumed to be constant. The swell sea force is computed through the *Morison* formula, which assumes a drag and a massive components of the forces (for further information see [26]):

$$F = \frac{1}{2} \cdot D \cdot \rho \cdot C_D \cdot |u| \cdot u + \rho \cdot \frac{\pi D^2}{4} \cdot C_M \cdot \frac{\partial u}{\partial t},$$

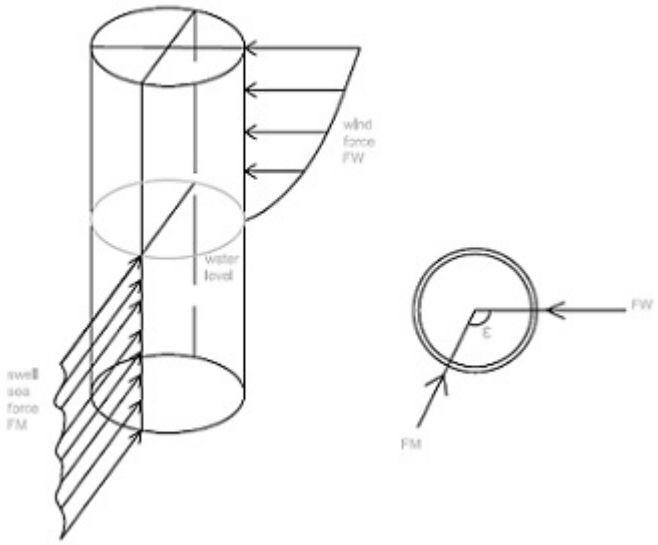

Figure C.1: Misalignment of the force of the wind and the swell sea (*source: self elaboration*).

where the first term is the drag term and the second one is the massive component (and u stands for the velocity of the water at a certain depth). In our particular case we will be doing the following hypothesis: we will assume that the direction of the swell sea forces will be constant with depth, as it has been summarized in Figure C.3. In other words, even though the value for the force will vary along depth, the direction will be always the same, and will always have an angle ε with the wind force.

The value for the force at a certain depth depends on C_D, C_M, u and $\frac{\partial u}{\partial t}$(acceleration), which will be random variables, as they have been defined in the parameters of the model. Therefore, since the value for the swell sea force is a combination of random variables, f_M will be a random variable as well. Therefore, its value will be computed through simulation for several depths (so the final expression we will get will be similar to the point expression of the forces on the blades).

In order to calculate the values for $C_D, C_M, u, \frac{\partial u}{\partial t}$ to be able to apply the *Morison* formula, the following variables are necessary:

- H_m= significant swell sea wave height, in meters (it is an external action, its value will be an input),
- T_m= swell sea period, in seconds (it is an external action, its value will be an input),
- d=total depth, equal to 12 meters,
- s=particular depth of a point ($s \in [0, d]$),
- D=diameter of the column (4 meters),
- L=wave length of the swell sea wave (it will be calculated from H_m and T_m).

With reference to the computation of L, the following expression will be used, according to [40]:

$$L = \frac{gT_m^2}{2\pi} \cdot \tanh\left(\frac{2\pi d}{L}\right),$$

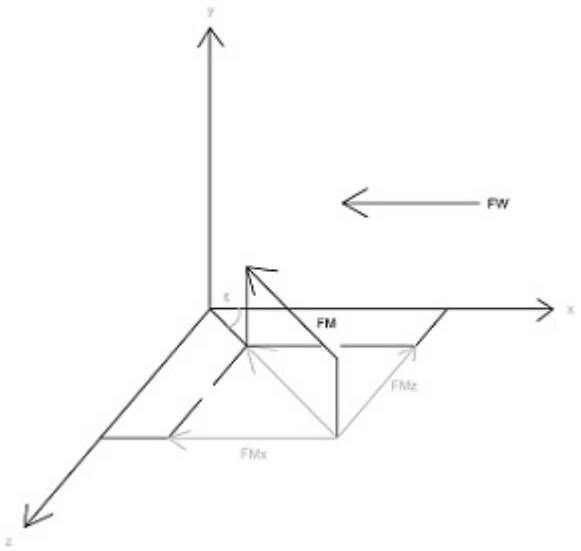

Figure C.2: Split of the swell sea wave force into two components (the vertical component is null by hypothesis) (*source: self elaboration*).

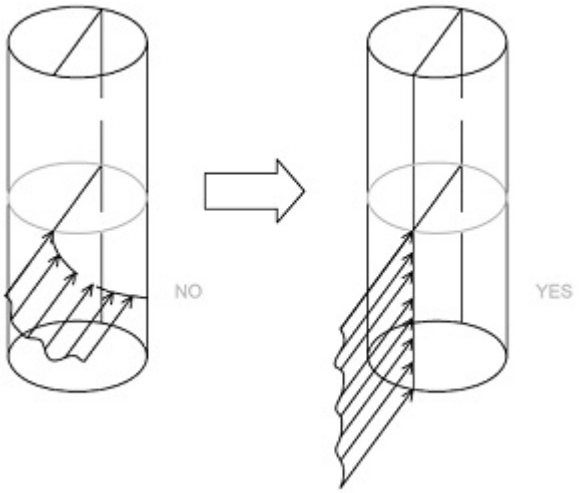

Figure C.3: Profile of the swell sea force according to the hypothesis of uniformity in the swell direction (*source: self elaboration*).

expression where the value for L has to be found through iteration.

Once these parameters are fixed (note that it is only necessary to provide the external actions values H_m and T_m), the values for the components of the *Morison* formula can be calculated.

Nevertheless, F_M is a cyclical force, according to the nature of the waves. In the references [18] it is stated:

$$u = u(t) = u \cdot \cos \omega t,$$
$$a = a(t) = a \cdot \cos \omega t,$$

which is equivalent to say that in case all the parameters are kept constant, both the velocity and the acceleration vary cyclically. Moreover, since:

$$a = \frac{\partial u}{\partial t},$$

the velocity term (drag term) and the massive term are out of phase.

Finally, once the previous remarks have been done, we will calculate the swell sea force as follows, according to the references. However, it is important to point out that in the present formula non-dimensional parameters have been used (like in reference [18]):

$$u^* = \frac{uT_m}{H_m},$$
$$L^* = \frac{L}{H_m},$$
$$d^* = \frac{d}{H_m},$$
$$s^* = \frac{s}{H_m},$$
$$a^* = \frac{aT_m^2}{H_m},$$
$$H^* = \frac{H_m}{D},$$
$$T^* = \frac{uT_m}{D}.$$

Finally, by applying the same methodology as in [18]:

$$F_M = F_{M,MAX} = C_D \cdot \frac{\rho D}{2} \cdot \left(\frac{H_m}{T_m} u^*\right)^2 \cdot \left(1 + \frac{1}{4} \cdot \left(\frac{C_M \cdot \frac{\rho \pi D^2}{4} \cdot \frac{H_m}{T_m^2} a^*}{C_D \cdot \frac{\rho D}{2} \cdot \frac{H_m \cdot u^*}{T_m}}\right)^2\right).$$

C.2 Computation of the wind wave force F_S

It has been said that the presence of wind in the windmill induces the formation of additional waves, waves we have called wind waves. With reference to these waves, they will be applied from the bottom part of the tower until the crest of the wave. The force diagram will be similar to the one summarized in Figure C.4, and as it can be checked in the figure this force will increase as we approach the surface.

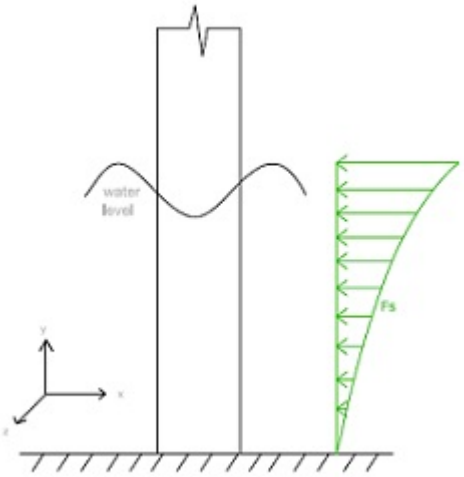

Figure C.4: Wind wave force on the tower (*source: self elaboration*).

Before computing the value for the forces on the tower, we have to state that we have used the nomenclature that can be seen in Figure C.5. This nomenclature is the conventional one assumed in all the references (for instance, see [40]), but it is important to keep the parameters clear to avoid mistakes. The evolution of the waves in time is modelled with a sinusoid. Therefore, the pressure supplied to the tower varies cyclically. In particular, the pressures on the tower are maximal and minimal in the crests and troughs. In order to calculate the values for these pressures the following hypotheses have been considered with respect to the sea water, according to [40]:

1. homogeneous and incompressible fluid,
2. surface tension is negligible,
3. Coriolis effect is negligible,
4. constant and uniform pressure on the surface,

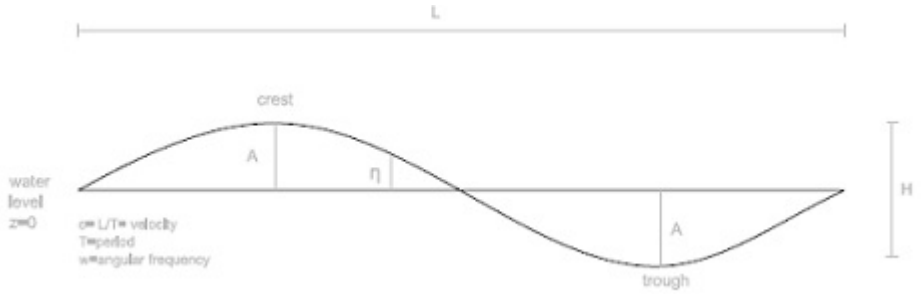

Figure C.5: Main magnitudes for wave analysis, according to [40] (*source: self elaboration*).

5. ideal fluid (non viscous),
6. irrotarional flow,
7. plane waves or "long crested waves",
8. small wave amplitude and homogeneous shape of the wave along space and time.

From the previous hypotheses the evolution of the waves is modelled. In particular, this problem is approached through solving the Laplace associated equation (conservation of mass):

$$\frac{\partial u}{\partial x} + \frac{\partial w}{\partial z} = 0,$$

$$\nabla^2 \phi = \frac{\partial^2 \phi}{\partial x^2} + \frac{\partial^2 \phi}{\partial z^2} = 0,$$

where u is the horizontal velocity of the water, w the vertical velocity and $v = \nabla\phi$ (so ϕ is the potential of the velocity).

Once this problem is solved, the following expression for ϕ is obtained:

$$\phi = \frac{Hc}{2} \cdot \frac{\cosh(k(z+h))}{\sinh(kh)} \cdot \sin(kx - \omega t),$$

where:

- $H = 2A$ is the wave height,
- c is the celerity (wave length over period),
- k is the wave number,
- z stands for depth,
- h is the total depth of the water, and
- ω is the angular frequency.

From the previous expression, the horizontal and vertical velocities can be found:

$$u = \frac{\partial \phi}{\partial x} = \frac{\pi H}{T} \cdot \frac{\cosh(k(z+h))}{\sinh(kh)} \cdot \cos(kx - \omega t),$$

$$w = \frac{\partial \phi}{\partial z} = \frac{\pi H}{T} \cdot \frac{\cosh(k(z+h))}{\sinh(kh)} \cdot \sin(kx - \omega t).$$

These velocities, at it can be easily seen, are cyclical with time, and the water particles experiment an elliptical trajectory. Depending on whether we are on shallow or deep waters, the behaviour will be slightly different, according to Figure C.6 (for further information see reference [40]).

For the reasons exposed above, our problem will only have to focus on the horizontal velocity. In particular, we will only have to focus on the maximum and minimum forces, which occur at the crests and troughs of the waves and have opposite signs, as it can be verified in Figure C.7. By applying the generalised Bernoulli formula:

$$\frac{\partial \phi}{\partial t} + \frac{1}{2} \cdot \left(\left(\frac{\partial \phi}{\partial x} \right)^2 + \left(\frac{\partial \phi}{\partial z} \right)^2 \right) + gz + \frac{p}{\rho} = 0,$$

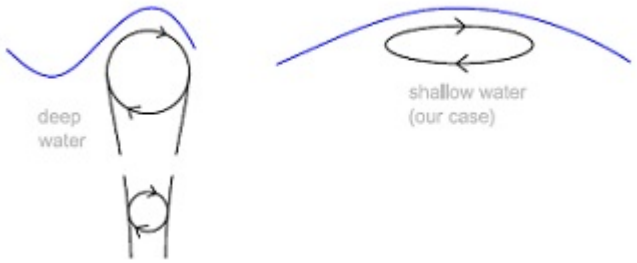

Figure C.6: Differences in the velocity fields along time in shallow and deep waters (*source: self elaboration*).

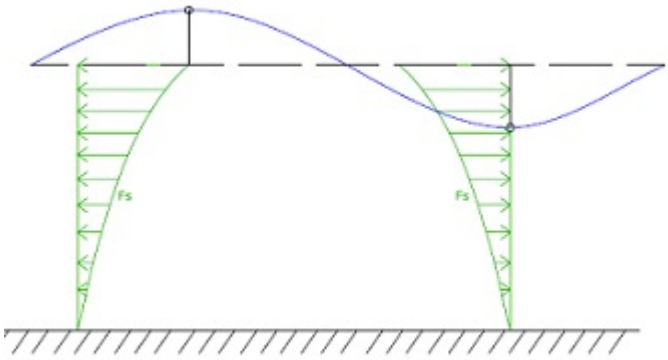

Figure C.7: Maximum and minimum values for the wind wave force on the tower (*source: self elaboration*).

we can obtain an expression for the wind wave pressure, which we have called p' (since p stands for the total pressure which includes the hydrostatic and atmospheric pressures):

$$p' = \frac{\rho g H \cosh(k(z+h))}{2\cosh(kh)} \cdot \cos(kx - \omega t).$$

If we consider the maximum and minimum values for p', which are reached in the crests and the troughs, respectively, the following expressions are found:

$$p'_{MAX} = p'_{crest} = \frac{\rho g H \cosh(k(z+h))}{2\cosh(kh)},$$

$$p'_{MIN} = p'_{trough} = -\frac{\rho g H \cosh(k(z+h))}{2\cosh(kh)},$$

It is important to remark that in order to study the vulnerability of the windmill we only need to consider the extreme situations where this force is maximum and minimum. Therefore, we will not be interested in the evolution with time.

Once the expressions for the forces have been set out, we have to say that, even though the parameters are H, T and L (because all the other parameters are either dependent on them or are related to the evolution of the wave with time so they are irrelevant), the only independent variable is the wind speed, since these waves are created because the presence of the wind. With regard to L, the same equation we used before is still applicable (see [40]):

$$L = \frac{gT^2}{2\pi} \cdot \tanh\left(\frac{2\pi d}{L}\right),$$

so the only variables we need are H and T. In order to compute their value we have used the expressions provided by the Shore Protection Manual (regarded as [11] in the bibliography). However, it is important to highlight that in these formulas there is one extra parameter that needs to be fixed. This parameter is regarded as F, which stands for the fetch. By literally paraphrasing [11] (page 3-39), "a fetch has been defined subjectively as a region in which the wind speed and direction are reasonably constant". The wind waves characteristics are dependent on this parameter, so in order to get an approach to H and T we have had to fix an approximate location for the windmill so an estimation for the fetch can be made.

As the present project has been inspired in the windmill plant "Horns Rev I" in Denmark, we have assumed a location similar to where that off-shore plant is located. According to [1], the distance from the wind farm "Horns Rev I" to the shore is 14-20 km, so for our project we have assumed a value for the fetch equal to 30 km.

In the Shore Protection Manual the explicative wind speed which is used is the wind speed at 10 meters above the sea level (see [11] page 3-44). Therefore, before computing anything, we have to convert our v_{hub} velocity (61 meters above the sea) to the 10 meter height equivalent. This conversion will be made through the formula provided by the norm EN-61400 (see [3]):

$$v_{10} = v_{hub} \cdot \left(\frac{z_{hub} - 51}{z_{hub}}\right)^{0.2}$$

From that velocity, according to the Manual the adjusted wind speed U_A is calculated

$$U_A = 0.71 \cdot v_{10}^{1.23}$$

Finally, the expressions for the wave height H and the period T are:

$$H = \frac{U_A^2}{g \cdot 1.6 \cdot 10^{-3}} \cdot \left(\frac{g \cdot F}{U_A^2} \right)^{1/2},$$

$$T = \frac{U_A}{g \cdot 2.857 \cdot 10^{-1}} \cdot \left(\frac{g \cdot F}{U_A^2} \right)^{1/3}.$$

Consequently, as long as the value for v_{hub} is known, the values for the wave height and the period can be calculated easily, so the numerical value for L can be found afterwards. From this information, it is straightforward to compute the value for the maximum and minimum wave pressure, which can be integrated to finally obtain the force supplied by the wind waves:

$$F_S = \int_0^{12} f_s ds = \int_0^{12} p'_{max} ds.$$

Appendix D

Results of the simulation

In total, 100 sets of values have been simulated, so in the end we have obtained 100 3-component-vectors which constitute our *experimental data* to use in order to fit a linear regression model. However, we have already stated that in fact, though being 3-component-vectors, there are only 2 degrees of freedom since we are always under the restriction that the sum has to be 1. As we set in the regression chapter, these 3-component-vectors are not on the real scale, so they are not appropriate to define a conventional regression fitting. In fact, this data *requires to be treated* in order to be consistent when building the regression model. This treatment (compositional treatment, according to [21] and [22]), consists on obtaining the ILR coordinates, which are orthogonal coordinates which are on the real scale and therefore admit a conventional regression fitting.

In the following table we have presented the 100 sets of values (fixing a set of values consists on fixing what we have called along the project *the external actions*, v_{hub}, H_m, T_m and fat), with their 3-component-vector of probabilities we have obtained through Monte Carlo simulation and the 2-component-vector with the ILR coordinates associated to the probabilities. It is important to keep in mind that the regression has been built for the ILR coordinates.

v_{hub} [m/s]	H_m [m]	T_m [s]	fat [%]	p_0	p_1	p_2	UD1	UD2
10	0.3	10	30	0.99964	0.00036	0.00000	22.34643	27.50071
10	1	60	30	0.99646	0.00354	0.00000	21.69596	29.60352
10	1	40	25	0.99971	0.00029	0.00000	26.35089	34.14226
10	2	60	25	0.99745	0.00255	0.00000	24.51001	34.01338
10	3	90	90	0.00537	0.98673	0.00790	-2.28535	3.41388
10	3	110	80	0.01400	0.98562	0.00038	-0.26417	5.55846
20	0.3	10	80	0.00109	0.46439	0.53453	-5.00344	-0.09946
20	0.3	15	60	0.01837	0.95587	0.02576	-1.75119	2.55543
20	1	40	20	0.98267	0.01733	0.00000	13.58920	17.82670
20	2	60	60	0.01878	0.94856	0.03267	-1.82735	2.38195
20	2.5	85	60	0.01879	0.94647	0.03473	-1.85077	2.33702
20	3	110	25	0.54833	0.45167	0.00000	7.82741	13.28322
20	3	120	40	0.20006	0.79990	0.00004	2.91146	7.00274
26	2	60	40	0.95442	0.04558	0.00000	8.50759	10.43400
30	3	90	50	0.54712	0.45029	0.00259	2.26541	3.64833
30	0.3	10	60	0.26874	0.70979	0.02147	0.63517	2.47368
32	1	40	50	0.47745	0.51636	0.00619	1.74184	3.12777
37	1	50	35	0.82548	0.17291	0.00161	3.18553	3.30681
30	1.5	60	70	0.09325	0.68923	0.21752	-1.16240	0.81550
40	2	80	50	0.14157	0.37419	0.48424	-0.89889	-0.18231
30	3	100	70	0.08362	0.61624	0.30014	-1.33714	0.50868
30	3	110	85	0.00627	0.19152	0.80221	-3.37610	-1.01286
50	2	80	15	0.97209	0.00201	0.02591	4.00406	-1.80880
50	1	50	35	0.14473	0.12404	0.73123	-0.59836	-1.25448
50	1	40	15	0.98124	0.00197	0.01679	4.19639	-1.51501
50	1	35	20	0.88998	0.02207	0.08795	2.45410	-0.97748
50	2	60	40	0.03346	0.05911	0.90743	-1.57975	-1.93122
50	3	100	50	0.00084	0.00557	0.99359	-3.66443	-3.66517
70	0.3	15	10	0.02283	0.00010	0.97706	0.67022	-6.47310
65	1	40	35	0.00002	0.00004	0.99994	-4.53872	-7.22209
70	2	60	40	0.00094	0.00572	0.99334	-3.58275	-3.64663
60	1	30	25	0.03029	0.00986	0.95985	-0.95284	-3.23710
60	2	60	20	0.03014	0.00951	0.96035	-0.94198	-3.26351
45	0.3	10	40	0.08711	0.00824	0.90465	0.00723	-3.32238
45	1	30	30	0.25525	0.29600	0.44875	-0.29080	-0.29423
45	1.5	50	50	0.02505	0.10522	0.86973	-2.03410	-1.49348
40	0.3	15	30	0.89890	0.09907	0.00203	3.38786	2.74906
40	1	40	35	0.74538	0.23328	0.02134	1.92494	1.69127
40	1	50	45	0.02522	0.10465	0.87014	-2.02664	-1.49770
45	1.5	65	30	0.73240	0.15545	0.11216	1.39884	0.23080
45	0.3	15	25	0.92632	0.05661	0.01707	2.77157	0.84772
45	2	60	20	0.98553	0.00961	0.00487	4.05859	0.48087
45	1	30	50	0.73246	0.15557	0.11197	1.39925	0.23256
45	3	110	40	0.17671	0.20427	0.61902	-0.57098	-0.78395
15	1	30	60	0.04284	0.95685	0.00030	0.75296	5.69686
35	2	60	50	0.36003	0.56200	0.07797	0.44279	1.39669
35	3	100	40	0.71499	0.27861	0.00640	2.31003	2.66829
35	0.3	20	35	0.86450	0.13538	0.00012	4.37196	4.95042
20	1	40	50	0.06376	0.93541	0.00084	0.67259	4.96340

v_{hub} [m/s]	H_m [m]	T_m [s]	fat [%]	p_0	p_1	p_2	UD1	UD2
15	1	30	60	0.04284	0.95685	0.00030	0.75296	5.69686
15	2	60	75	0.00816	0.94192	0.04992	-2.67771	2.07712
20	0.3	10	65	0.06344	0.93570	0.00086	0.65716	4.94417
20	0.3	40	55	0.06357	0.93549	0.00094	0.62113	4.87862
20	1	30	80	0.00089	0.45104	0.54807	-5.16783	-0.13777
20	1	50	50	0.06354	0.93572	0.00074	0.71792	5.04728
20	1.5	50	45	0.11462	0.88529	0.00008	2.11566	6.55546
15	0.3	40	80	0.00464	0.88504	0.11033	-3.43789	1.47233
15	0.3	50	65	0.02458	0.97299	0.00243	-0.55768	4.23636
25	1	60	55	0.60421	0.39578	0.00001	4.66715	7.48546
25	3	140	70	0.22291	0.73828	0.03881	0.22474	2.08289
25	2	120	55	0.60315	0.39682	0.00003	4.21615	6.71047
15	3	170	65	0.00437	0.50645	0.48918	-3.86676	0.02454
15	1	70	70	0.01413	0.97289	0.01298	-1.69274	3.05266
35	1	60	40	0.71903	0.27891	0.00207	2.77567	3.46832
35	0.3	30	50	0.37223	0.58096	0.04681	0.66469	1.78086
35	2	40	45	0.53685	0.44249	0.02066	1.40880	2.16672
35	2.5	50	35	0.86436	0.13516	0.00049	3.81211	3.97861
35	1.5	70	55	0.21763	0.60544	0.17693	-0.33316	0.86990
35	1.5	30	60	0.11045	0.54062	0.34894	-1.11800	0.30959
35	2.5	60	65	0.04271	0.35088	0.60642	-1.94297	-0.38688
35	3	150	65	0.03038	0.25212	0.71750	-2.15478	-0.73954
25	3	100	65	0.33001	0.66588	0.00411	1.50387	3.59754
25	2	70	80	0.09477	0.79833	0.10690	-0.91919	1.42170
25	1	60	70	0.23111	0.76141	0.00748	0.91364	3.26859
20	1	40	90	0.00016	0.16343	0.83641	-6.30720	-1.15451
20	1	25	85	0.00046	0.28706	0.71248	-5.62627	-0.64281
15	1	40	95	0.00052	0.43833	0.56114	-5.59628	-0.17465
15	3	130	90	0.00108	0.52997	0.46896	-5.01149	0.08648
45	0.3	30	58	0.00341	0.03714	0.95946	-3.27803	-2.29934
45	0.3	55	62	0.00099	0.01650	0.98251	-3.96830	-2.88977
50	0.3	50	20	0.90655	0.02160	0.07185	2.56050	-0.84972
50	1	70	25	0.66146	0.07880	0.25974	1.25019	-0.84341
50	1.5	100	15	0.97737	0.00198	0.02065	4.10585	-1.65671
40	1.5	120	20	0.90653	0.02202	0.07145	2.55498	-0.83244
40	3	160	15	0.90716	0.02191	0.07092	2.56051	-0.83050
40	2	120	30	0.89614	0.09787	0.00599	2.94854	1.97536
40	2	160	25	0.92735	0.02350	0.04914	2.69966	-0.52156
35	1	100	35	0.86387	0.13599	0.00013	4.33770	4.89849
35	2	160	40	0.65726	0.25674	0.08600	1.21405	0.77340
35	2.5	90	50	0.86371	0.13610	0.00019	4.19985	4.66114
25	3	190	60	0.18026	0.21316	0.60658	-0.56381	-0.73948
40	1	70	40	0.53716	0.37873	0.08411	0.89961	1.06395
50	2	100	30	0.31789	0.11394	0.56817	0.18181	-1.13614
40	1	70	40	0.53716	0.37873	0.08411	0.89961	1.06395
50	2	100	30	0.31789	0.11394	0.56817	0.18181	-1.13614
27	1	90	65	0.25836	0.73166	0.00998	0.90352	3.03707
35	2	130	55	0.20613	0.57871	0.21516	-0.43893	0.69964
28	3	150	60	0.31563	0.62353	0.06085	0.39411	1.64546
29	0.5	50	65	0.19790	0.76156	0.04054	0.09708	2.07394
56	2	70	25	0.12830	0.02852	0.84318	-0.15470	-2.39476